
Defense Special Weapons Agency
Alexandria, VA 22310-3398


DSWA-TR-97-30

# High Voltage Water Breakdown Studies

Magne Kristiansen
Lynn L. Hatfield
Texas Tech University
Pulsed Power Lab
Department of Electrical Engineering
Lubbock, TX 79409

January 1998

Technical Report



CONTRACT No. DNA 001-94-C-0117

DESTRUCTION NOTICE:

Destroy this report when it is no longer needed.
Do not return to sender.

PLEASE NOTIFY THE DEFENSE SPECIAL WEAPONS AGENCY, ATTN: CSTI, 6801TELEGRAPH ROAD, ALEXANDRIA, VA 22310-3398, IF YOUR ADDRESS IS INCORRECT, IF YOU WISH IT DELETED FROM THE DISTRIBUTION LIST, OR IF THE ADDRESSEE IS NO LONGER EMPLOYED BY YOUR ORGANIZATION.

ERRATA

for

DSWA-TR-97-30

High Voltage Water Breakdown Studies

UNCLASSIFIED

dated January 1998

Two changes were made to referenced report after it was printed and distributed. An additional author's name was added to the front cover, SF 298 block 6, and the Distribution List. In addition, the Project Officer's name in SF 298 block 9 was changed. Please make pen and ink changes as follows:

a. Add David Lojewski to the two names presently appearing on the front cover and in SF 298 block 6.

b. Change EST/Larson to read EST/Ware in SF 298 block 9.

c. Add 2 CY ATTN: D. Lojewski to TEXAS TECH UNIVERSITY on page Dist-3 of the Distribution List.

The added author is being furnished two copies of the finished product.

# REPORT DOCUMENTATION PAGE

*Form Approved*
*OMB No. 0704-0188*



| 1. AGENCY USE ONLY (Leave blank) | 2. REPORT DATE | 3. REPORT TYPE AND DATES COVERED |
|---|---|---|
| | 980101 | Technical 940726 - 970102 |

**4. TITLE AND SUBTITLE**
High Voltage Water Breakdown Studies

**5. FUNDING NUMBERS**
C - DNA 001-94-C-0117
PE - 62715H
PR - AB
TA - RF
WU - DH00033

**6. AUTHOR(S)**
Magne Kristiansen and Lynn L. Hatfield

**7. PERFORMING ORGANIZATION NAME(S) AND ADDRESS(ES)**
Texas Tech University
Pulsed Power Lab
Department of Electrical Engineering
Lubbock, TX 79409

**8. PERFORMING ORGANIZATION REPORT NUMBER**
DNA-F-97

**9. SPONSORING/MONITORING AGENCY NAME(S) AND ADDRESS(ES)**
Defense Special Weapons Agency
6801 Telegraph Road
Alexandria, VA 22310-3398
EST/Larson

**10. SPONSORING/MONITORING AGENCY REPORT NUMBER**
DSWA-TR-97-30

**11. SUPPLEMENTARY NOTES**
This work was sponsored by the Defense Special Weapons Agency under RDT&E RMC Code B4662D GE 00033 3300A AB 25904D.

**12a. DISTRIBUTION/AVAILABILITY STATEMENT**
Approved for public release; distribution is unlimited.

**12b. DISTRIBUTION CODE**

**13. ABSTRACT** (*Maximum 200 words*)

The breakdown voltage and time to breakdown for electrodes in water has been measured. Reports in Russian journals describe increases of a factor of three in the holdoff voltage for water subjected to some treatment which is not described. Several electrode treatments and water treatments were tried in an effort to uncover the secret. Electrode treatments included: anodizing aluminum electrodes, coating electrodes with polyethersulfane and polycarbonate, and coating the electrodes with black wax. Electrodes with integral magnets were tried. Water treatments included: dissolved $SF_6$, solutions with $HC\ell$ and solutions with the surfactants dodecylamine and laric acid. None of these schemes produced a large increase in holdoff voltage although some did produce small but statistically significant increases. Some produced significant decreases. This report also includes an extensive bibiliography of articles and electrical breakdown and conduction in water.

**14. SUBJECT TERMS**
Electrical Breakdown in Water

**15. NUMBER OF PAGES**
138

**16. PRICE CODE**

| 17. SECURITY CLASSIFICATION OF REPORT | 18. SECURITY CLASSIFICATION OF THIS PAGE | 19. SECURITY CLASSIFICATION OF ABSTRACT | 20. LIMITATION OF ABSTRACT |
|---|---|---|---|
| UNCLASSIFIED | UNCLASSIFIED | UNCLASSIFIED | SAR |

NSN 7540-280-5500

Standar d Form 298 ((rev. 2-89)
Precribed by ANSI Sta. 239-18
298-102

CLASSIFIED BY:

N/A since Unclassified.

DECLASSIFY ON:

N/A since Unclassified.

## SUMMARY

Electrical breakdown due to high voltage applied between electrodes in water has been investigated in a series of experiments. This work was undertaken after a number of reports by Russian scientists that voltage levels much higher than conventional limits could be achieved by use of special treatments. Unfortunately, the nature of these special treatments was not disclosed. There was some hint that these special treatments were somehow related to the water-electrode interface.

A chamber was constructed which would hold two electrodes at a spacing of 1.27 cm immersed in water. The water was circulated so that purification, addition of chemicals, and addition of gases could be controlled. A pulse generator delivered a fast rise pulse to the electrodes at up to 400 kV. Experiments in pure water established a baseline breakdown voltage which agreed with previous researchers results. In all of these experiments, the measured parameters included the time to breakdown, the breakdown voltage, and the fall time of the voltage across the electrodes. These parameters were extracted from the wave form recorded by use of a capacitive probe on the high voltage pulse line at the input to the water chamber.

The following special conditions were tried: magnetic fields at the electrodes using embedded magnets; $SF_6$ gas dissolved in the water; several concentrations of $HC\ell$ in the water; anodized aluminum electrodes; coating of the electrodes with black wax and with two polymers, polyethersulfane and polycarbonate; and treatment of the water with two surfactants, dodecylamine and laric acid.

A sophisticated analysis of the data showed small but statistically significant increases in breakdown voltage for the magnetic field application but no improvements as large as even ten percent for any case. Some treatments, such as laric acid in the water, lowered the overall performance.

## CONVERSION TABLE

Conversion factors for U.S. Customary to metric (SI) units of measurement.

| MULTIPLY → / TO GET ← | BY → / BY ← | TO GET / DIVIDE |
|---|---|---|
| angstrom | 1.000 000 X E -10 | meters (m) |
| atmosphere (normal) | 1.013 25 X E +2 | kilo pascal (kPa) |
| bar | 1.000 000 X E +2 | kilo pascal (kPa) |
| barn | 1.000 000 X E -28 | meter$^2$ ($m^2$) |
| British thermal unit (thermochemical) | 1.054 350 X E +3 | joule (J) |
| calorie (thermochemical) | 4.184 000 | joule (J) |
| cal (thermochemical/$cm^2$) | 4.184 000 X E -2 | mega joule/$m^2$ ($MJ/m^2$) |
| curie | 3.700 000 X E +1 | *giga becquerel (GBq) |
| degree (angle) | 1.745 329 X E -2 | radian (rad) |
| degree Fahrenheit | $t_k = (t^\circ f + 459.67)/1.8$ | degree kelvin (K) |
| electron volt | 1.602 19 X E -19 | joule (J) |
| erg | 1.000 000 X E -7 | joule (J) |
| erg/second | 1.000 000 X E -7 | watt (W) |
| foot | 3.048 000 X E -1 | meter (m) |
| foot-pound-force | 1.355 818 | joule (J) |
| gallon (U.S. liquid) | 3.785 412 X E -3 | meter$^3$ ($m^3$) |
| inch | 2.540 000 X E -2 | meter (m) |
| jerk | 1.000 000 X E +9 | joule (J) |
| joule/kilogram (J/kg) radiation dose absorbed | 1.000 000 | Gray (Gy) |
| kilotons | 4.183 | terajoules |
| kip (1000 lbf) | 4.448 222 X E +3 | newton (N) |
| kip/inch$^2$ (ksi) | 6.894 757 X E +3 | kilo pascal (kPa) |
| ktap | 1.000 000 X E +2 | newton-second/$m^2$ ($N\text{-}s/m^2$) |
| micron | 1.000 000 X E -6 | meter (m) |
| mil | 2.540 000 X E -5 | meter (m) |
| mile (international) | 1.609 344 X E +3 | meter (m) |
| ounce | 2.834 952 X E -2 | kilogram (kg) |
| pound-force (lbs avoirdupois) | 4.448 222 | newton (N) |
| pound-force inch | 1.129 848 X E -1 | newton-meter (N·m) |
| pound-force/inch | 1.751 268 X E +2 | newton/meter (N/m) |
| pound-force/foot$^2$ | 4.788 026 X E -2 | kilo pascal (kPa) |
| pound-force/inch$^2$ (psi) | 6.894 757 | kilo pascal (kPa) |
| pound-mass (lbm avoirdupois) | 4.535 924 X E -1 | kilogram (kg) |
| pound-mass-foot$^2$ (moment of inertia) | 4.214 011 X E -2 | kilogram-meter$^2$ ($kg\cdot m^2$) |
| pound-mass/foot$^3$ | 1.601 846 X E +1 | kilogram/meter$^3$ ($kg/m^3$) |
| rad (radiation dose absorbed) | 1.000 000 X E -2 | **Gray (Gy) |
| roentgen | 2.579 760 X E -4 | coulomb/kilogram (C/kg) |
| shake | 1.000 000 X E -8 | second (s) |
| slug | 1.459 390 X E +1 | kilogram (kg) |
| torr (mm Hg, 0° C) | 1.333 22 X E -1 | kilo pascal (kPa) |

*The becquerel (Bq) is the SI unit of radioactivity; 1 Bq = 1 event/s.
**The Gray (GY) is the SI unit of absorbed radiation.

TABLE OF CONTENTS

TABLE OF CONTENTS (Continued)

FIGURES

FIGURES (Continued)

FIGURES (Continued)

FIGURES (Continued)

FIGURES (Continued)

# TABLES

# SECTION 1
# INTRODUCTION

The Water Breakdown System was designed to investigate various techniques for increasing the high voltage breakdown strength of water and increase the time before breakdown. The interest in water for high voltage applications has been around since the 1950s. The reason for this interest is water's unusually high dielectric constant ($\varepsilon_r$) which is typically 80. This is about 30 to 40 times higher than most other insulator materials. If we could improve the insulating ability of water, then high energy capacitors could be made 30 to 40 times smaller than they presently are. Much of the initial work in characterizing water insulation was done by J. C. Martin; however, most of his work was done for systems with limited surface area. Many of the pulsed power systems today are much larger than they were in Martin's time, and his equations are limited to smaller surface areas than we are seeing today, but Martin's work is still used for comparison with the work being done today. Martin's equations are discussed in Appendix A.

The Russians have also done considerable work with water insulation. Recently claims of quadrupling the field strength above the J. C. Martin levels over large areas [1] has brought considerable interest into this area. Some of the Russian work will be discussed in Section 2.

As can be seen, the interest in water has been around for a long time. One reason for this is that water exhibits the quality of being self-healing; if there is a breakdown in the water, it quickly returns to its original and undamaged state. Other liquid insulators are prone to carbonization after breakdown and tend to lose some of their voltage holdoff strength.

The drawback to using water is the short length of time it can hold off the voltage, typically in the microsecond ($\mu s$) range. Considerable research has been done to make water a more viable dielectric material. For now, water

capacitors are used for intermediate energy storage in pulsed power systems. This is usually in the form of peaking capacitors placed between the Marx bank and the load. The use of peaking capacitors sharpens the rise time of the pulse before it goes to the load. What we would like to see is the use of water in the primary energy storage portion of the pulsed power system. Water is relatively inexpensive and is environmentally safe. These characteristics along with the high dielectric constant make water an excellent choice for building large capacitors. If a way can be found to increase the voltage holdoff time and the field strength, then there will be more applications for water capacitors.

A review of the literature is given in Section 2. This consists of a discussion of a subset of over 225 articles that were reviewed for this work and a review of some of the Russian literature. Section 3 presents a description of the experimental setup and an analysis of the electrical circuit model developed for this experiment. Experimental design and data are given in Section 4 and a discussion of the data is in Section 5. Conclusions are given in Section 6 along with some suggestions for future work.

As mentioned above, Appendix A goes through some of the information on J. C. Martin's equation and some of the more resent work done in that area. Appendix B contain the list of articles found in the literature search.

# SECTION 2
# LITERATURE REVIEW

The literature search for this project consisted of a review of over 225 journal articles and books that pertained to high voltage breakdown in liquids with the emphasis on water. The literature review is presented in two sections; the first will be a discussion of thirteen representative articles that deal with techniques to increase the ability of the water insulator to hold-off high electric fields and, the second, presents a discussion of the prebreakdown phenomena described by Russian scientists at the Siberian Scientific-Research Institute of Power Generation, Novosibirsk, Russia. A reading list of all of the articles reviewed is included at the end of this report in Appendix B.

## 2.1 HIGH VOLTAGE WATER BREAKDOWN REVIEW.

In the course of this review, there were so many variables involved that attempting to analyze the work that had been done was like comparing "apples and oranges." Thirteen articles were selected that provided a good representation of the research previously done.

An analysis of the data showed three overriding effects. Any change made to the water affected (1) its voltage breakdown strength which was usually measured as its electric field breakdown ($E_{BD}$) strength, (2) its dielectric constant ($\varepsilon_r$), and/or (3) its effective time ($\tau_{eff}$) of holdoff. Typically, there were tradeoffs between these three effects, e.g., something that improves $E_{BD}$ causes a decrease in $\varepsilon_r$.

A matrix of Variables versus Effects was developed from the 13 journal articles to show these relationships (see Table 2-1). The numbers in the matrix relate to the references listed at the end of this report. The variables that have been researched are pressure, additives (ethylene glycol and alcohol),

electrode material, polarity, temperature, resistivity, distillation, diffusion electrodes, and electrode coatings. The respective effects of each of these variables will be summarized. More in-depth information can be found by reviewing the articles referenced in Table 2-1.

Table 2-1. Matrix of Variables versus Effects in water breakdown research (numbers in table refer to reference numbers at the end of this report).

| Variables / Effects | $E_{BD}$ | $\varepsilon_r$ | $\tau_{eff}$ |
|---|---|---|---|
| Pressure | 2,3 | | 2,3 |
| Ethylene Glycol/Water | 4 | 4 | 4 |
| Alcohol/Water | | 5 | |
| Same Electrode Material (anode and cathode) | 6,7 | 8,9,10 | |
| Different Electrode Material (anode and cathode) | 6 | 10 | |
| Polarity | | 10 | 11 |
| Temperature | 3 | 5,12,14 | 3,12 |
| Resistivity (Conductivity) | | 12 | 12 |
| Diffusion Electrodes | 13 | | 13 |
| Electrode Coatings | 7 | | |

Abramyan and Kornilov [2] did considerable work looking at the effects of pressure on the voltage breakdown and the time to breakdown. They showed that an increase in the pressure from 1.7 MPa to 13.4 MPa increased $E_{BD}$ from 360 kV/cm to 640 kV/cm, effectively doubling $E_{BD}$. Figure 2-1 shows the nearly linear relationship between the breakdown field and pressure. Over the range of pressures that were measured, the relationship between the $E_{BD}$ and pressure was approximately 24 kV/(cm MPa). They also reported an increase in the time until breakdown ($\sim\tau_{eff}$) from 50 ns to 10 μs with an increase in pressure from 0.3 MPa to 10.1 MPa. According to Abramyan and Kornilov, this suggested a gaseous process occurring in the water during the breakdown.

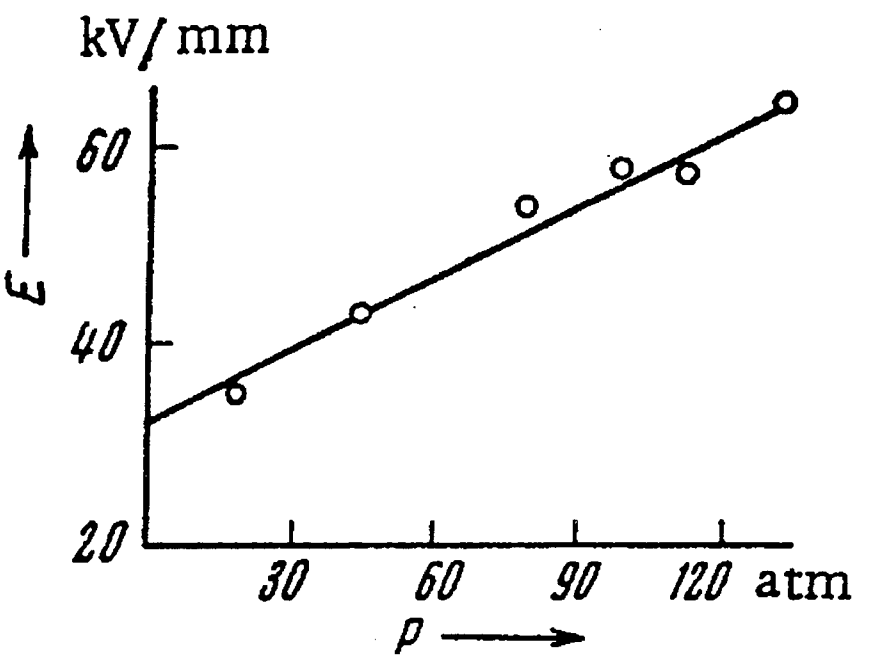


Figure 2-1. Relationship between pressure and electric breakdown strength of water [2].

Sincerny [3] looked at flow rate, temperature, resistivity, pressure, and percentage of deaeration on $E_{BD}$ and $\tau_{eff}$. He varied the water pressure from 101 kPa to 308 kPa with an increase of $E_{BD}$ from 218 kV/cm to 236 kV/cm, and an increase in $\tau_{eff}$ from 2.9 μs to 3.5 μs. Even though he claims no effect due to temperature, a small effect was seen when three measurements were made at different temperatures: 8°C, 20°C, and 33°C. The electric breakdown field ($E_{BD}$) went from 220 kV/cm to 224 kV/cm, and $\tau_{eff}$ went from 2.9 μs to 3.1 μs as the temperature decreased.

Varying the deaeration level from 0% to 90% did not have any significant effect on the electrical breakdown level but did have an effect on the recovery time of the test cell. The level of deaeration affected the amount of time required to wait between shots to allow the bubbles that formed in the water to dissipate. Without deaeration, this typically took about an hour.

The flow rate of the water was varied between 126 ml/s and 630 ml/s with no significant effect seen on $E_{BD}$ or $\tau_{eff}$. He did observe a difference in the breakdown site on the electrode with a difference in flow rate. The breakdown region tended to be more localized when there was no flow as opposed to a more generalized breakdown region with the higher flow rate. This was attributed to the arc following the motion of the particles involved in the discharge as they are being swept across the surface of the electrode. The resistivity of the water was varied from 14 MΩ-cm to 37 MΩ-cm. There was no significant effect on breakdown strength with the change of resistivity of the water.

Fenneman [4] looked at the effects of mixing ethylene glycol with the water on $E_{BD}$, $\varepsilon_r$, and $\tau_{eff}$. With pure water at room temperature and no ethylene glycol, he measured $E_{BD}$ at 130 kV/cm. With a 95% mixture of ethylene glycol at +28°C, $E_{BD}$ went up to 270 kV/cm, effectively doubling the breakdown voltage. By varying the water/ethylene glycol mixture and the temperature, he was able to get an $\varepsilon_r$ of 80 with a 60% mixture cooled to –30°C, and was able to get $\tau_{eff}$ up to 1 ms with an 80% mixture cooled to –10°C. Table 2-2 summa-

rizes the data on the water and ethylene glycol investigation. By varying the amount of ethylene glycol added to the water and the temperature of the mixture, Fenneman was able to vary $E_{BD}$, $\varepsilon_r$, and $\tau_{eff}$.

Table 2-2. Electrical breakdown strength properties of mixtures of ethylene glycol and water [4].

| Mix (%) | T (C) | $\varepsilon_r$ | $\tau_{eff}$ (ms) | $E_{BD}$ (kV/cm) |
|---|---|---|---|---|
| 0 | 0 | 88 | 0.25 | 130 |
| 40 | 25 | 67 | 0.10 | 160 |
| 40 | -11 | 79 | 0.40 | 160 |
| 60 | 30 | 58 | 0.18 | 160 |
| 60 | -23 | 77 | 0.97 | 140 |
| 80 | 25 | 49 | 0.45 | 210 |
| 80 | -10 | 60 | 1.00 | 170 |
| 95 | 28 | 40 | 0.20 | 270 |

Noyel, Jorat, Derriche, and Huck [5] looked at the change in the dielectric constant with different mixtures of alcohol and supercooled water. The alcohols used were methanol, ethanol, propanediol 1-2, and propanetriol 1-2-3. They determined the relationship between temperature (T), molar fraction ($x$) of the alcohol, and static dielectric constant ($\varepsilon_s$) to be

$$\varepsilon_{s,x} = A_x + \frac{B_x}{T} + \frac{C_x}{T^2}, \tag{2.1}$$

where A, B, and C are constants that were determined experimentally and varied with the molar fraction of the alcohol used. They showed that an increase in alcohol decreased $\varepsilon_s$ while a decrease in temperature increased $\varepsilon_s$ (Figure 2-2). The highest value of $\varepsilon_s$ was found to be 120 by using a 40% methanol molar fraction cooled to −100°C. They did not look at $E_{BD}$ or $\tau_{eff}$.

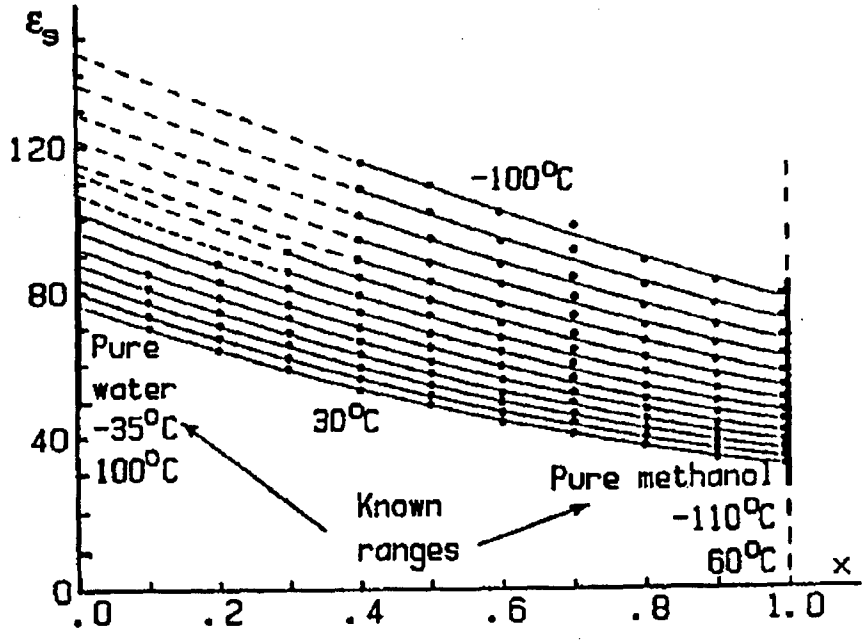


Figure 2-2. Isothermal static permittivity versus molar fraction $x$ for mixtures $(\text{methanol})_x$ / $(\text{water})_{1-x}$ [5].

Zahn, Ohki, Rhoads, LaGasse, and Matsuzawa [6] looked at the $E_{BD}$ of different types of electrodes. They found that stainless steel (SS) electrodes performed better than aluminum (Al) and were able to increase $E_{BD}$ from 110 kV/cm (Al) to 125 kV/cm (SS). Overall, brass electrodes had the best holdoff with an $E_{BD}$ of 145 kV/cm. Copper electrodes had the most consistent

holdoff (least variation) with an average $E_{BD}$ of 135 kV/cm. They also looked at using different materials for the anode and cathode. The most significant finding was that brass for the cathode and aluminum for the anode gave the worst holdoff with an $E_{BD}$ of 90 kV/cm. Table 2-3 summarizes the data from this investigation.

These data were taken using parallel plane electrodes, 1 m x 3.2 cm, placed 1 cm apart. This may explain why the $E_{BD}$'s are lower than what is seen in other research. The larger is the surface area, the lower the $E_{BD}$. They did not look at $\varepsilon_r$ or $\tau_{eff}$.

Szklarczyk, Kainthla, and Bockris [7] compared platinum, copper, iron, nickel, gold, and cobalt electrodes. Figure 2-3 shows the current density-voltage ($j$-$v$) relationship for various types of electrodes with a 5 mm gap. The horizontal axis is the voltage ($v$) in volts and the vertical axis is the current density ($j$) in amps/cm$^2$. Shown in Figure 2-3, of the four materials used, copper (Cu) had the best response. Figure 2-4 describes the various portions of the $j$-$v$ curve and what the mechanism was at various parts of the curve. The section of the curve at $A$ is due to the electrode kinetics for $H_2$ and $O_2$ evolution in a low conductance solution. In this region, the current is limited by the solution resistance. The next portion of the curve ($B$) represents the dissociation of the water molecules. The electric field is high enough to cause the ionization and dissociation of the water. The next stage is the plateau region ($C$) where so much $H_2$ has built up on the electrode surface that the water will no longer be in contact with the electrode surface, thus preventing the increase of the current density. At the end of the plateau region ($D$), an intermittent glow discharge is seen. Region $E$ represents the breakdown of the gap. Szklarczyk et al. suggest that at the breakdown point ($D$) the Fermi level of the electrons in the cathode is equal to the conduction band of the water. They also looked at gold (Au) and nickel (Ni) electrodes with the

Table 2-3. Summary of the data with a history of the highest applied voltages without breakdown [6].

| | |
|---|---|
| Stainless Steel + / Stainless Steel –<br>110 kV/cm (12 times)<br>115 kV/cm (12 times)<br>120 kV/cm (4 times)<br>125 kV/cm (16 times) | Aluminum + / Aluminum –<br>110 kV/cm (29 times)<br>115 kV/cm (9 times)<br>120 kV/cm (2 times) |
| Brass + / Brass –<br>115 kV/cm (9 times)<br>125 kV/cm (10 times)<br>130 kV/cm (1 time)<br>145 kV/cm (2 times) | Copper + / Copper –<br>135 kV/cm (24 times) |
| Stainless Steel + / Aluminum –<br>125 kV/cm (4 times)<br>130 kV/cm (14 times)<br>140 kV/cm (2 times) | Aluminum + / Stainless Steel –<br>105 kV/cm (20 times)<br>110 kV/cm (1 time) |
| Brass + / Copper –<br>110 kV/cm (19 times)<br>115 kV/cm (8 times) | Copper + / Brass –<br>110 kV/cm (10 times)<br>115 kV/cm (8 times)<br>120 kV/cm (1 time) |
| Stainless Steel + / Brass –<br>115 kV/cm (20 times)<br>120 kV/cm (6 times) | Brass + / Stainless Steel –<br>125 kV/cm (19 times) |
| Stainless Steel + / Copper –<br>115 kV/cm (19 times)<br>125 kV/cm (2 times)<br>130 kV/cm (1 time) | Copper + / Stainless Steel –<br>110 kV/cm (19 times)<br>115 kV/cm (3 times) |
| Aluminum + / Brass –<br>90 kV/cm (19 times)<br>95 kV/cm (17 times) | Brass + / Aluminum –<br>125 kV/cm (22 times)<br>130 kV/cm (13 times)<br>135 kV/cm (2 times) |
| Aluminum + / Copper –<br>110 kV/cm (20 times) | Copper + / Aluminum –<br>100 kV/cm (19 times)<br>125 kV/cm (2 times) |

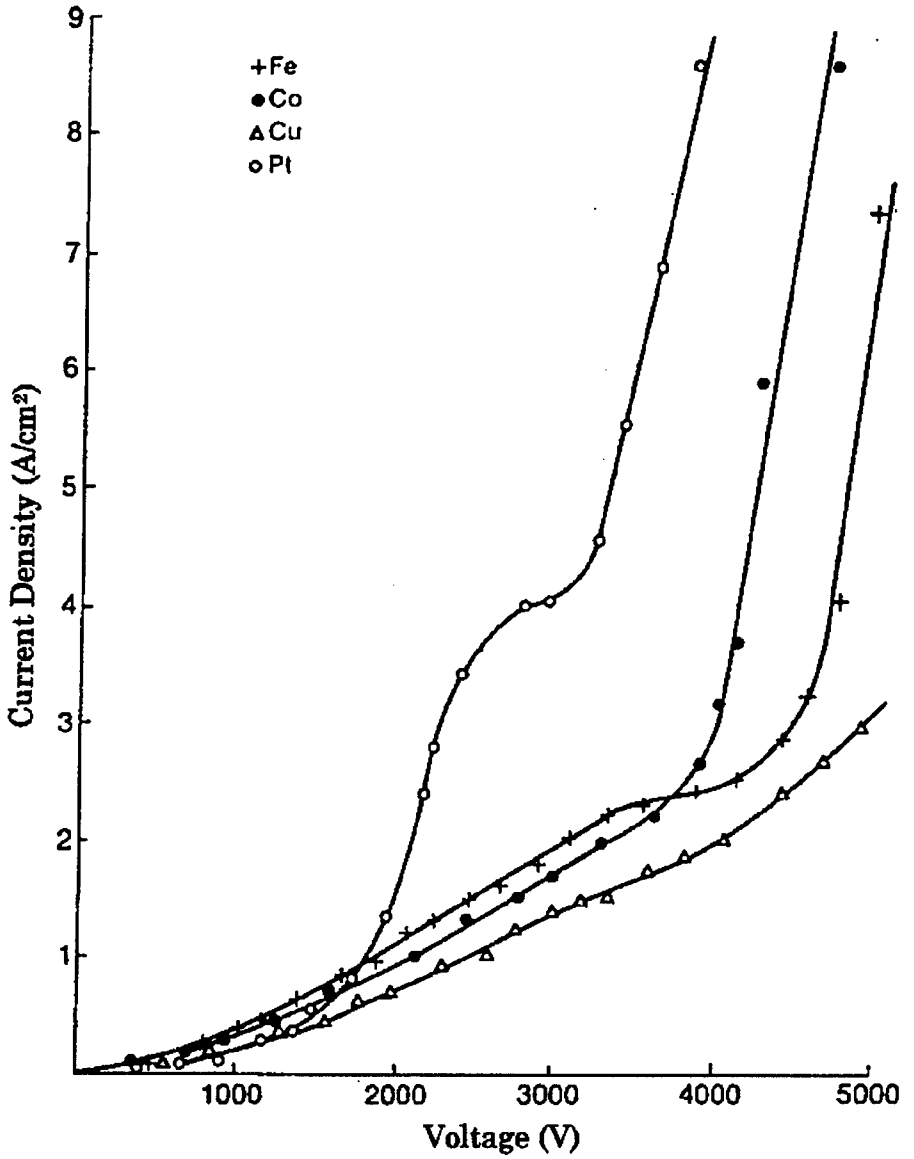


Figure 2-3. The *j-v* dependence for different cathode materials for the same spacing between the cathode and the anode [7].

results shown in Figure 2-5. Comparing Figures 2-3 and 2-5 shows that Au performs much better than Cu, and Ni was the worst.

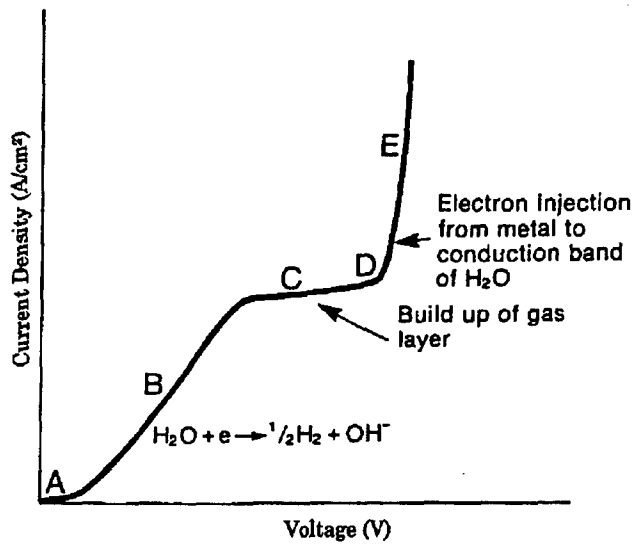


Figure 2-4. Schematic representation of the *j-v* curves obtained with different electrodes in pure water [7].

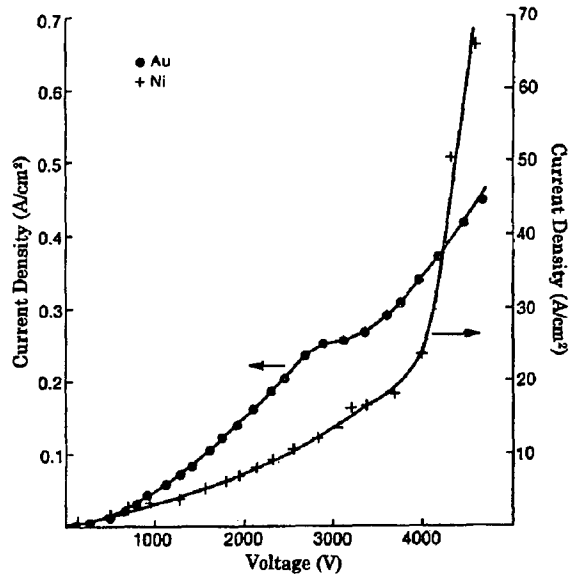


Figure 2-5. The *j-v* dependence for Au and Ni electrodes for the same spacing between the cathode and the anode [7].

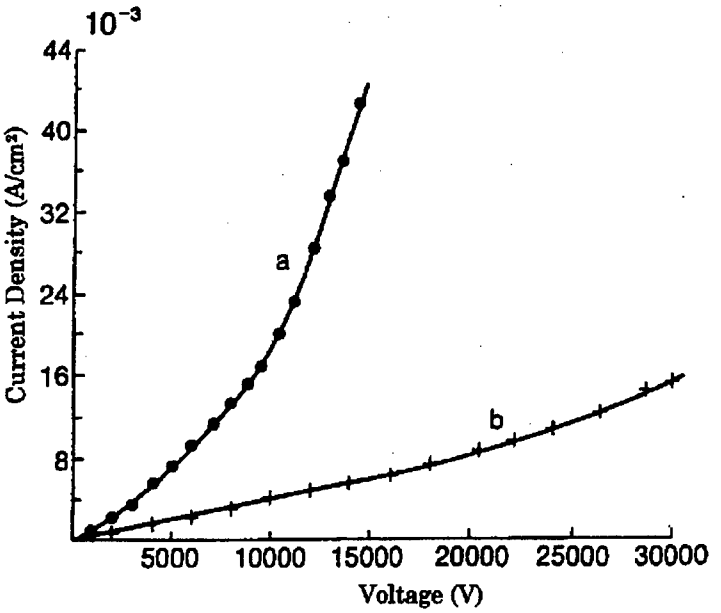


Figure 2-6. The *j-v* dependence for a platinum electrode covered with (a) 0.1 mm and (b) 0.5 mm thick film of black wax [7].

Szklarczyk et al. also looked at coatings of paraffin and black wax on the anode. Figure 2-6 shows the results of the black wax coating on the electrode. The black wax showed the best overall performance with an $E_{BD}$ of about 60 kV/cm with a 0.5 mm thick film of black wax on a platinum electrode compared with only about 8 kV/cm without. No explanation was offered as to why the $E_{BD}$'s were low compared to other field strengths seen in similar research. The electrodes consisted of a 100 μm diameter planar tip platinum anode and a 0.6 cm diameter platinum cathode. The wax was placed on the anode. The small size of the electrodes and gap may explain he low breakdown values.

Fenneman [8] looked at the performance of copper (Cu), steel (SS), brass, and aluminum (Al) electrodes. Using J. C. Martin's relationship, Fenneman measured the value of *M* from Martin's equation (see Appendix A).

$$E_{\max}\tau_{eff}^{1/3} = \frac{M}{A^{1/10}}, \qquad (2.2)$$

as a measure of the performance of the different electrodes where $E_{max}$ was the maximum electric field in MV/cm, $\tau_{eff}$ was the effective time in μs, $A$ was the electrode area in $cm^2$, and $M$ was a value usually between 0.3 and 0.6. Figure 2-7 shows the values of $M$ over a sequence of 200 shots for each of the different electrode materials. Fenneman averaged each set of 20 shots ($<M>_{20}$) for the plot in Figure 2-7. The most significant result was the poor performance of Al to withstand repeated breakdowns.

Gehman [9] examined various electrode materials and measured their action density (AD) which is a figure of merit defined as the energy density multiplied by the effective time ($\tau_{eff}$). Figure 2-8 shows the AD for Al, anodized Al, brass, and Cu. Of these four electrode types, the anodized Al had the best performance. Also shown in Figure 2-8 for the various electrode types are the threshold breakdown strengths $\left(V_B^{TH}\right)$ which were calculated by dividing the maximum voltage before the onset of breakdown by the electrode spacing. Figure 2-9 shows the AD for SS for various configurations of bead blasted and electropolished passivated electrodes. Passivation forms a contiguous layer of chromic oxide across the surface of the steel to prevent metal ions from contaminating the water. To do this, the electrodes were dipped into a solution of nitric acid and potassium dichromate which was heated to 43.3°C. If both electrodes had the same surface preparation, the data points are labeled either with "BB" or "EP" for bead blasted or electropolished passivated, respectively. For the trials run with a mix of surface treatment, the data points are labeled "EP(+), BB(–)" for an electropolished passivated anode and a bead blasted cathode, and "BB(+), EP(–)" for a bead blasted anode and an electropolished passivated cathode. The electropolished SS had the best performance. Comparing Figure 2-9 with Figure 2-8, the SS had overall better performance than the other materials.

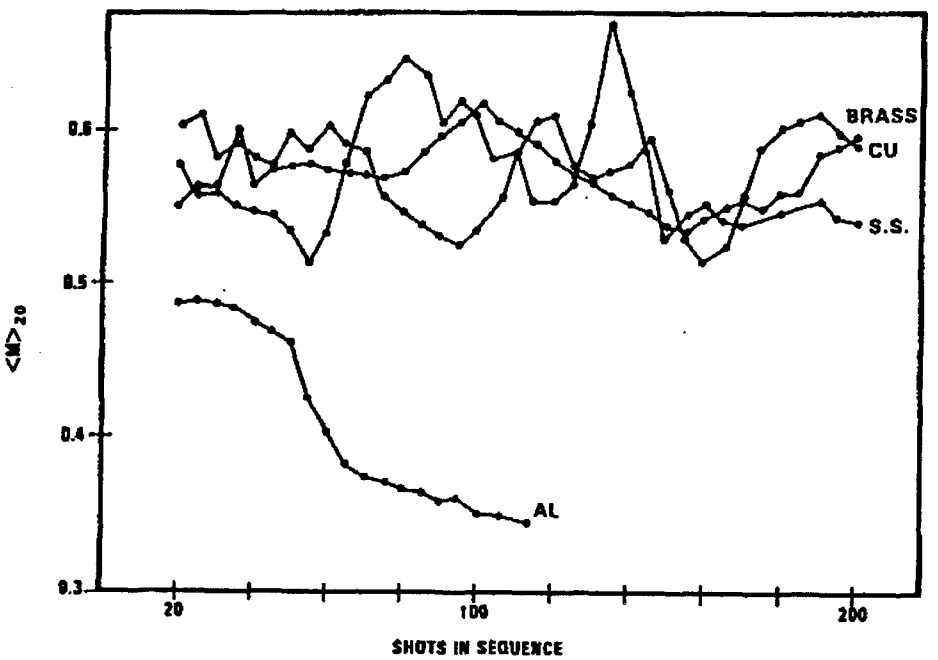


Figure 2-7. The value of $\langle M \rangle_{20}$ as a function of the shot sequence number [8]

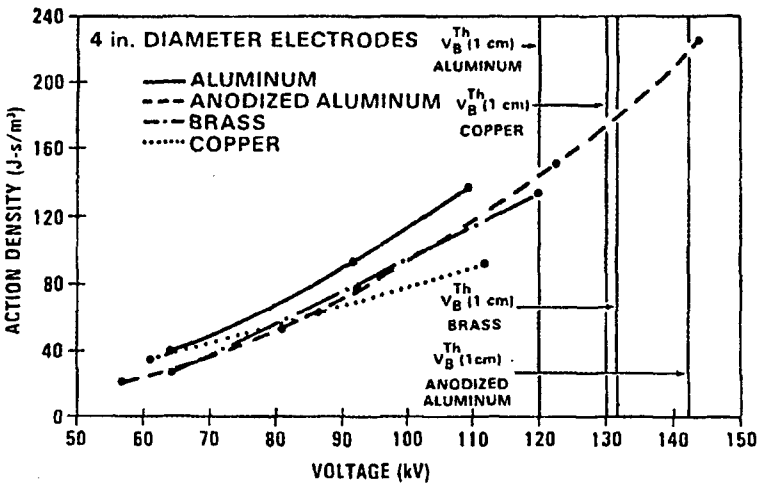


Figure 2-8. Action density as a function of applied voltage for various electrode materials. The threshold breakdown voltages (Vth) are included [9].

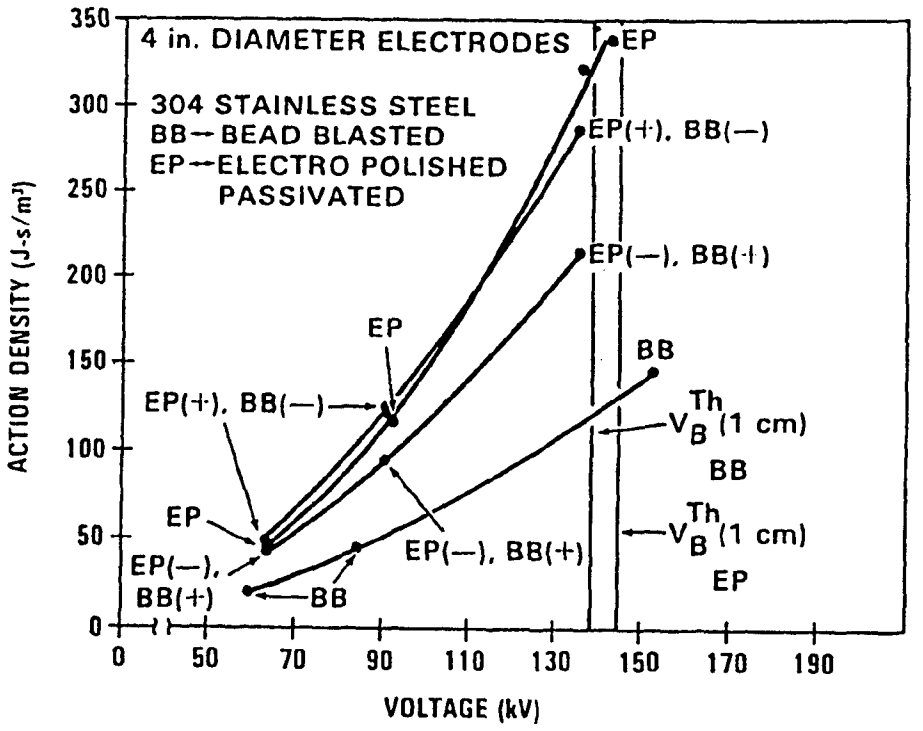


Figure 2-9. Action density as a function of applied voltage for #304 stainless steel. The threshold breakdown voltages ($V_{th}$) are included [9].

McLeod and Gehman [10] looked at several different types of SS and Al electrodes, and compared their voltage holdoff capability. There were four SS electrodes: #304, #310, #316, #430, and four Al electrodes: #7075, #5083, #2024, #6061. The best performance was achieved with #430 SS and #6061 Al which both showed an average breakdown strength of 170 kV/cm. By using mixed electrodes of #304 SS and #2024 Al, he showed that with +SS and –Al, $E_{BD}$ was 145 kV/cm; with –SS and +Al, $E_{BD}$ was 100 kV/cm; but after the electrodes stayed in the water for 23 days, $E_{BD}$ was about the same for both polarities. The authors state the reason for this is "related to the theoretical modeling of the breakdown initiation process".

Kuzhekin [11] looked at the effects that the polarity and the type of electrode had on voltage breakdown and the time to breakdown ($\tau$). He used a rod electrode 0.8 cm in diameter and a plane electrode which was SS, 25 cm in diameter. Kuzhekin demonstrated a polarity effect at 95 kV/cm using a +rod and –plane, $\tau$ was 0.5 $\mu$s; with –rod and +plane, $\tau$ was 20 $\mu$s; which increased $\tau$ by a factor of 40. This shows the importance of the polarity of the machine if the electrodes are non-symmetrical.

Buttram and O'Malley [12] showed that the water temperature affected both the resistivity and the dielectric constant of the water. By purifying the water to its intrinsic resistivity level, $\rho$ = 18 M$\Omega$-cm (room temperature), and then chilling the water to near freezing, T $\approx$ 0°C, they could get the water up to its theoretical maximum resistivity of 80 M$\Omega$-cm. Using water at its maximum resistivity, they were able to get an $\varepsilon_r$ of 90 and $\tau_{eff}$ of 640 $\mu$s.

Vorov'ev, Kapitonov, and Kruglyakov [13] used "diffusion" electrodes with cupric sulfate ($CuSO_4$) diffusing out of the upper electrode, which was the anode, and iron chloride ($FeCl_3$) diffusing out of the lower electrode. The different solutions were used to keep the diffusion layer close to the surface of the electrode by the difference in densities between the water and the two solutions. The electrodes were SS with 2 $\mu$m to 5 $\mu$m pores for introducing the solutions into the experimental chamber. They were able to show an increase in $E_{BD}$ from 0.3 MV/cm to 1.3 MV/cm by using the diffusion electrodes. This was for pulse lengths of less than 3 $\mu$s; above 3 $\mu$s, the diffusion electrodes did not perform as well.

Hasted [14] looked at much of the research done on the static dielectric constant ($\varepsilon_s$) of water and showed that there was a very complicated relationship between water temperature and $\varepsilon_s$. Figure 2-7 shows a comparison of findings by eight different researchers. These were plots of the differences between Malmberg and Maryott's [15] equation for $\varepsilon_s$ which was given by

$$\log(\varepsilon_{SMM}) = 1.94404 - \frac{1.991 \cdot 10^{-3}}{T}, \qquad (2.3)$$

and the actual data. Figure 2-10 shows that there was a lot of variation between the different sets of data.

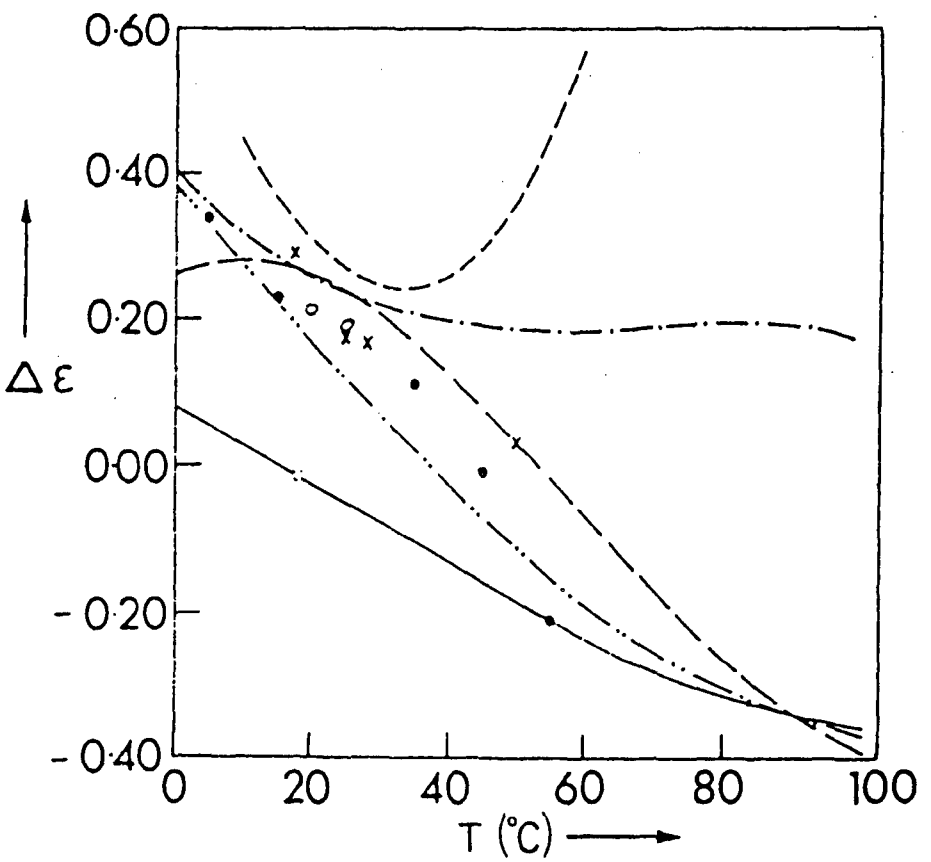


Figure 2-10. Differences between measurements of $\varepsilon_s$ as a function of temperature.

---

$\Delta\varepsilon = \varepsilon_s - \varepsilon_{SMM}$ (Malmberg and Maryott) [14]. □ mean of 17 values selected from literature by Lattey et al.;
x Albright; —·— Wyman and Ingalls;
—— Lattey et al.; ° Jones and Davies;
• Albright and Gosting; --- Drake et al.;
- - Wyman; —·— Akerlof and Oshry.

## 2.2 PREBREAKDOWN PHENOMENA.

Many theories have been proposed in an attempt to describe what is occurring in the water during the breakdown. It is important to understand the phenomena that lead to the breakdown so that ways can be devised to delay or prevent the breakdown. Probably the most extensive investigation of the prebreakdown phenomena has been conducted by the Academy of Sciences of the USSR, Scientific-Research Institute of Energetics, Novosibirsk, USSR. Their development and use of the electrooptical bridge made it possible to study the effects of a high voltage pulse on the water between the electrodes [15].

Yanshin, Ovchinnikov, and Vershinin [16] describe the primary mechanism of charge transport through the water gap as proton motion, similar to "hole" motion in semiconductors. Figure 2-11 shows how this motion occurs. The water molecule ($H_2O$) is pictured on the right as it would be oriented in an electric field in the direction shown on the top of the figure. On the left side of the figure, an $H^+$ ion is shown combining with an $H_2O$ molecule to form a hydronium ion ($H_3O^+$). According to the authors,

> when a voltage is applied across the discharge gap, electron vacancies appear on the anode with a surface charge density $\sigma = \varepsilon_o\varepsilon_r E$. The appearance of vacancies is accompanied by an adiabatic or nonadiabatic transition of electrons from nearby water molecules to these vacancies; hydronium ions form. The subsequent motion of charge carriers occurs by the mechanism described above, which converts electric-field energy into thermal energy. (pp. 1305-1306)

This thermal energy causes the water to "boil" causing bubble formation.

In a later article, Yanshin, Yanshin, and Korobeynikov [17] concluded that the bubble formation in the water was due to gas released from micropores on the electrode surface by a mechanism similar to cavitation. They used the Kerr effect in nitrobenzene to study the prebreakdown fields because of its high Kerr constants. A 50 kV to 150 kV pulse was applied to the test gap

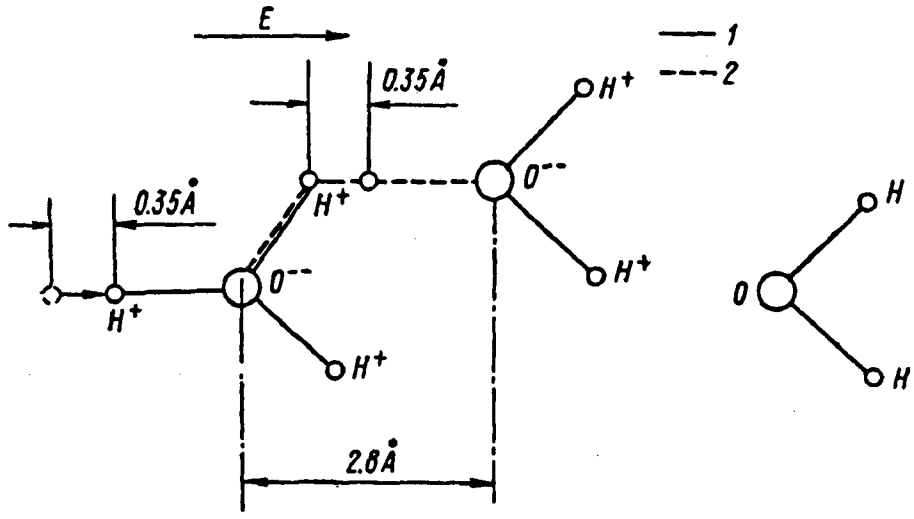


Figure 2-11. Proton mobility mechanism in water. (1) Displacement of a proton and (2) displacement of an electron [16].

that contained a 0.1 mm to 0.3 mm stainless steel electrode and a plane electrode. Field strengths in the gap were between 500 kV/cm and 1 MV/cm. They looked at the formation of space charges and bubbles in the electrode gap. Their conclusion based on the results of the experiment was that the bubbles appeared as a result of gases being released from micropores on the electrode surface due to Coulomb forces and electro-hydrodynamic (EHD) flow.

Ovchinnikov, Yanshin, and Yanshin [18] were able to show through the use of the Kerr effect and a streak camera that there was not a space charge buildup around the cathode even with fields up to 10 MV/cm. They interpret this to mean that the electron mobility in the water is very low and that the electrons are bound to the water molecules even under high electric fields. The electron velocity in water was estimated to be less than $1.5 \times 10^5$ cm/sec with a field of 10 MV/cm. This gives an electron mobility of less than

$1.5 \times 10^{-2}$ $cm^2/Vsec$. This supports the contention by Yanshin et al. [16] that it is proton motion that carries the charges across the water gap.

The development of a new technology that creates conductive layers in the liquid near the electrode was recently claimed by E. V. Yanshin at the Pulsed Power Conference [19]. This technology supposedly builds on the findings generated by the diffusion electrode experiments and provides a practical means of quadrupling the breakdown field strength. No explanation was given as to what this new technology is and how it works. Whatever the conductive layer is made of, it does not diffuse into the water and can be used in any configuration since it is not dependent on gravity to hold it in place as was needed with the diffusion electrodes.

SECTION 3

EXPERIMENTAL SETUP AND MODELS

## 3.1 SYSTEM DESCRIPTION.

### 3.1.1 Overview.

Figure 3-1 shows a simple diagram of the components that make up the pulsed power system. It consists of a Marx bank, a coaxial line, and the test chamber. The system also includes a control panel, power supply, screen room, and diagnostics. Each of these components will be described in detail in the following sections.

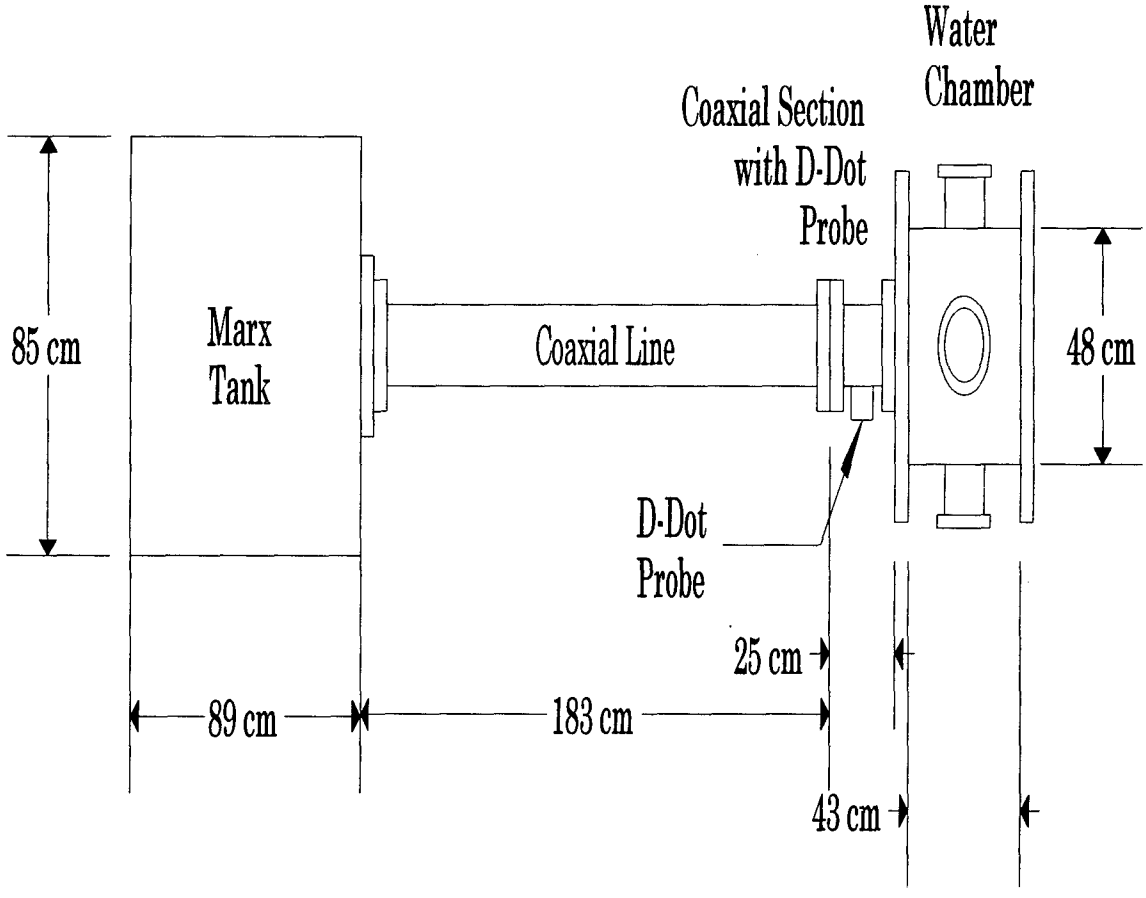


Figure 3.1. High voltage breakdown in water system diagram, side view.

### 3.1.2 Marx Bank.

The Marx bank consisted of six Maxwell Model 31334 capacitors which were rated at 0.1 μF, 100 kV, and 20 nH; these were later replaced with Model 31885 capacitors which were rated at the same capacitance but only 75 kV and 40 nH. The total capacitance of the erected Marx bank was the series capacitance of the capacitors which would simply be

$$C = \frac{0.1\ \mu\text{F}}{6} = 16.6\ \text{nF}. \tag{3.1}$$

The inductance of the bank was the series inductance of the capacitors and the inductance of the connections between the bank and the center coaxial line. The inductance of the Marx bank connections was estimated by modeling them as a rectangle of rectangular wire. Terman [20] gives the following equation for a rectangle that has sides that are $S_1$ by $S_2$ and is made up of a rectangular bar that is $b$ by $c$,

$$L = 0.02339\left[(S_1+S_2)\log\left(\frac{2S_1S_2}{b+c}\right) - S_1\log(S_1+g) - S_2\log(S_2+g)\right]$$

$$+ 0.01016\left[2g - \frac{S_1+S_2}{2} + 0.447(b+c)\right]\ \mu\text{H}, \tag{3.2}$$

where $g$ is the diagonal distance in the rectangle formed by $S_1$ and $S_2$. All distances are in inches. For $S_1$ equal to 12 inches (30.48 cm); $S_2$, 22 inches (55.88 cm); $b$, 1/16 inch (0.16 cm); and $c$, 1 inch (2.54 cm), the inductance of the Marx bank connectors is 1.185 μH. The capacitors used were rated at 20 nH each, so the total inductance would be 1.305 μH. The impedance of the Marx bank would be

$$Z = \sqrt{\frac{L}{C}} = 8.9\ \Omega. \tag{3.3}$$

This produced a very low impedance Marx bank.

The capacitors are charged to 66 kV to give an erected voltage of about 400 kV. The capacitors are linked together with Physics International Model 670

air pressure spark gaps which are rated at 100 kV at 415 kPa air pressure. The pressure in the spark gaps is set at about 345 kPa with the pressure in the last sparkgap set to 415 kPa.

The charging resistors are water resistors made from 1.9 cm diameter polyvinyl tubing with 1.9 cm copper end caps. Electrical connectors are soldered to the flat portion of the end caps. The tubing that makes up the body of the resistors is about 9 cm long and the end caps are forced into the end of the tubing. The resistors are filled with 0.008 grams/liter of $CuSO_4$ in purified water.

The switches and resistors are attached to the capacitors by copper plates, the same as those described by Coulter [21]. These had to be modified when the new capacitors were used because the capacitor cases were wider and the mounting hardware would not allow the switches to fit properly. The bank is assembled on a fiberglass frame and is made up of a row of three capacitors on the bottom of the frame and another row above them. Because of the size of the Marx tank, the Marx bank could not be assembled with six capacitors in one row. This configuration caused some erection problems and some changes had to be made to the Marx bank.

A sparkgap trigger was added to the Marx generator. This is used to trigger the first switch of the bank. This consists of a BIMBA Model 041-D air pressure cylinder connected to a Ross Engineering HV Relay Model E-DTA-30-2, 7.6 cm, high-voltage switch. Figure 3-2 shows the connections for the air lines. The electric solenoid was removed from the HV switch and the BIMBA air pressure cylinder was attached to the end of the fiberglass rod.

The switch was placed into a Lexan cylinder 46 cm long with 1.3 cm Lexan end plates. The connections to the air valve and the HV switch are made through the top end plate. The whole assembly is pressured with 140 kPa of air to prevent breakdown between the ends of the switch during

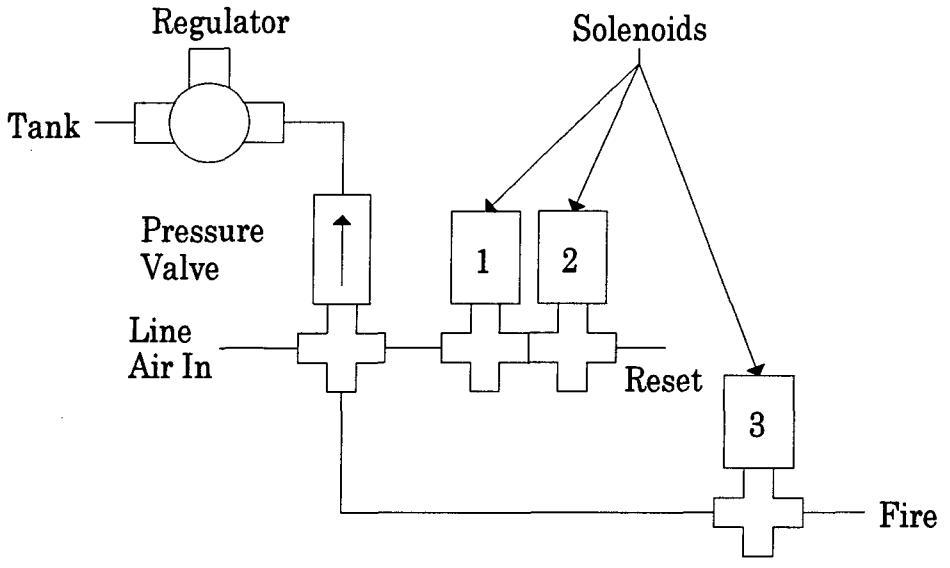


Figure 3.2. Air line diagram for trigger switch.

charging. Figure 3-3 shows the electrical connections to the HV switch. In the open position, the trigger capacitors, which are two Maxwell Model 31247, 0.02 μF, 50 kV capacitors connected in series, are charged by the main power supply. When the switch is closed, the connection between the capacitors and the trigger pin in the first sparkgap switch is closed. This provides 66 kV between the end of the trigger point and the ground electrode in the first switch. The trigger point is approximately 0.6 cm from the edge of the electrode which gives it a 110 kV/cm field between the two points which is more than enough field strength to initiate a breakdown in the sparkgap switch. There was a 50 ms time delay measured between the signal from the firing switch to the actual closing of the trigger switch, so that signal could not be used to initiate the trace on the oscilloscope.

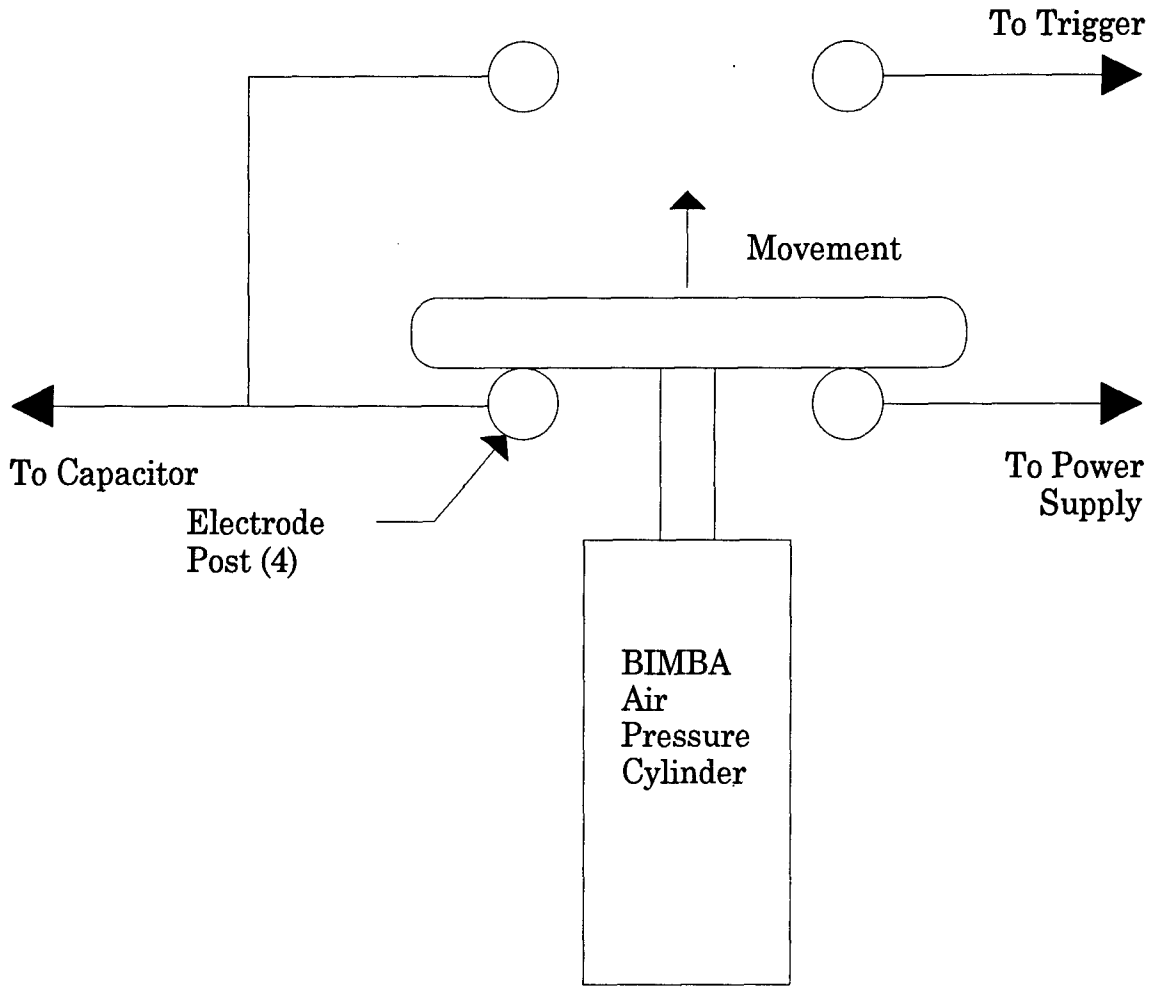


Figure 3-3. Trigger switch electrical connections.

### 3.1.3 Coaxial Line.

The coaxial line consists of an aluminum outer electrode which has an inside diameter of 16.4 cm and a stainless steel center electrode which is 2.3 cm in diameter. The distance from the Marx tank to the test chamber is 208 cm. The coaxial line is filled with transformer oil which is circulated continuously through the coaxial line and the Marx tank. A water-lock filter is used to remove any moisture that was present in the oil and also removed any contaminants, including carbonization caused by occasional arcs in the Marx tank.

The capacitance and inductance of the line is needed in order to calculate the impedance of the coaxial line. The capacitance of the coaxial line is given by the equation

$$C = \frac{2\pi\varepsilon_r\varepsilon_o l}{\ln\left(\frac{b}{a}\right)} = 130 \text{ pF}, \tag{3.4}$$

where $\varepsilon_r$ is equal to 2.2 for transformer oil, $\varepsilon_o$ is the permittivity of free space, $a$ is the radius of the inner conductor, $b$ is the inner radius of the outer conductor, and $l$ is the length of the coaxial line. The inductance is given by the equation

$$L = \frac{\mu_0 l}{2\pi} \cdot \ln\left(\frac{b}{a}\right) = 817 \text{ nH}, \tag{3.5}$$

where $\mu_o$ is the permeability of free space. Then the impedance of the coaxial line is

$$Z = \sqrt{\frac{L}{C}} = 79 \ \Omega. \tag{3.6}$$

We also needed to know the one-way transit time in the coaxial line. This can be calculated by

$$t = \frac{l\sqrt{\varepsilon_r}}{c} = 10.3 \text{ ns}, \tag{3.7}$$

where $c$ is the speed of light in free space. This gives us an estimate of the delay between the erection of the Marx bank and the voltage at the D-Dot probe located at the end of the coaxial line.

Previous work by Coulter looked at ways to increase the operating voltage of the system but these were not successful. The limiting factor on the maximum voltage of the system was the coaxial line. The maximum voltage of a coaxial line is given by the equation [23]

$$V_{max} = aE_{max} \ln\left(\frac{b}{a}\right), \tag{3.8}$$

where $a$ is the radius of the inner conductor, and $b$ is the radius of the outer conductor. For the values listed above with $E_{max}$ of 200 kV/cm (nominal value for transformer oil), then $V_{max}$ = 450 kV. In order to prevent a breakdown in the coaxial line, the Marx bank was charged to 66 kV in order to have an erected voltage of about 400 kV.

### 3.1.4 Experimental Chamber.

The test chamber is a cylinder with a 48 cm inside diameter and 43 cm in length. The end plates were made from 5 cm thick Lexan. There are six ports evenly spaced around the chamber. The tank is filled with deionized water which is continuously circulated through two deionizing bottles at about 3.8 *l*/min. This provides water with a resistivity of over 10 MΩ-cm measured with a Myron L Series 570 Resistivity Meter. The circulation clears away any contaminants from the test chamber. The water was initially filtered through two U. S. Filter, poly string wound, 5 μm cartridge filters and put into a storage tank before pumping it through the deionizer bottles and into the test chamber. This method removes only particulate matter from the water, not organic contaminants such as solvents. Air bubbles are removed from the water by the difference in pressure between the experi-

mental chamber and the storage tank due to the weight of the water; this is not the same as deaeration.

As with the coaxial line, the impedance of the experimental chamber is calculated by treating the chamber as a coaxial line. The capacitance is given by the equation

$$C = \frac{2\pi\varepsilon_r\varepsilon_o l}{\ln\left(\frac{b}{a}\right)} = 630 \text{ pF}, \tag{3.9}$$

where $\varepsilon_r$ is equal to 80 for the water, $\varepsilon_o$ is the permittivity of free space, $a$ is the radius of the inner conductor, $b$ is the radius of the outer conductor, and $l$ is the length of the water chamber. The inductance is given by the equation

$$L = \frac{\mu_o l}{2\pi} \cdot \ln\left(\frac{b}{a}\right) = 261 \text{ nH}, \tag{3.10}$$

where $\mu_o$ is the permeability of free space. Then the impedance of the coaxial line is

$$Z = \sqrt{\frac{L}{C}} = 20 \ \Omega. \tag{3.11}$$

The one-way transit time to the center of the water gap ($l$/2) is calculated to be

$$t = \frac{l\sqrt{\varepsilon_r}}{c} = 6.4 \text{ ns}, \tag{3.12}$$

where $c$ is the speed of light in free space. This is also the transit time from the gap to the load resistor since the gap is centered in the chamber.

The electrodes in the experimental chamber consist of two copper-tungsten rods 2.3 cm in diameter with a 7.6 cm radius of curvature on the electrode surface. The edge of the electrode surface is rounded to reduce field enhancements. For most of the data collected, the gap was set at 1.27 cm. The average breakdown strength of water is typically given to be 150 kV/cm, so, with a 1.27 cm spacing, the gap should break down at approximately 120 kV.

With the Marx bank delivering a 400 kV pulse, there should be sufficient over-voltage to ensure gap breakdown regardless of the treatment given to the water.

### 3.1.5 Load Resistor.

The load resistor was built by Coulter [21] and provided both matching and damping of the voltage at the end of the experimental chamber. It consists of two 160 Ω water resistors, in parallel, 14 cm in diameter and 36 cm in length, connected together at the inner conductor extending from the end of the experimental chamber and connected to two of the return paths around the experimental chamber.

### 3.1.6 D-Dot Probe.

The use of a D-Dot probe for the Water Breakdown System was recommended by both Mr. Van Kenyon [24] from the Naval Surface Warfare Center and Mr. Richard Miller [25] from Maxwell Laboratories. The design resulted from a paper provided by Mr. Miller which is referenced in the probe model section later in the chapter.

There were several attempts made to calibrate the probe without any success. The initial attempt used a Mercury Relay Pulse Generator Model L4 line pulser with a 1.6 kV, 200 ns, pulse. This was not sufficient voltage to measure an integrated signal at the oscilloscope because of the voltage drop across the probe and across the integrator. By using a high voltage power supply and a mechanical switch, it was determined that in order to calibrate the probe, a 10 kV pulse was needed. The equipment needed to generate a test signal with a fast rise time and with a short pulse duration, and the equipment needed to make a direct measurement was not available. To get around this, the experiments were designed to look at changes in the voltage pulse

rather than being concerned about the actual value of the voltage seen across the gap.

### 3.1.7 Cable.

The probe is connected to the screen room with LDF 2-50 semi-rigid coaxial cable, commonly referred to as "foam" cable. Initial measurements made with the Tektronix 7104 oscilloscope were plagued by noise. This resulted in a lot of back-writing on the oscilloscope trace which was due to changes in the oscilloscope's ground level. Considerable time was spent trying to eliminate ground loops between the experiment and the screen room. At one point, the main power to the screen room was disconnected and a 12 V battery and a power inverter was used to run the oscilloscope.

To completely eliminate the noise problem, the coaxial cable had to be covered with three layers of Olympic tinned copper flat braid, 2.54 cm wide (Allied #876-4169), along with 7.3 meters of 3.8 cm outside diameter solid conduit added from the probe towards the screen room. The solid conduit accounted for about 80% of the total cable length between the experiment and the screen room. In order to ensure there was no noise on the coaxial line when the machine was fired, the line was terminated at the probe end with a 50 Ω terminator and the outer shield was connected to the outer shell of the probe with aluminum tape. The machine was fired with the oscilloscope at its lowest input amplifier level (5 mV/div). The copper braid and the solid conduit was added to the coaxial cable until the machine could be fired without triggering the oscilloscope. The line was then connected to the probe, and the tinned copper braid and the solid conduit were connected to the outer shell of the probe with several layers of aluminum tape. This was also done to the connection at the screen room wall. Through trial and error, it was determined that the cable from the oscilloscope to the connection on the inside

of the screen room needed to be as short as possible. This completely eliminated the noise seen on the oscilloscope trace.

### 3.1.8 Power Supply.

The power supply for the Marx bank consists of a Beta Electric Corp. Model MP-120-50R, 120 kV, DC Power Supply connected to a Universal Voltronics Corporation High Voltage D. C. Power Supply transformer rated at 160 kV, 5.5 mA. This is set so that the Marx bank is charged with a 2.5 mA constant current up to 66 kV. The transformer is attached to the Marx bank with an RG-19 coaxial cable with the outer braid cut back about 30 cm from both ends and allowed to "float" electrically. The ground between the power supply and the Marx bank is through a single point (MECCA) ground connection.

### 3.1.9 Control Panel.

The control panel for the system was assembled by Coulter [21]. It provides control for the air pressure in the sparkgap switches, dump switch, warning buzzer and light, and circulation pumps for both the oil and water. Control for the air pressure switch for triggering the Marx bank was added later. Figure 3-4 shows the electrical connections for the trigger switch. The electrical control of the trigger switch consists of a main power switch, a keyed HV switch to prevent firing the machine if the key is removed, and a double-throw switch for firing and resetting the trigger switch.

### 3.1.10 Diagnostics.

Initially, diagnostics for the Water Breakdown System consisted of two Tektronix 7104 oscilloscopes using either a 7A29 plug-in (50 Ω input, 1 GHz BW) or a 7A16A plug-in (1 MΩ, 200 MHz BW) vertical amplifier, and a 7B15 or 7B10 horizontal time base. The 7A16A was used with the analog integra-

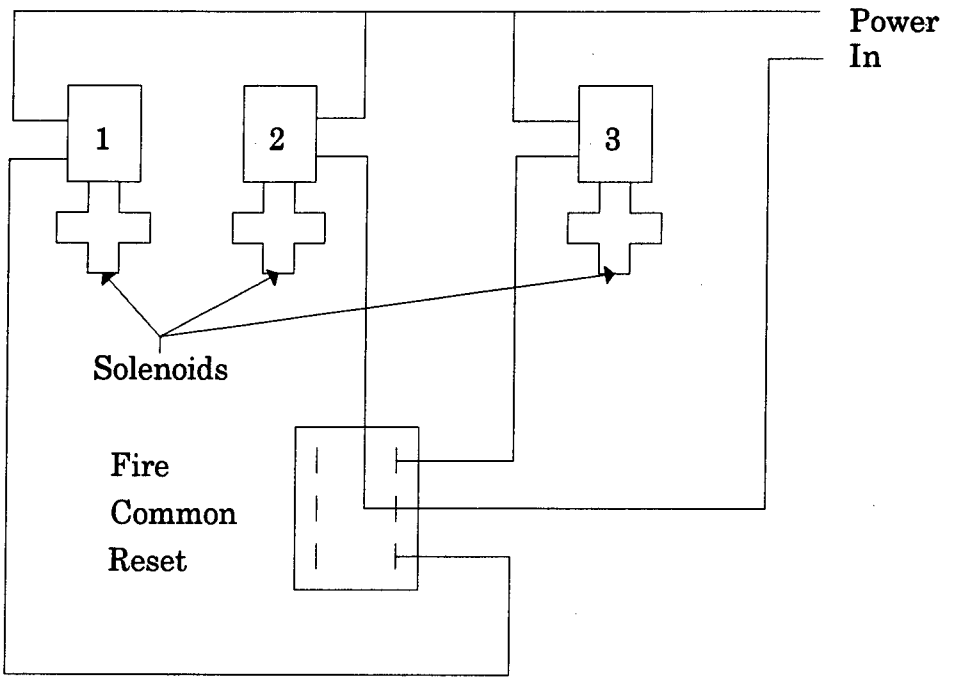


Figure 3-4. Electrical wiring diagram for the trigger switch.

tor. Initially, a Polaroid C-53 camera was used to capture the waveforms on Polaroid 667 film. This was later replaced with a Tektronix C1002R digital camera which was connected to a Tektronix DX01 video board installed in a COMPAQ 386/20 computer. Images from the digital camera were converted into waveforms with the Tektronix DCS01GPH version 3.05 software and stored on the COMPAQ computer.

All of the signals were saved in the raw video format. These were then loaded into the DCS01GPH program and saved as a binary waveform file, and then printed out. For data analysis, the waveform file had to be converted to ASCII file format. To do this, the file was loaded into DCS01GPH and saved as an ASCII file through the Save File function. Several files could be saved this way at one time, usually a complete set of signals were

saved as a group with a unique filename prefix -- first four characters of the filename. The software then saved the group of files adding the corresponding letter of the alphabet of the waveform to the fifth character of the filename and the video port number as the last three characters. This gave us an eight character filename.

We would then exit the software to DOS. Using the rename command (ren), the video port number could be stripped off of the filename. For example, entering the following at the DOS prompt

"ren file?258.asc file?.asc"

would get rid of the video port number. In order to import the file into MATLAB for analysis, the text header had to be stripped from each of the files. This would take out all the text that DCS01GPH put at the beginning of the file and then check to see if there were 512 data points in the file. For some reason, some of the ASCII files would have an extra character added at the end of the file which would look like an extra data point to the MATLAB program. To do more than one file, the following DOS command

"for %a in (*.asc) do stripasc %a"

would run the STRIPASC.COM program for each file.

One problem encountered with the Tektronix DX01 video board and the DCS01GPH software was the inability of the program to follow fast changing signals. The waveform that was generated tended to have the signal peaks rounded off. This caused us to lose the high frequency components of the waveforms. This was particularly prevalent when the D-Dot signal was measured without an integrator. Adjusting the intensity of the trace and the threshold level did not improve the waveform generated by the software. It seemed to be an inherent problem with the program.

The Tektronix 7104s have been replaced by Tektronix SCD-5000 digitizers. These are on loan from the Defense Nuclear Agency (now DSWA). These provide 4.5 GHz bandwidth input with 1024 points over the signal's time-

width. The high bandwidth made it possible to measure the D-Dot signal directly and integrate it digitally. The high frequency components of the signal are preserved. The digitizers were controlled through the computer with the Data Acquisition, Archival, Analysis, and Instrument Control ($DA^3C$) System software provided by DNA which was prepared by Voss Scientific, Inc.

## 3.2 MODELS.

### 3.2.1 System Model.

Figure 3-5 shows the PSPICE model used for the Water Breakdown system. The Marx bank was modeled as a single 16.6 nF capacitor ($C_1$) with an initial charge of 400 kV and a 1.305 μH ($L_1$) inductor between the Marx bank and the rest of the circuit. This inductance was the rated inductance of the capacitors specified by the manufacturer (120 nH) plus the estimated inductance of the Marx bank connections (1.185 μH). The coaxial line was modeled as a lumped parameter transmission line with a total inductance of 817 nH and a capacitance of 130 pF ($L_2 = L_3 = 408.5$ nH, $C_2 = 130$ pF). These values were the calculated values using Eqs. (10) and (11). The water chamber was modeled as two transmission lines, one before the gap and one after

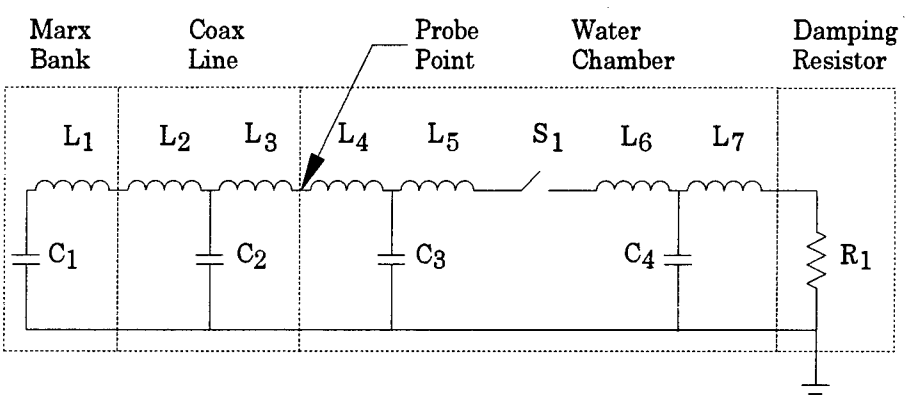


Figure 3-5. System model for simulation.

the gap ($L_4 = L_5 = L_6 = L_7 = 65.25$ nH, $C_3 = C_4 = 315$ pF). The water gap was modeled as a voltage controlled switch ($S_1$) with the controlling voltage the voltage seen across the switch. The damping resistor ($R_1$) was modeled as a simple 80 Ω resistor.

Figure 3-6 shows the output measured at the point where the D-Dot probe would be located. The waveform was similar to the actual waveform seen with the D-Dot probe.

To get an idea of what the rise time of the system would be, the ringing frequency was needed. This was done by modeling the system as a CLC circuit. The first capacitor was the total capacitance of the erected Marx bank which was calculated to be 16.7 nF. The second capacitor was the calculated capacitance of the coaxial line which was calculated to be 130 pF. The inductor is the sum of the bank inductance and the coaxial inductance. The bank inductance was 1.305 μH and the coaxial inductance was calculated to be 817

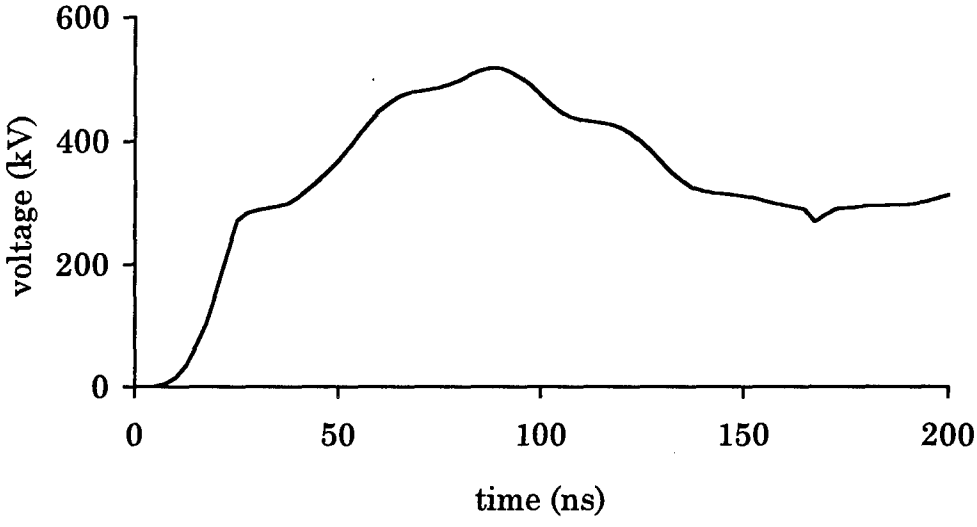


Figure 3-6. Output of system model at the probe point.

nH for a total of 2.122 μH. Solving the CLC circuit for the voltage across the second capacitor gives the equation

$$V_{C2} = \frac{V_o}{\omega L}(1 - \cos\omega t), \tag{3.13}$$

with

$$\omega = \sqrt{\frac{1}{L}\left(\frac{1}{C_1} + \frac{1}{C_2}\right)}. \tag{3.14}$$

Dividing Eq. (20) on both sides by $2\pi$ gives us the ringing frequency equation

$$f = \frac{1}{2\pi}\sqrt{\frac{1}{L}\left(\frac{1}{C_1} + \frac{1}{C_2}\right)}. \tag{3.15}$$

For the values listed above, the ringing frequency is 9.6 MHz. If a sinusoidal shaped pulse is assumed, the risetime ($t_r$) for a sinusoid can be calculated by

$$t_r = \frac{1}{2\pi f}\left[\sin^{-1}(.9) - \sin^{-1}(.1)\right], \tag{3.16}$$

which simplifies to

$$t_r = \frac{0.16227}{f}. \tag{3.17}$$

For a frequency of 9.6 MHz, $t_r$ would be 16.9 ns. This gave us an idea of the signal that the system would be capable of producing. To compare this to an actual system, a sine wave was produced and then overlaid on an actual signal from the Water Breakdown System. Figure 3-7 shows how the initial portion of the actual signal (solid line) and a 5 MHz sine wave have the same rise time. After the initial rise in voltage, the capacitances and inductances in the rest of the system begin to affect the waveform. A 5 MHz sine wave has a risetime of about 33 ns. This is a factor of about two greater than what the CLC model gives for the risetime. This would require a factor of about four increase in the combination of the inductance and capacitance of the Mark bank and the coaxial line. The total inductance of the Marx bank would be expected to be more than the rated inductance of just the individual

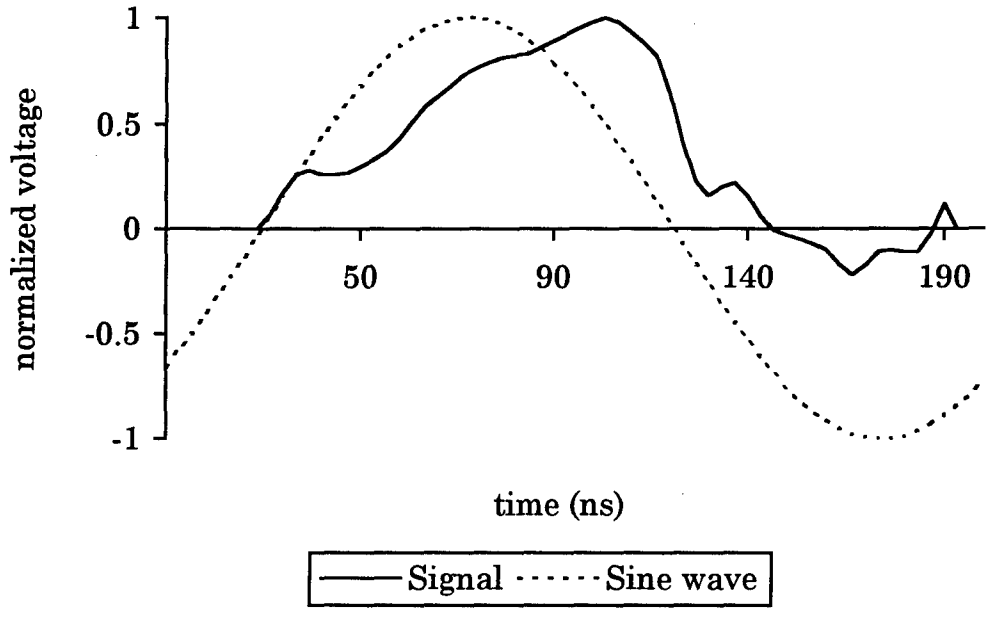


Figure 3-7. Comparison of an actual signal with a 5 MHz sine wave.

capacitors and the loop inductance approximation calculated earlier due to the inductance of the Marx bank connections and the inductances of the individual spark gap switches.

3.2.2 Probe Model.

The model used for the D-Dot probe was described by Wilkinson [26]. Figure 3-8 shows a graphic representation of the probe as it would look connected to the system. The probe was modeled as a capacitive divider with the two capacitances, $C_1$ and $C_2$, connected to an RC integrator as shown in Figure 3-8. The first capacitor was the capacitance between the face of the center section of the probe and the inner conductor of the coaxial line. This value was estimated by assuming a flat plate capacitor with the surface area equal to the cross sectional area of the probe's center section. The second capacitor of the

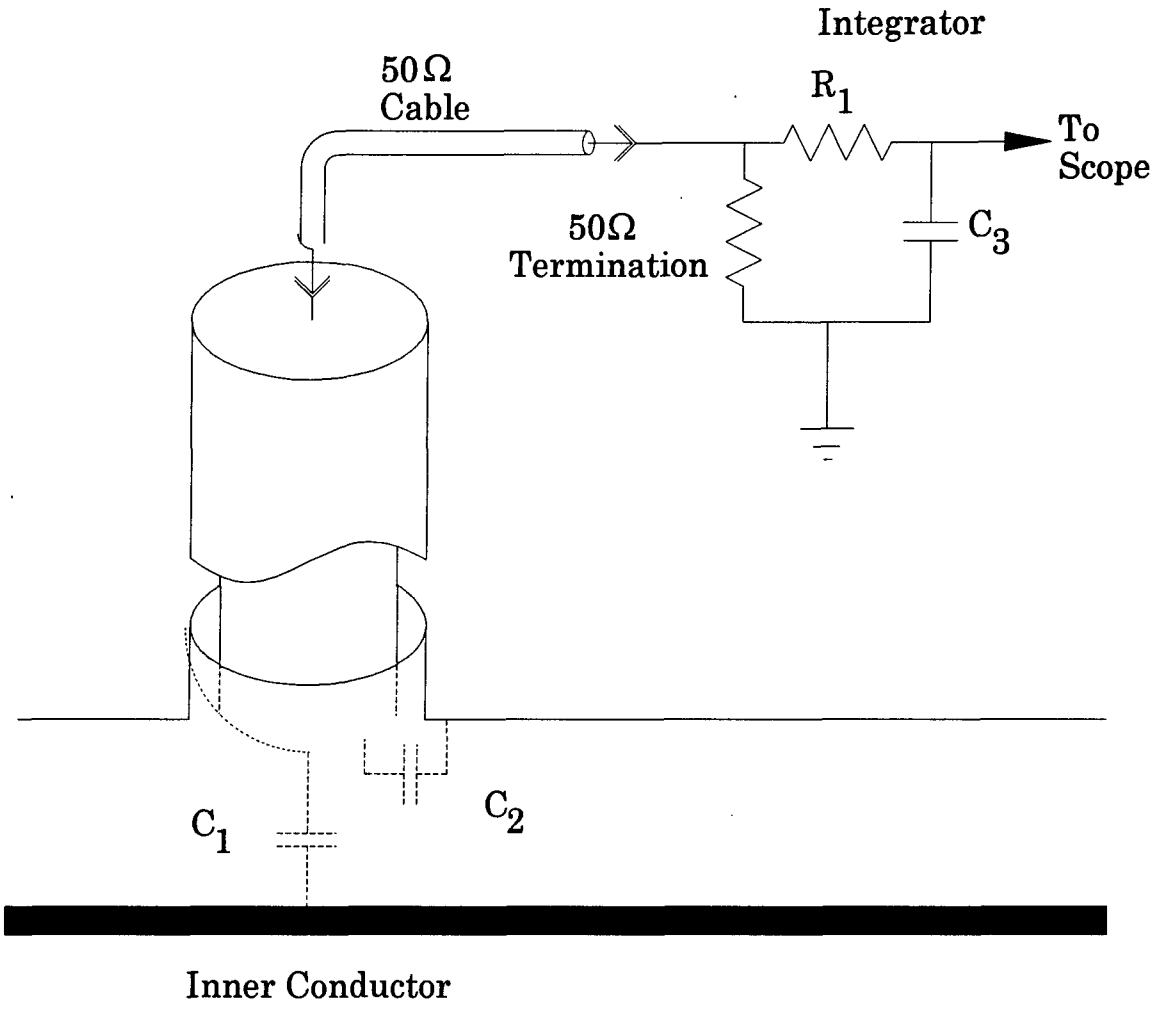


Figure 3-8. Diagram of the D-Dot probe.

capacitive divider was the capacitance between the side of the probe's center section and the outer shell of the probe body. This value was estimated by assuming a coaxial capacitor.

The probe was connected to a 50 Ω cable and terminated into a 50 Ω resistor either at the oscilloscope or the integrator. The integrator was modeled as a simple RC circuit. In practice, simple resistors and capacitors could not be used because of the high frequency components of the signal from the probe.

The signal had to be integrated digitally or through the use of a special high-bandwidth integrator.

Figure 3-9 shows the circuit model used for the derivation and simulation of the probe. For simulation, the following values were used: $C_1$ = 0.65 pF, $C_2$ = 32.5 pF, $C_3$ = 1.66 nF, R = 50 Ω, and $R_1$ = 1.21 kΩ. Figure 3-10 shows the output of the probe model using PSPICE. Actual measurement of $C_2$ was done with the Tektronix Type 130 LC meter and was found to be 67 pF. This was over twice what was expected and was due to not including the capacitance at the connector end of the probe. The PSPICE simulation was run again to see what effect the increase in $C_2$ would have on the output of the probe. Figure 3-11 shows the output of the probe with $C_2$ equal to 32.5 pF (calculated value), solid line, and then equal to 67 pF (measured), dotted line, to the same 400 kV square input (solid line) in Figure 3-10. As can be seen, there was little effect on the output signal.

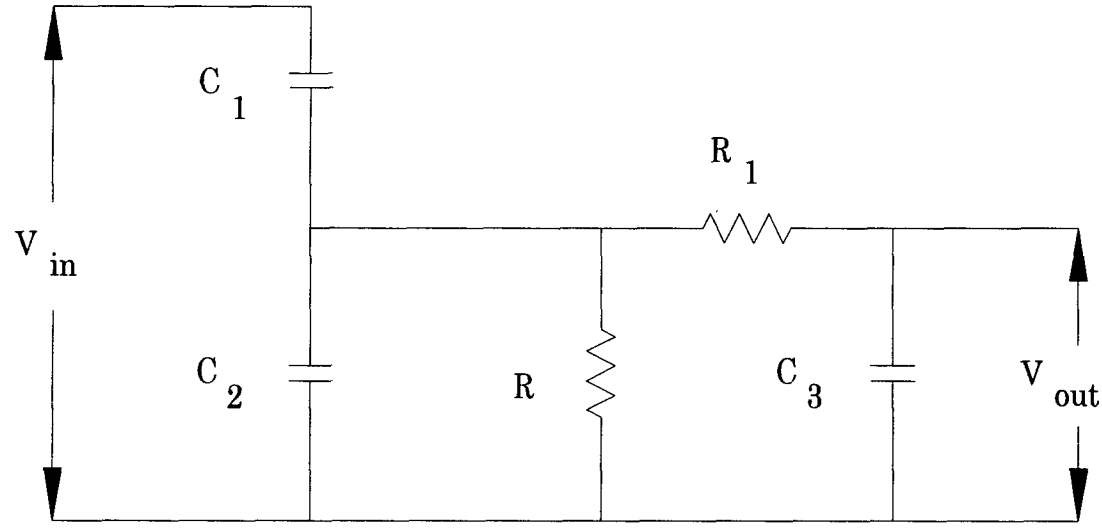


Figure 3.9. Circuit model used for the D-Dot probe.

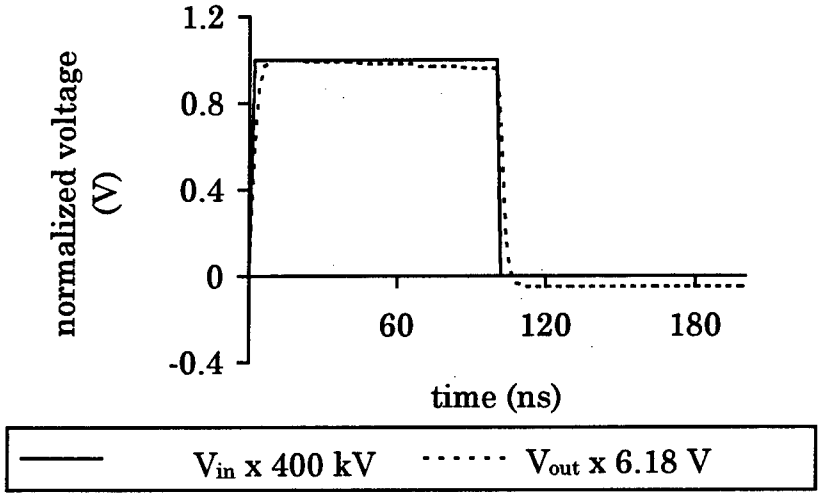


Figure 3-10..Normalized input and output voltages for the D-Dot probe simulation.

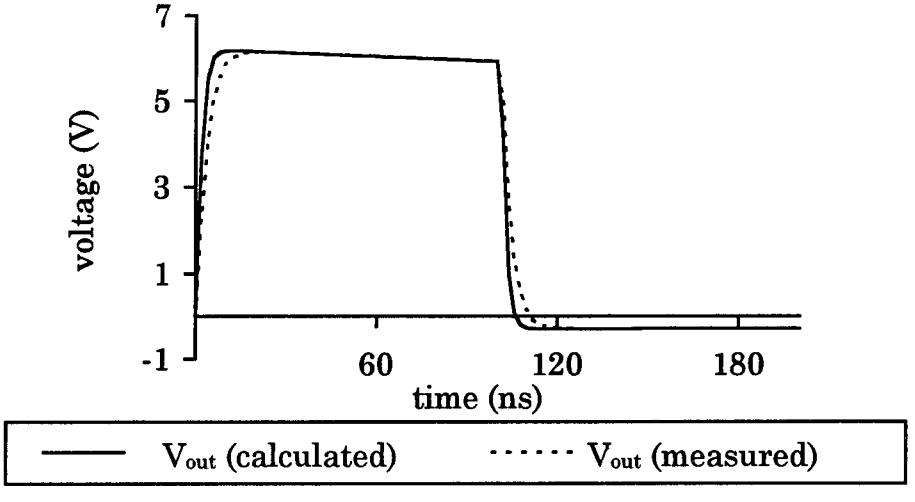


Figure 3-11. Comparison of D-Dot probe with calculated versus measured $C_2$.

# SECTION 4
# EXPERIMENT DESIGN AND DATA

## 4.1 EXPERIMENT DESIGN.

### 4.1.1 Magnetic Fields.

Several experiments were planned using magnets in the electrodes to look at possible effects of magnetic fields on the breakdown process. The magnets used were Cookson neodymium iron boron (NdFeB) disc magnets, 35NERR32, which were 1.27 cm in diameter and 4.7 cm in length. The field strength of the magnets was measured with a F. W. Bell Model 4048 Gauss Meter with a T-4048-001 Cal 1735 Transverse Probe. On the end of the magnet along the center line and near the surface, the magnetic field measured 0.2 T. When one of the magnets was placed in the Copper-Tungsten (CuW) electrode, the field measured at the surface of the electrode was about 15 mT.

The first experiment looked at using a single magnet in either the anode or the cathode. The polarity of the magnetic field was also investigated in this experimental series. The second experiment investigated the use of magnets in both the anode and cathode, and with the fields opposing or aligning.

The first series of trials investigated the magnet in the cathode. The procedure was to run five baseline shots, five shots with the magnetic North Pole pointing into the gap, and five shots with the magnetic South Pole pointing into the gap. The procedure was repeated for a total of thirty shots.

Normally, when using statistics, the experiment is designed so that the data are collected in random order. However, because of the nature of pulsed power research and the difficulty in completely randomizing the shots, the shots were planned to help eliminate possible series effects. Many shots were fired on the system before the experiments were started to ensure that the system was reliable and series of shots were fired periodically between ex-

periments to guarantee that any effects seen in the experimental trials were due to the experimental process and not a change in the pulsed power system. Analysis of Variances (ANOVA's) were calculated to find statistically significant effects. This procedure is described in Bruning and Kintz [27] and was programmed to run in MATLAB. The results of the ANOVA's were then looked up in an F distribution table and a result was considered significant if its probability level ($\alpha$) value was less than 0.050. At $\alpha < 0.050$, there is more than a 95% certainty that something statistically significant has occurred in the data. If the ANOVA was found to be significant, a *t*-test for a difference between two independent means was run between each of the three groups: Baseline versus North Pole, Baseline versus South Pole, and North Pole versus South Pole. The results of the *t*-test were looked up in the *t* statistic table and again, a result was considered significant if $\alpha < 0.050$. Several parameters were analyzed for each of the data groups. The maximum voltage ($V_{max}$), the effective time ($\tau_{eff}$) which is defined as the time that the voltage is above 63% of $V_{max}$, the fall-time, and the fall-rate, which is the change of voltage divided by the fall-time, were investigated. ANOVA's and, if significant, *t*-tests were calculated for each of these parameters.

The next series of thirty shots were run in the same fashion except with the magnet in the anode. The polarity of the charging system was reversed so that the anode was on the electrode that extended from the end of the experimental chamber. This made the data collection much easier because the experimental chamber did not have to be opened between data series to insert the magnet into the electrode. Changing the polarity seemed to have an adverse effect on the capacitors in the Marx Bank and caused several to self-destruct when the bank was fired. For this reason, a complete ANOVA was not run on the combined data with the magnet in the cathode and the magnet in the anode.

An ANOVA was calculated for the thirty shots and *t*-tests were run on the three data groups for the same parameters listed above: Baseline versus North Pole, Baseline versus South Pole, and North Pole versus South Pole. The last series of magnet tests looked at the effects of using a magnet in each of the electrodes. For this series, five baseline shots were fired then a magnet was placed in each electrode. Initially, the North Pole of each magnet was pointing towards the gap; this was labeled Opposing Fields. Five shots were fired in this configuration then the magnet in the anode was reversed so that the South Pole was pointing towards the gap; this was labeled Aligning Fields. The sequence was repeated for a total of ten shots in each data set: Baseline, Opposing Fields, and Aligning Fields.

### 4.1.2 Sulfur Hexafluoride.

$SF_6$ is used in many pulsed power applications because of its electonegativity. This is used a lot in spark gap switches to increase the voltage holdoff of the switch. For this reason, the effect of adding $SF_6$ to the water was looked at. Ten shots were fired for a baseline, then the gas was added at the suction side of the water pump. The pressure on the gas line was increased until $SF_6$ bubbles were seen coming out of the drain line at the bottom of the experimental chamber. This was allowed to go on until there was about 2 cm of water displaced at the top of the experimental chamber. The gas pressure was then reduced until the water started circulating through the chamber again. Ten shots were planned but the loss of several Marx Bank capacitors made it possible to collect only four shots.

Two more series of experiments were run using $SF_6$. The second series was run the same as the first series. It consisted of ten baseline shots and ten $SF_6$ shots. The same *t*-tests were calculated for the second series of shots as were done on the first series. For the third experiment, the gas connection was moved to the top of the experimental chamber. The chamber was ini-

tially filled with water for the baseline shots, then the gas was added until it forced about 5 cm of water from the top of the chamber. The water was allowed to circulate through the gas layer to help draw gas bubbles into the water in the chamber. The deionizer bottles were bypassed so that the $SF_6$ would not be absorbed into the resin in the bottles. The water circulated for two hours and a series of ten shots were run. The system was left circulating for over 24 hours then the final ten shots were fired.

4.1.3 Hydrochloric Acid.

Hydrochloric acid (HCl) was used by Ovchinnikov and Yanshin [15] to decrease the conductivity of the water in their prebreakdown research. Since they were doing prebreakdown research, they did not measure the breakdown voltages. It was decided to see if there would be any effect on $V_{max}$, $\tau_{eff}$, fall-time, and fall-rate if HCl was added to the water. Several shots were measured using different concentrations of HCl. Concentrations of $2.0 \times 10^{-4}$ molar (M) and $10.0 \times 10^{-4}$ M were looked at. The HCl was added to the water and allowed to circulate only in the experimental chamber for an hour. Several shots were fired, then the water was drained from the experimental chamber. The water lines and chamber were flushed with water to ensure there was no contamination of the deionizer bottles.

A second experiment was run using five different concentrations of HCl: $0.1 \times 10^{-4}$ M, $0.5 \times 10^{-4}$ M, $1.0 \times 10^{-4}$ M, $5.0 \times 10^{-4}$ M, and $10.0 \times 10^{-4}$ M. Three shots were fired at each of the five concentration levels plus three baseline shots.

4.1.4 Polymer Coatings.

Two different polymer coatings were tried to see if they would have any effect on the voltage holdoff in the water gap. A thin layer of either poly(ethersulfone) (PES) or polycarbonate (PC) was air brushed onto stain-

less steel electrodes and then allowed to cure for at least 24 hours. A series of 15 shots with stainless steel electrodes was used for a baseline for comparison to the shots with the polymer coating. There were four sets of electrodes with each one of the two polymers so that the following combinations could be tried: PES on both electrodes, PC on both electrodes, PES on the anode and PC on the cathode, and PC on the anode and PES on the cathode.

4.1.5 Black Wax.

Stainless steel electrodes were coated with an about 1.25 mm thick coating of Apiezon-W black wax. The coating was allowed to harden for at least 24 hours before being used. Ten sets of electrodes were prepared and used for this experiment. The experimental chamber was drained after each shot.

4.1.6 Anodized Aluminum.

The last experiment consisted of two sets of aluminum electrodes made from #6061 aluminum and anodized in order to harden the surface of the electrodes. They were anodized by placing in a tank with a 20% concentration of sulfuric acid and the voltage was adjusted so that 20 amps went through the electrodes for 25 minutes. This experiment was planned to see if the results here would be similar to Gehman et al. [9]. Eight baseline shots were used for comparison to two shots with the anodized surfaces. The same four parameters measured in the previous experiments ($\tau_{eff}$, $V_{max}$, fall-time, and fall-rate) were used here.

At this point it was necessary for the graduate student (Major David Lojewski, USAF) to stop the experiments and write a dissertation. Two more experiments were undertaker by a technician and research associate. These two experiments were suggested by Prof. Harry Parker of the Texas Tech Chemical Engineering Department.

One of the pieces of information gleaned from the Russian experiments was that if an arc did occur, the system would "heal" in six hours. This suggested that the key is to grow some coating on the electrodes which would regrow over an area damaged by an arc. Therefore, two water soluble surfactants were chosen because it is known that these will grow polarized coatings on the electrode surfaces.

4.1.7 Surfactant Coatings.

The first surfactant tried was dodecylamine ($C_{12}H_{27}N$). This chemical is a base and must be dissolved in an acid solution. Enough dodecylamine (23 g) to saturate the water in the chamber was added to the reservoir and hydrochloric acid was added to bring the ph to 3.2. A series of five shots produced results not significantly different from the bench mark results with deionized water.

For the next set of tests a three volt bias was applied between the electrodes with the cathode negative. This bias would accelerate the growth of the surfactant molecules on the electrode surfaces. Three volts was chosen because no measurable current flowed at this voltage and therefore no electrolysis occurred. Electrolysis is undesirable because it produces gas in the water and could damage the electrodes or the surfactant molecules. After 3 hours, four test shots were recorded. No significant difference from benchmark voltage or breakdown time was observed.

New electrodes and a new fill of deionized water were used for tests with the dodecylamine without hydrochloric acid. The ph with 13 g of dodecylamine added to the water was 9.2. The surfactant may not have dissolved since small particles could be seen in the water as it circulated. A series of eight shots showed no difference from benchmark results. However, one of the damping resistors was destroyed and tests with dodecylamine were terminated.

The damping resistors were repaired and new electrodes and deionized water were used for benchmark tests at a ph of 7. Four shots gave results which agreed with previous benchmark tests. In preparation for the tests with the second surfactant, Lauric acid, the water was treated with 0.05 g of sodium hydroxide (NaOH) to produce a ph of 9. Four shots gave results no different from benchmark results. More NaOH was added to produce a ph of 11 and four more shots taken. These four shots showed an average breakdown voltage which was 82% of the benchmark test.

A total of 19 g of NaOH was added to dissolve 100 g of Lauric acid ($C_{12}H_{24}O_2$). This produced a ph of 10 and a white coating on the electrodes and walls of the chamber. Two shots were taken and the breakdown voltage was 50% of the benchmark tests. After these shots, white particles could be seen suspended in the water. An additional 5 g of NaOH was added to dissolve these particles and this raised the ph to 11. Three shots were taken and the breakdown voltage averaged 50% of benchmark. No further tests were conducted.

## 4.2 DATA.

The data for each experiment will be presented in graphic form. Each set of data will consist of a graph of the averaged signals to show the differences between the baseline and experimental groups. Each individual signal was adjusted to compensate for the starting point of the signal by adding a least-squared routine to the MATLAB data extraction program. After the individual signals were adjusted, each of the 512 data points were averaged to give the waveform for the graphs.

Four parameters were looked at for comparison between the experimental groups. These were $\tau_{eff}$, $V_{max}$, fall-time, and fall-rate. The rise-time was not used because there seemed to be very little difference in the rise-time from one shot to another and was probably governed by the system rather than the

closing of the water gap. The results of the four parameters are also presented in graphical form with the mean data points connected by a single line and the ± 1 standard deviation bars drawn above and below the mean points.

### 4.2.1 Magnetic Fields.

Figure 4-1 shows the average waveforms for the magnet in the anode. The three curves represent the average values for the baseline signals, the signals generated with the North Pole of the magnet facing towards the gap, and the signals generated with the South Pole of the magnet facing towards the gap. The values of $\tau_{eff}$ for each of the three groups are shown in Figure 4-2; $V_{max}$, Figure 4-3; fall-time, Figure 4-4; and fall-rate, Figure 4-5.
The next experimental set consisted of baseline shots and shots with the magnet placed in the cathode. Again there were three sets of signals, baseline, North Pole in, and South Pole in. The averaged waveforms are show in Figure 4-6; values of $\tau_{eff}$, Figure 4-7; $V_{max}$, Figure 4-8; fall-time, Figure 4-9; and fall-rate, Figure 4-10.
Two magnets were used in the last experimental series. The three sets of signals consisted of the baseline, aligning fields, and opposing fields. The averaged waveforms are show in Figure 4-11; values of $\tau_{eff}$, Figure 4-12; $V_{max}$, Figure 4-13; fall-time, Figure 4-14; and fall-rate, Figure 4-15.

### 4.2.2 Sulfur Hexafluoride.

Figure 4-16 shows the averaged waveforms for the first series of $SF_6$ experiments. The values of $\tau_{eff}$ for the two groups are shown in Figure 4-17; $V_{max}$, Figure 4-18; fall-time, Figure 4-19; and fall-rate, Figure 4-20. The second series was a repeat of the first series with the averaged waveforms in Figure 4-21; values of $\tau_{eff}$, Figure 4-22; $V_{max}$, Figure 4-23; fall-time, Figure 4-24; and

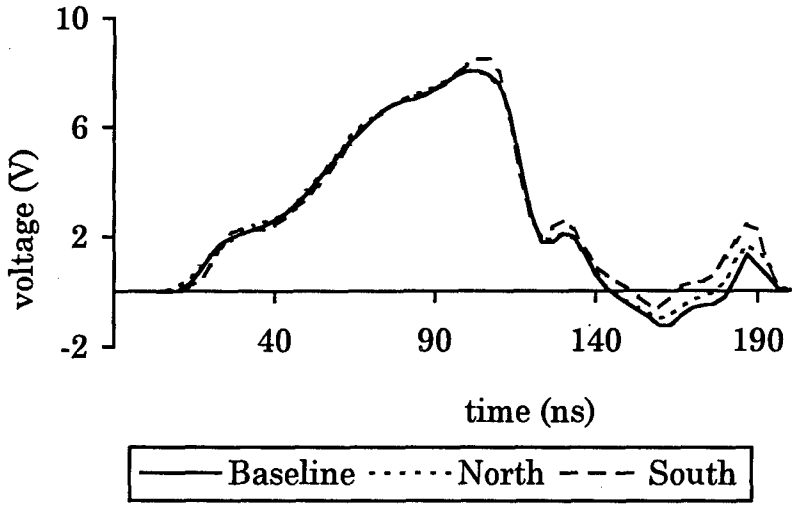


Figure 4-1. Average waveforms for the magnet in the anode.

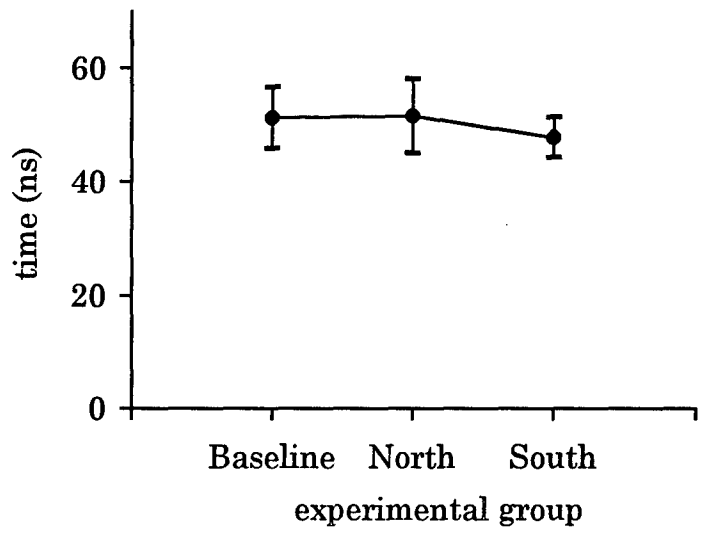


Figure 4-2. Effective time ($\tau_{eff}$) with a magnet in the anode.

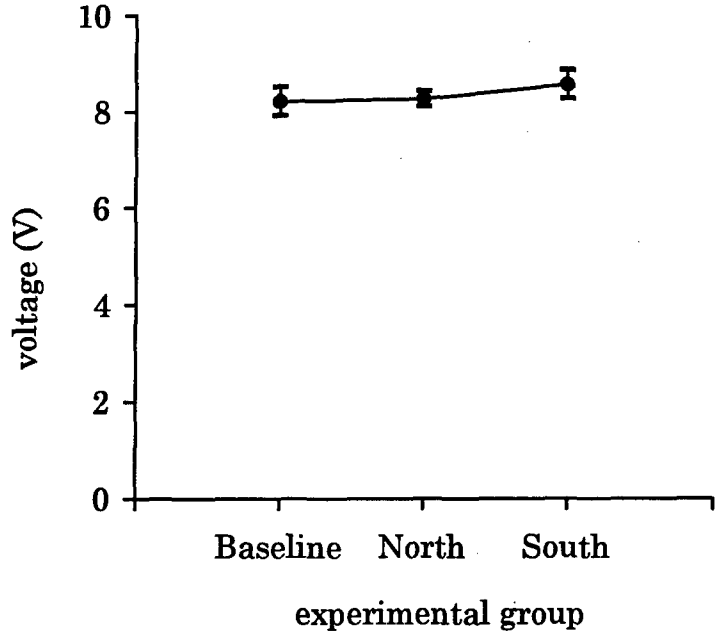


Figure 4-3. Maximum voltage ($V_{max}$) with a magnet in the anode.

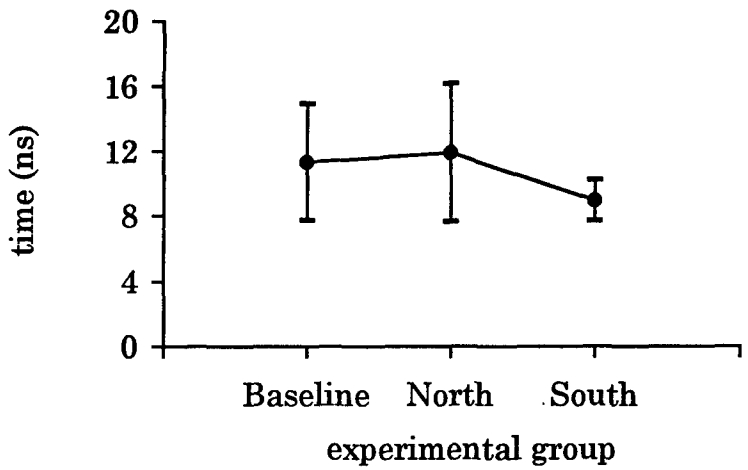


Figure 4-4 Fall-time with a magnet in the anode

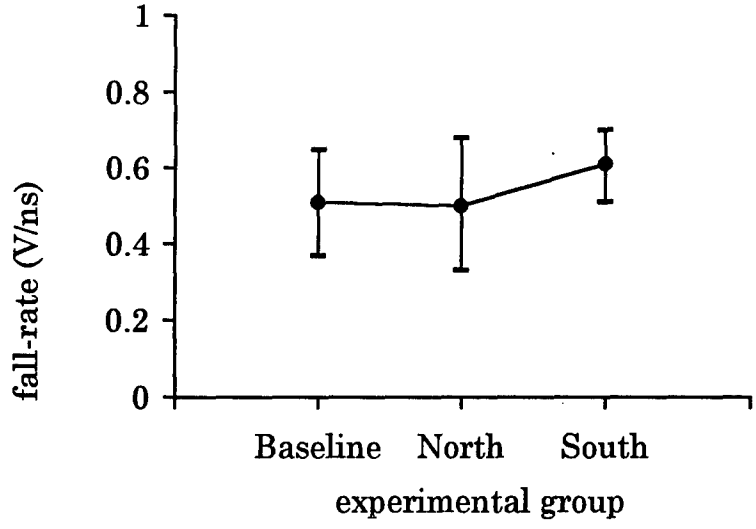


Figure 4-5. Fall-rate with a magnet in anode.

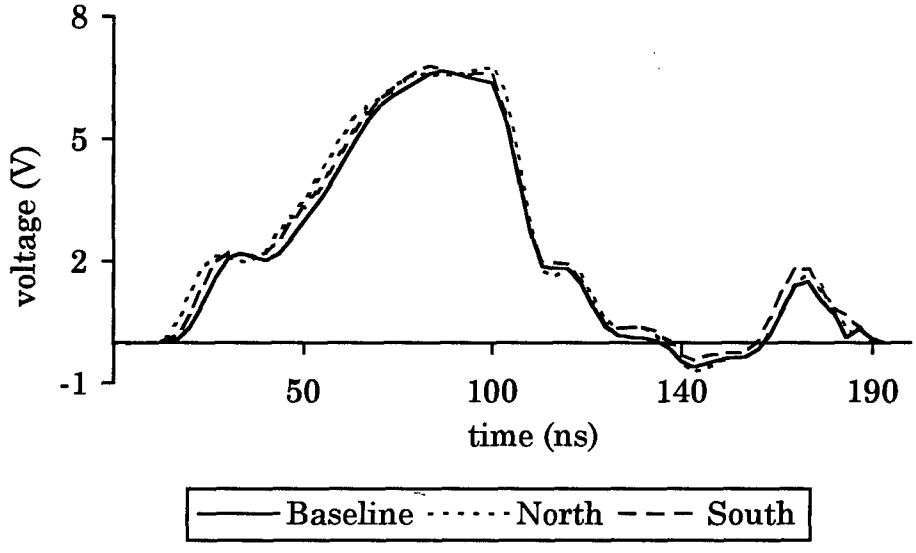


Figure 4-6. Average waveforms for the magnet in the cathode.

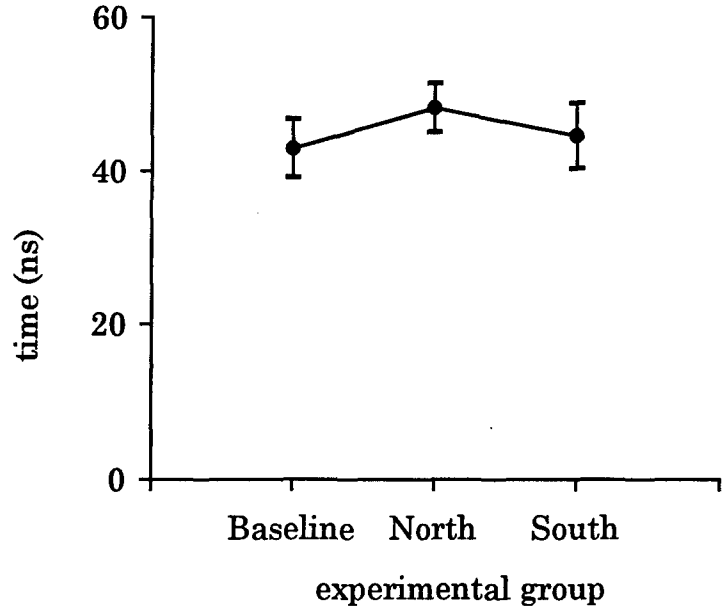


Figure 4-7. Effective time ($\tau_{eff}$) with a magnet in the cathode.

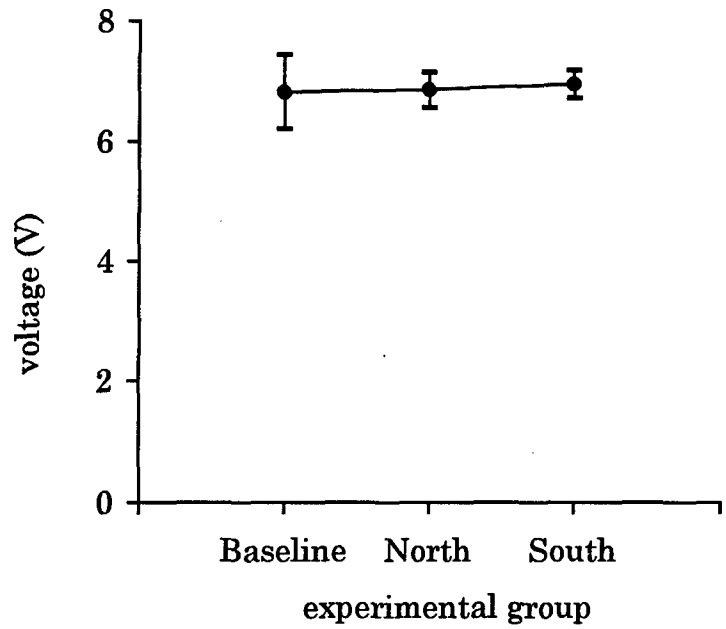


Figure 4-8. Maximum voltage ($V_{max}$) with a magnet in the cathode.

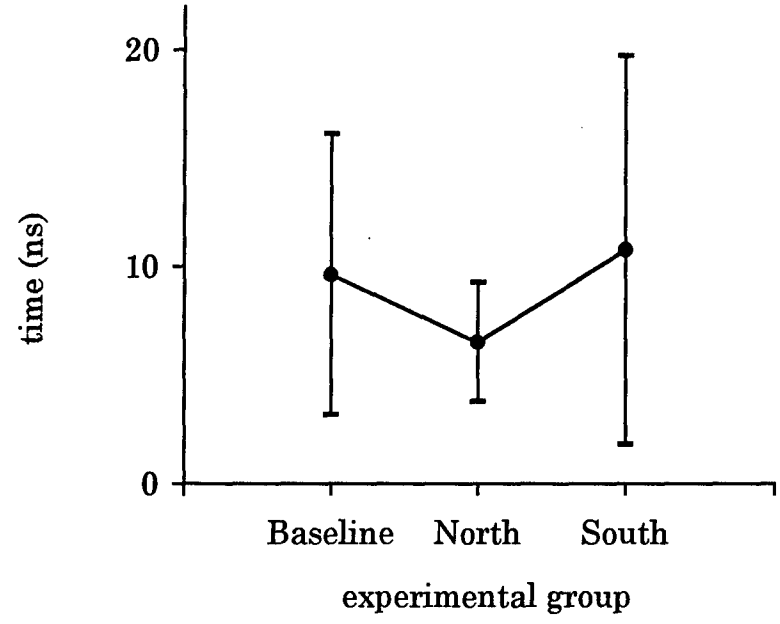


Figure 4-9. Fall-time with a magnet in the cathode.

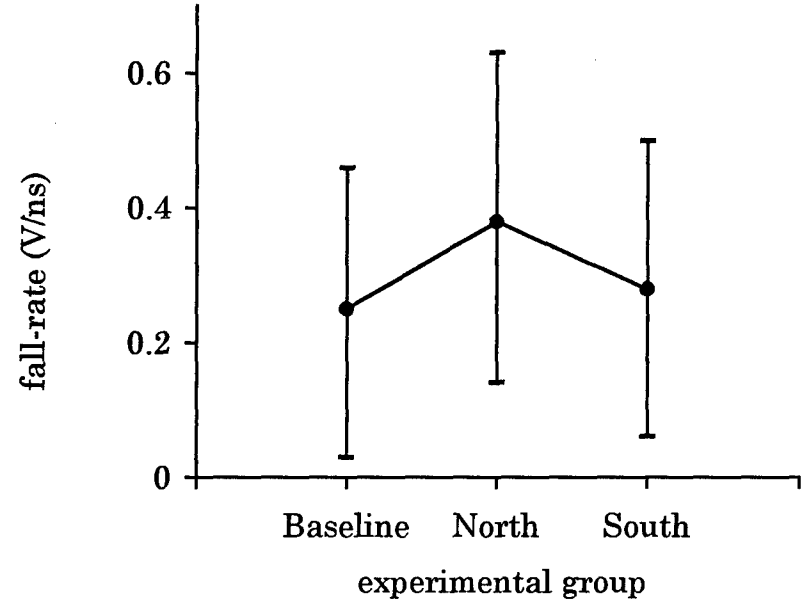


Figure 4-10. Fall-rate with a magnet in the cathode.

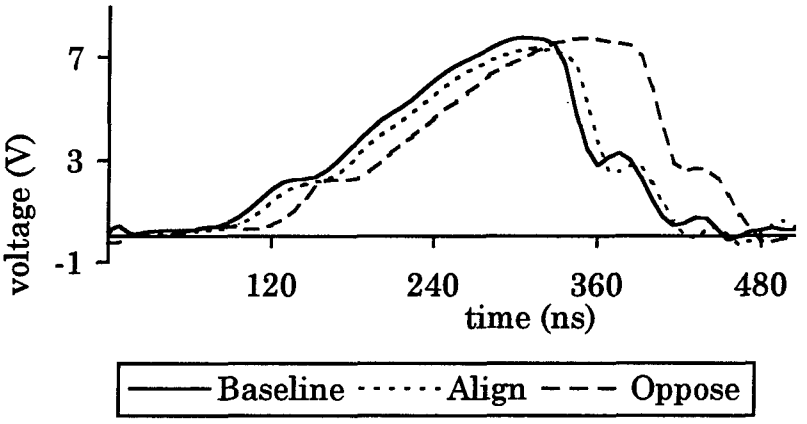


Figure 4-11. Average waveforms with magnets in the anode and cathode.

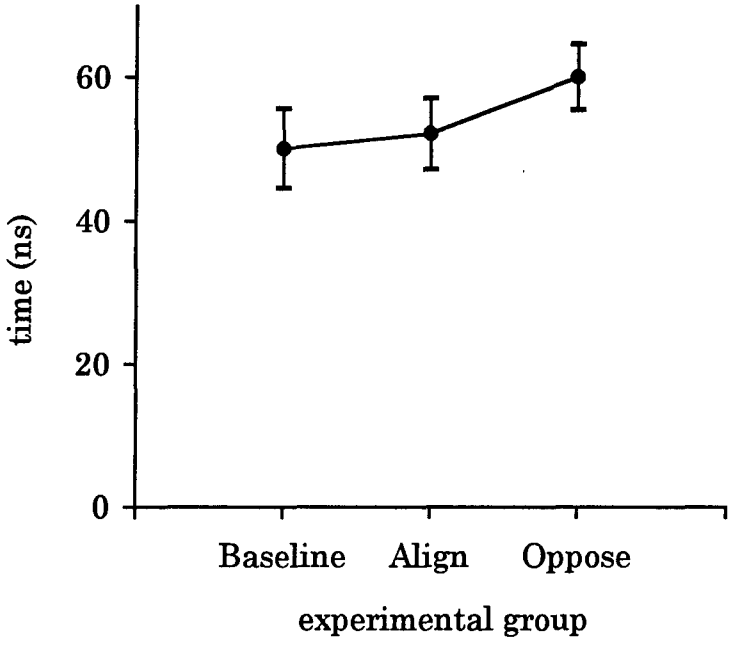


Figure 4-12. Effective time ($\tau_{eff}$) with magnets in anode and cathode.

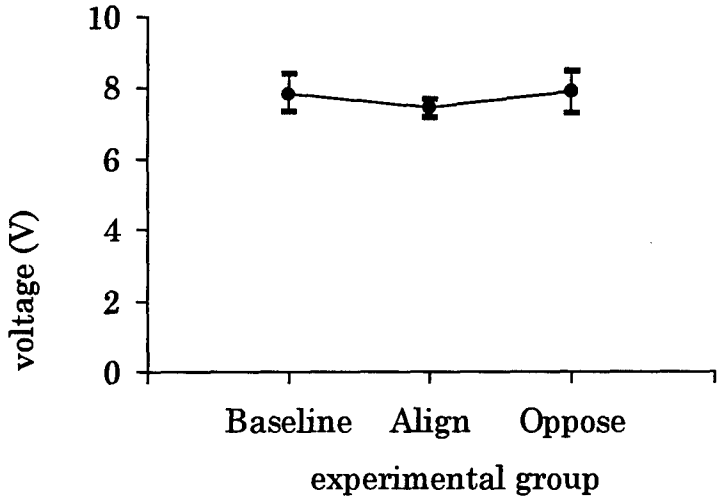


Figure 4-13. Maximum voltage ($V_{max}$) with magnets in the anode and cathode.

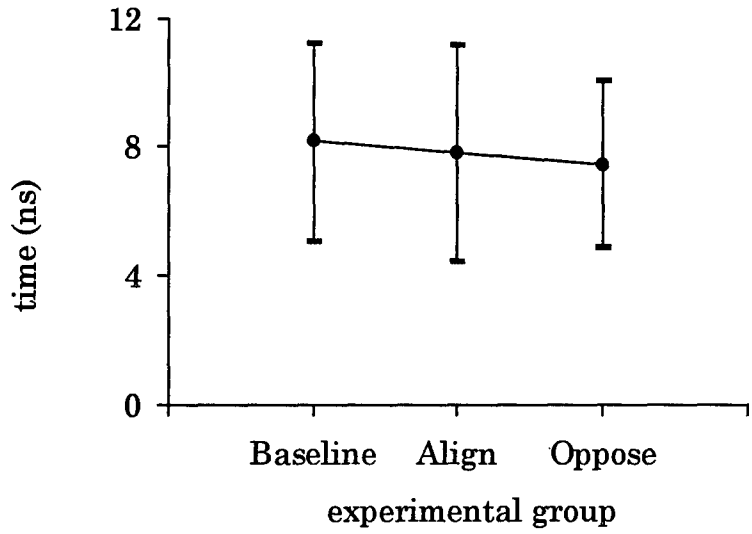


Figure 4-14. Fall-time with magnets in the anode and cathode.

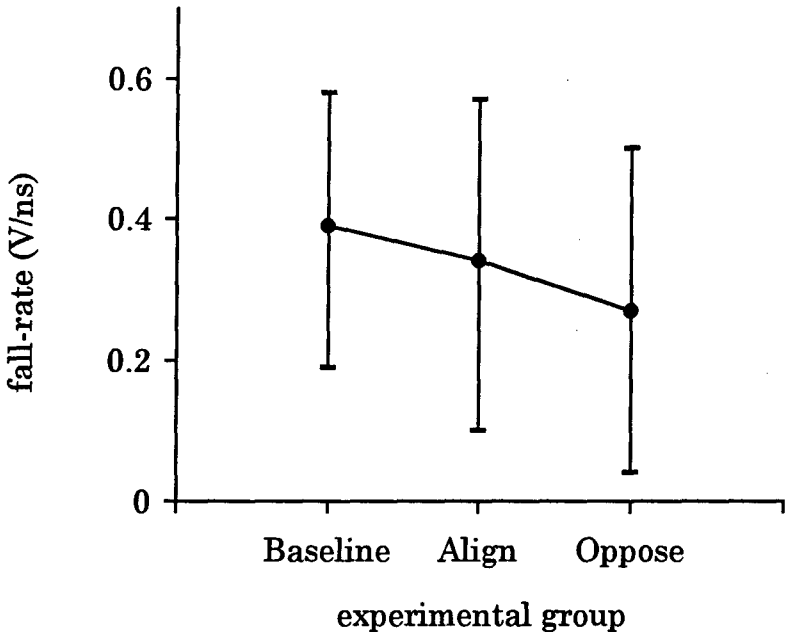


Figure 4-15. Fall-rate with magnets in the anode and cathode.

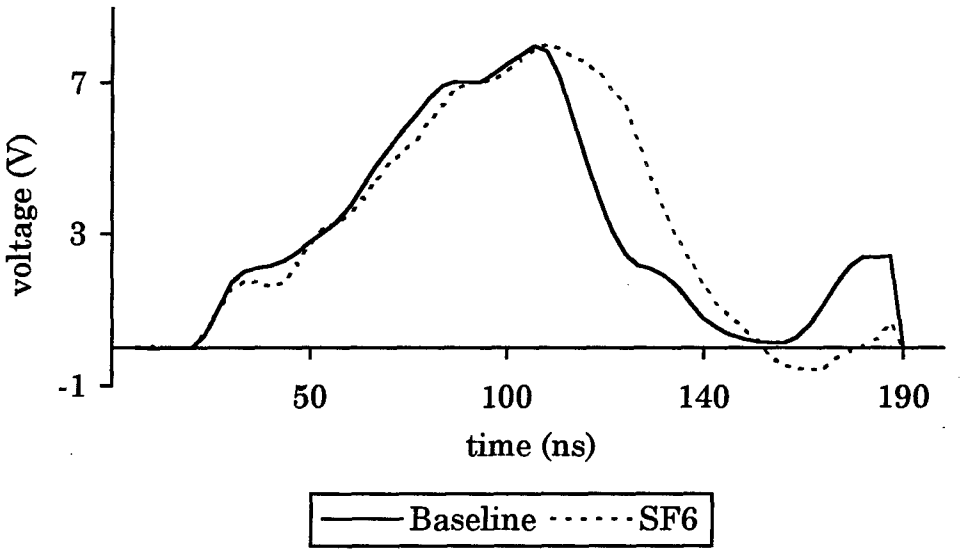


Figure 4-16. Average waveforms with $SF_6$ added to the water (first series).

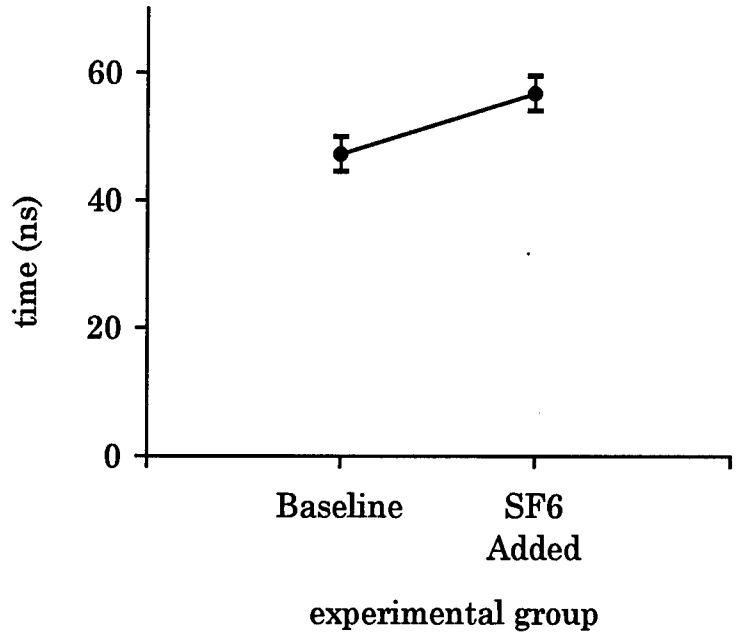


Figure 4-17. Effective time ($\tau_{eff}$) with $SF_6$ added (first series).

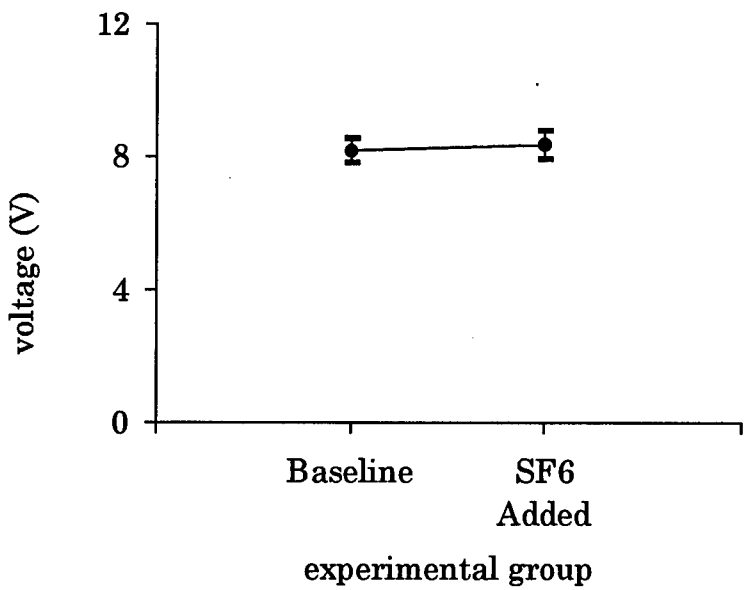


Figure 4-18. Maximum voltage ($V_{max}$) with $SF_6$ added (first series).

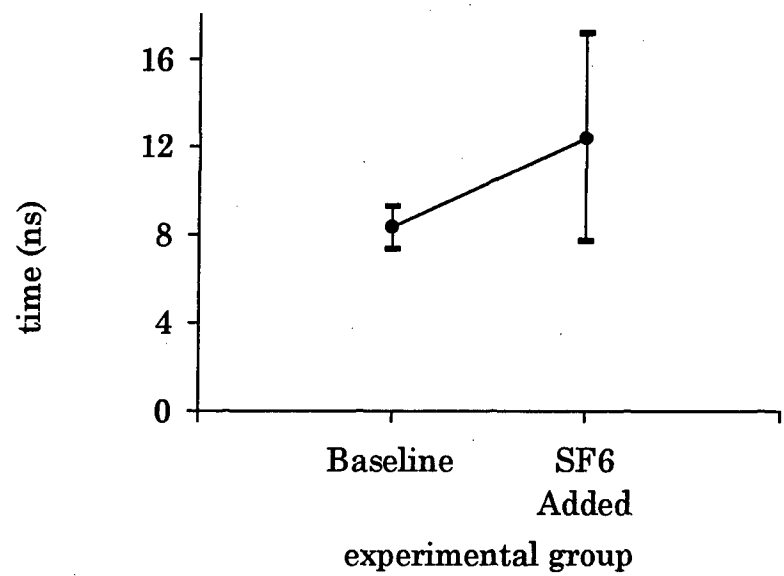


Figure 4-19. Fall-time with $SF_6$ added (first series).

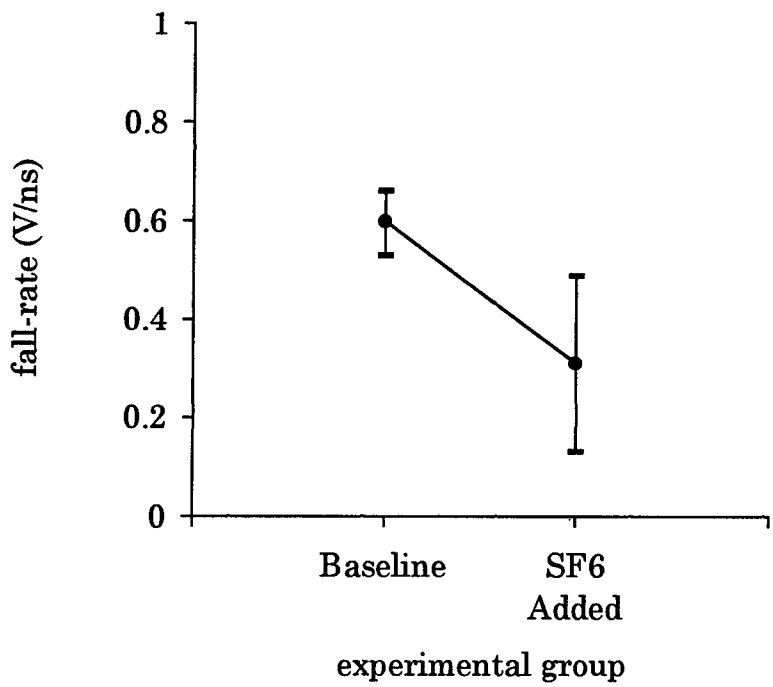


Figure 4-20. Fall-rate with $SF_6$ added (first series).

fall-rate, Figure 4-25. To show the effect the addition of the gas had on the individual waveforms, Figures 4-26 and 4-27 contain all twenty of the signals. The variation in the time-width of the signal can be seen by comparing the baseline signals in Figure 4-26 and the experimental signals in Figure 4-27.

An analog integrator was used on the last experiment using the $SF_6$ and accounts for the difference in the appearance of the waveforms and the absolute values of the signal parameters. Figure 4-28 shows the average waveforms of the three data groups: baseline, $SF_6$ (2 hours), and $SF_6$ (24 hours). The values of $\tau_{eff}$ for the two groups are shown in Figure 4-29; $V_{max}$, Figure 4-30; fall-time, Figure 4-31; and fall-rate, Figure 4-32.

### 4.2.3 Hydrochloric Acid.

Figure 4-33 shows the waveforms for several shots fired using two levels of HCl. The baseline signal and the $10x10^{-4}$ M HCl signal was captured with a 200 ns time window. The $2x10^{-4}$ M HCl signal was captured using a 500 ns time window. The first two signals were adjusted to fit on the 500 ns graph and accounts for the truncated appearance of the $10x10^{-4}$ M signal. Graphs for the four parameters used in the other experimental sets were not generated for this first set of signals. An ANOVA was not calculated for this data because of the different time windows used and was used to plan the second experiment. The analog integrator was not used for this series. For the second HCl experiment, five different levels of HCl were used along with the baseline. Figure 4-34 shows the averaged waveforms for the baseline, 0.1x10-4 M, 0.5x10-4 M, 1.0x10-4 M, 5.0x10-4 M, and 10.0x10-4 M. The same parameters were looked at as in the previous experiments: $\tau_{eff}$, $V_{max}$, fall-time, and fall-rate. Figures 4-35 through 4-38 show the mean values and the standard deviation for each of these parameters.

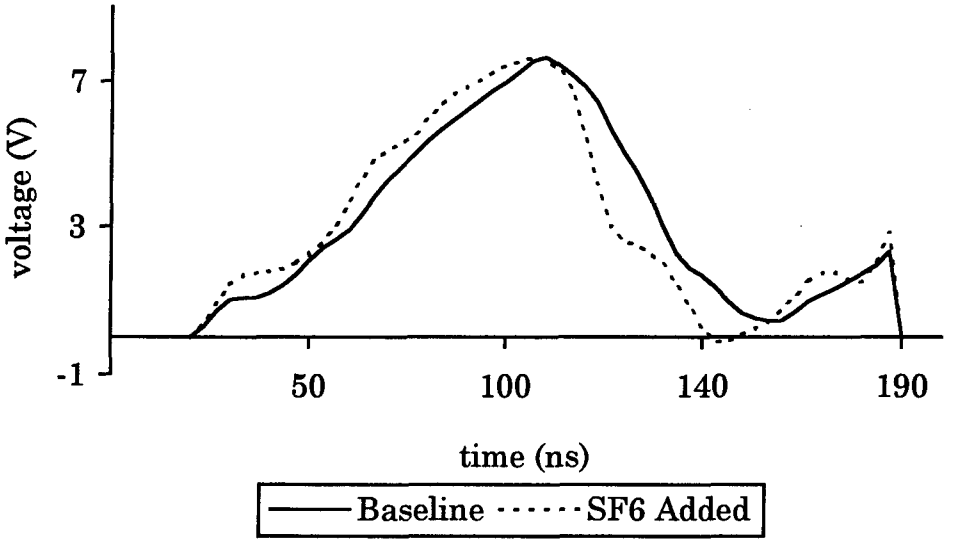


Figure 4-21. Average waveforms with $SF_6$ added to the water (second series).

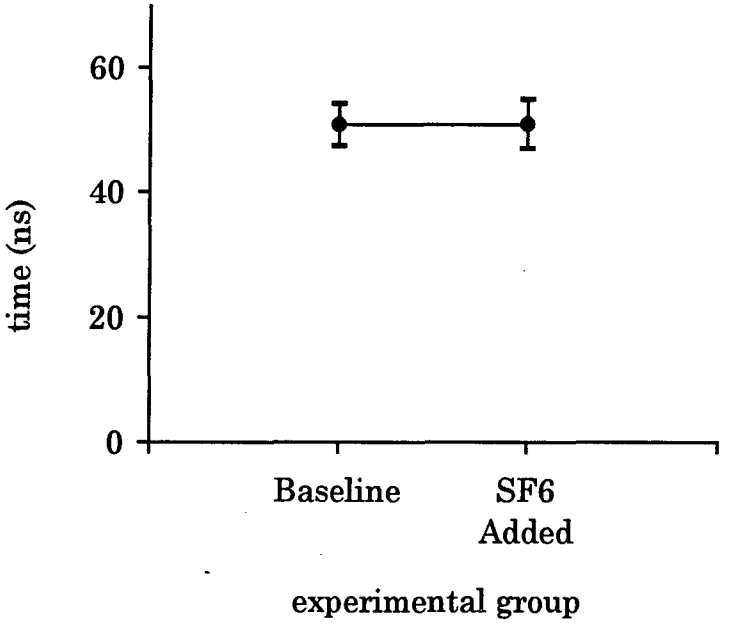


Figure 4-22. Effective time ($\tau_{eff}$) with $SF_6$ added (second series).

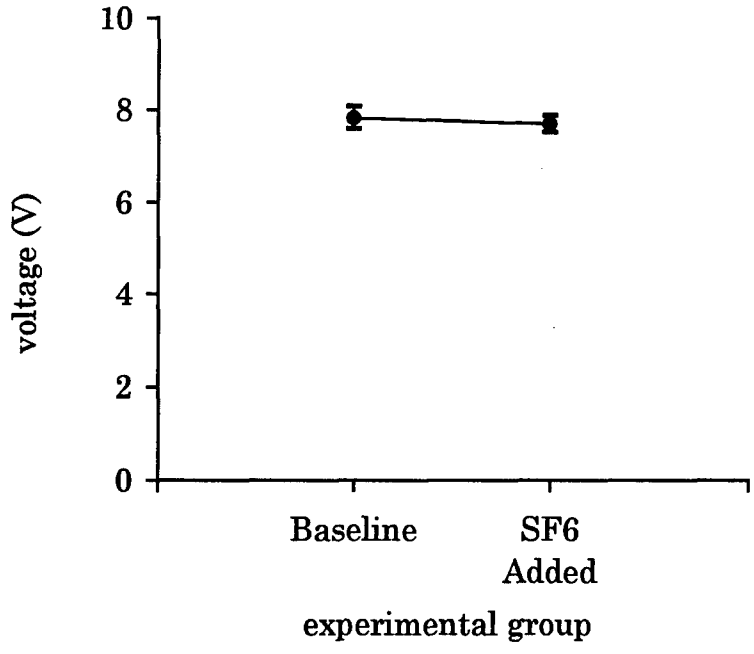


Figure4-23. Maximum voltage ($V_{max}$) with $SF_6$ added (second series).

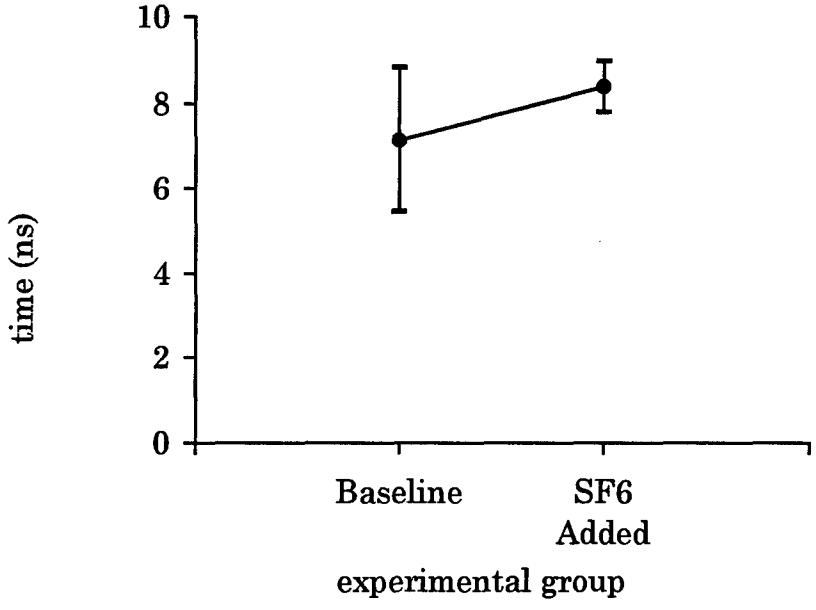


Figure 4-24. Fall-time with $SF_6$ added (second series).

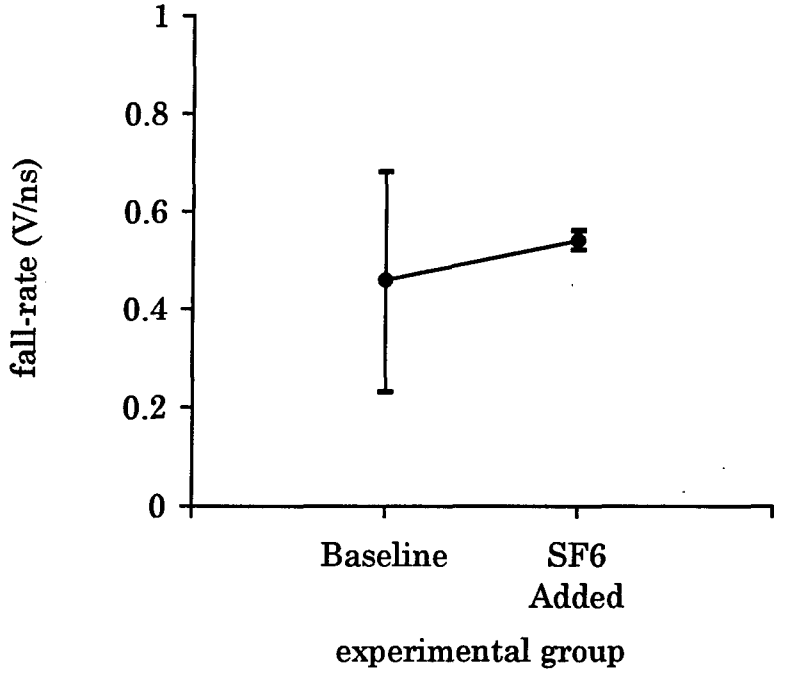


Figure 4-25. Fall-rate with $SF_6$ added (second series).

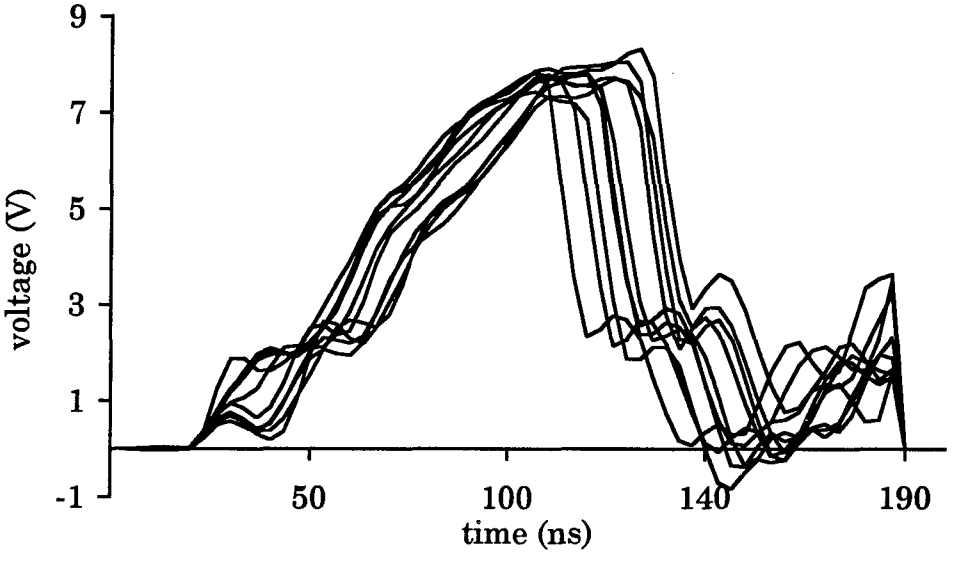


Figure 4-26. The ten baseline waveforms for the $SF_6$ second series of shots.

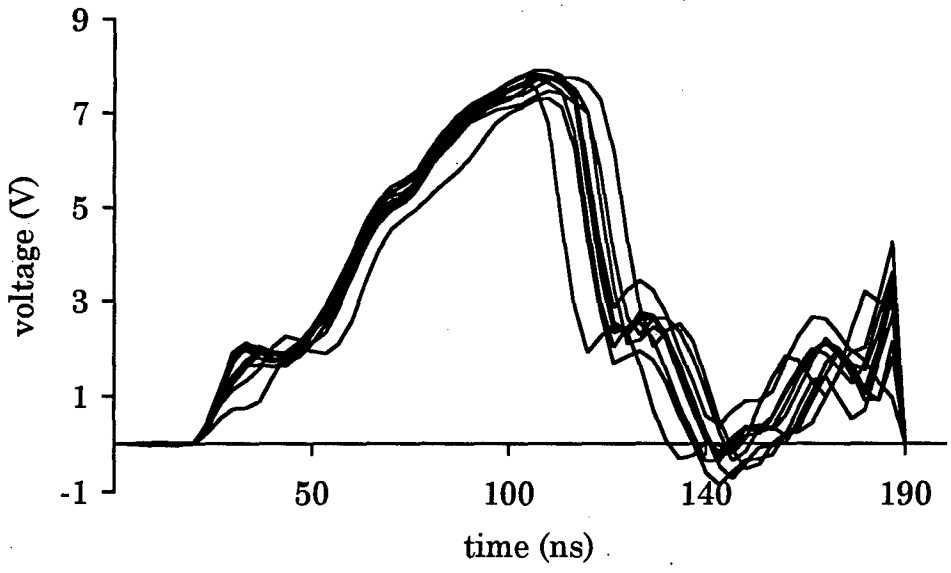


Figure 4-27. The ten waveforms with $SF_6$ added to the water (second series).

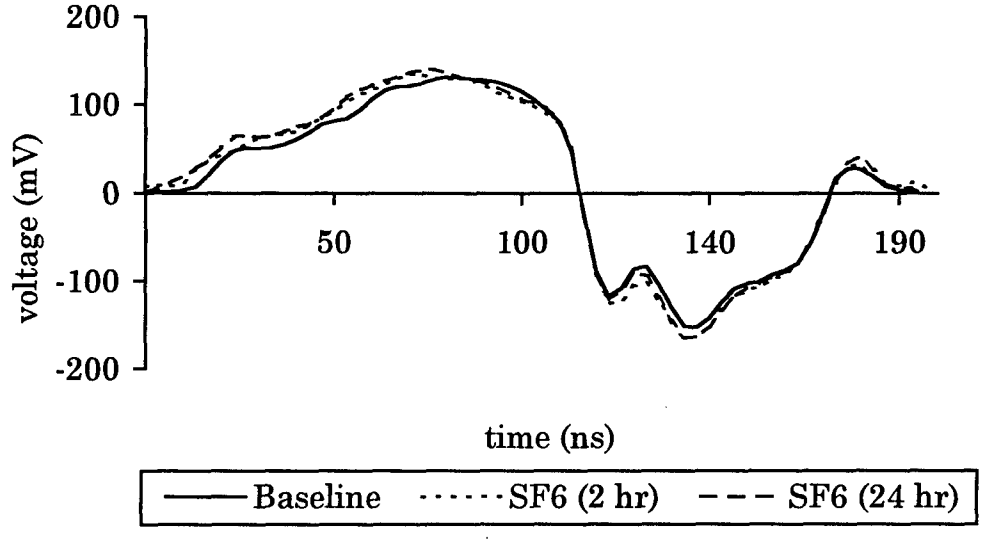


Figure 4-28. Average waveforms with $SF_6$ added to the water (third series).

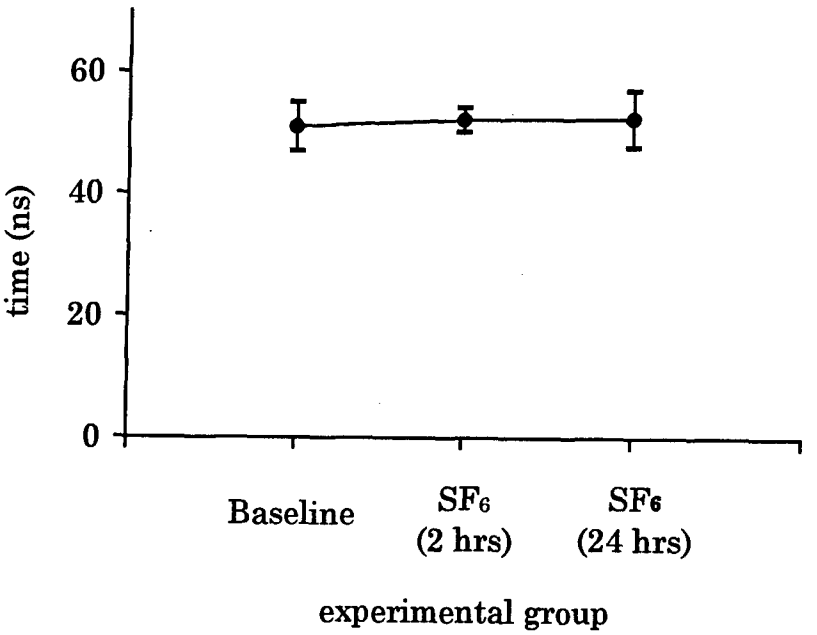


Figure 4-29. Effective time ($\tau_{eff}$) with $SF_6$ added (third series).

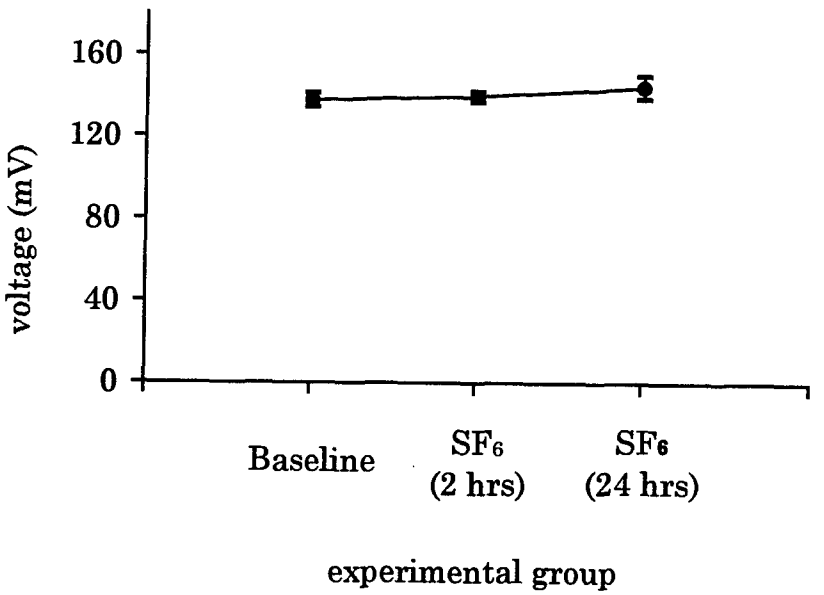


Figure 4-30. Maximum voltage ($V_{max}$) with $SF_6$ added (third series).

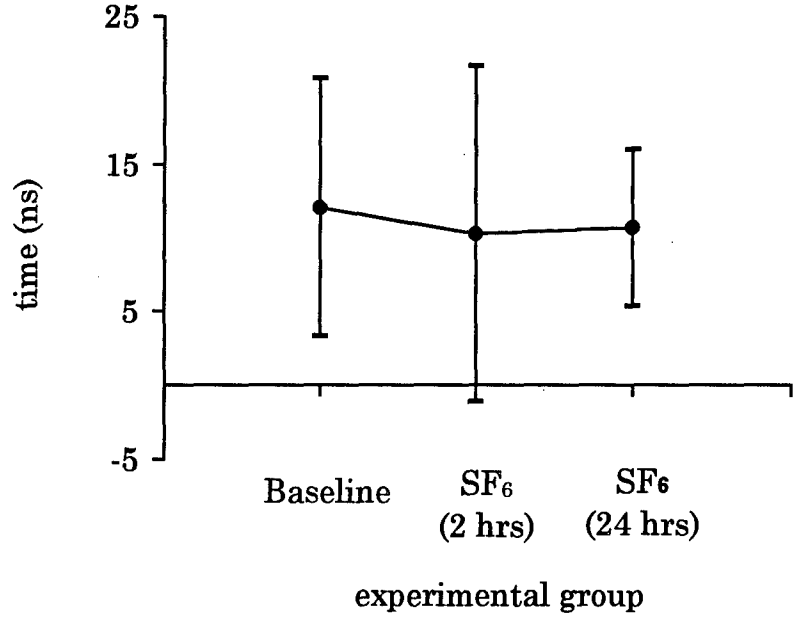


Figure 4-31. Fall-time with $SF_6$ added (third series).

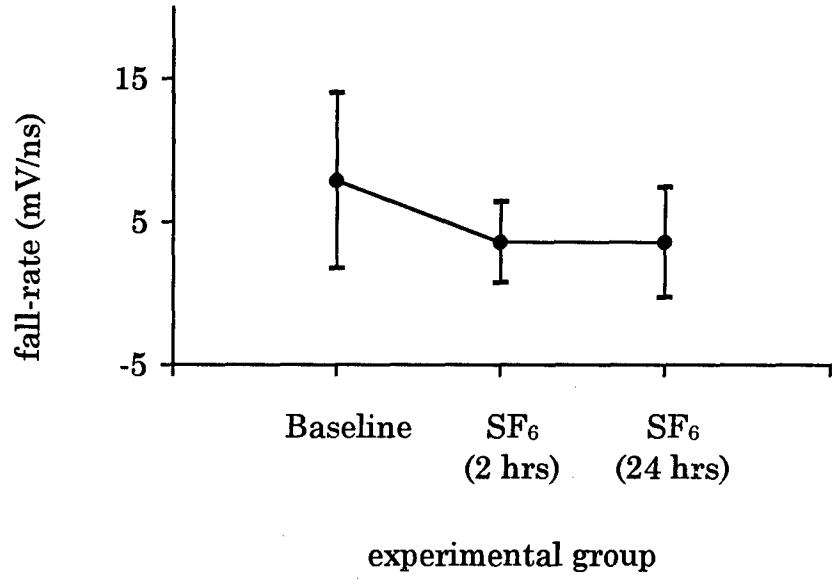


Figure 4-32. Fall-rate with $SF_6$ added (third series).

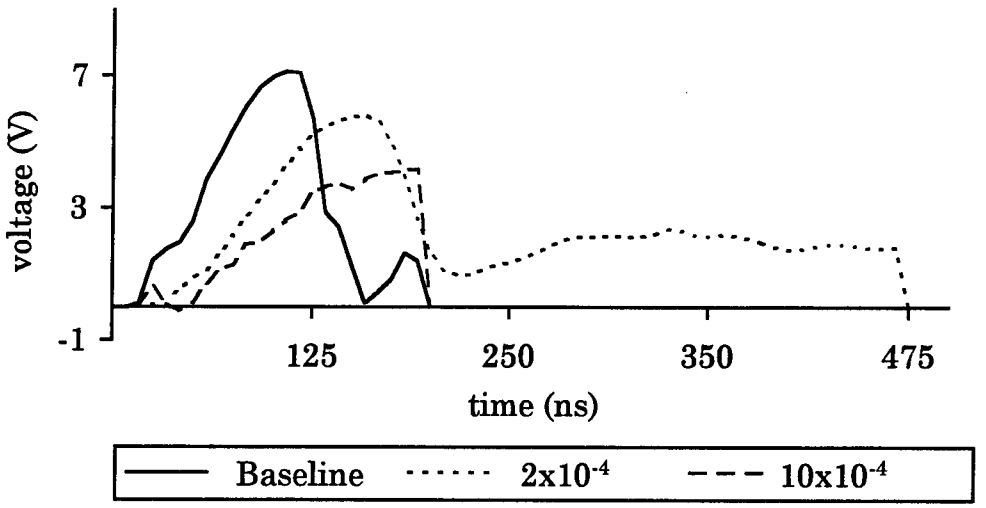


Figure 4-33. Waveforms for various amounts of HCl added to the water.

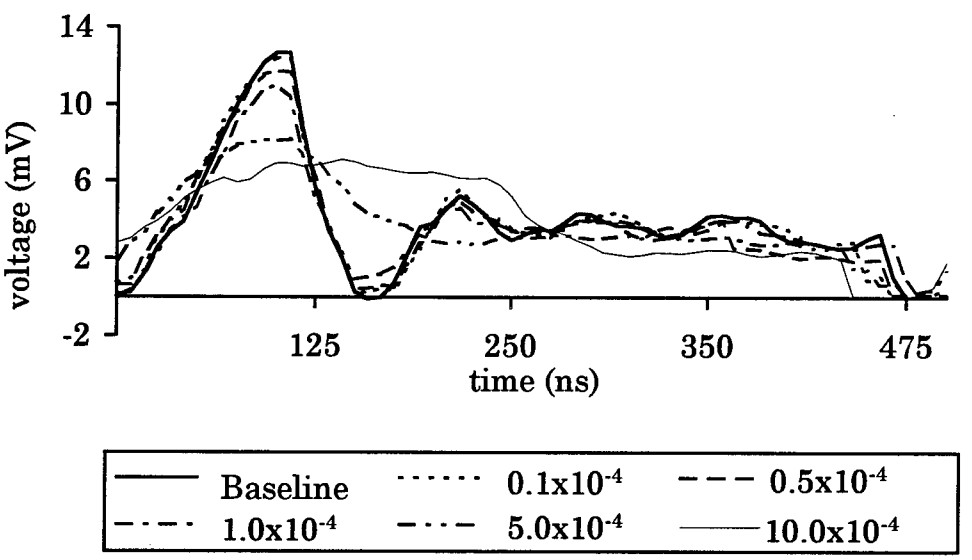


Figure 4-34. Average waveforms for various amounts of HCl added to the water (second series).

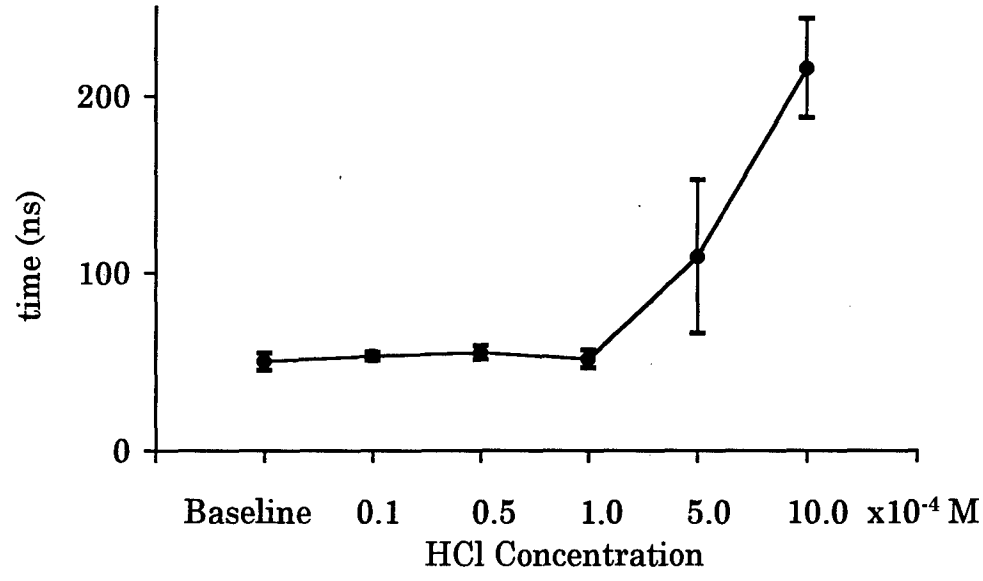


Figure 4-35. Effective time ($\tau_{eff}$) with HCl added (second series).

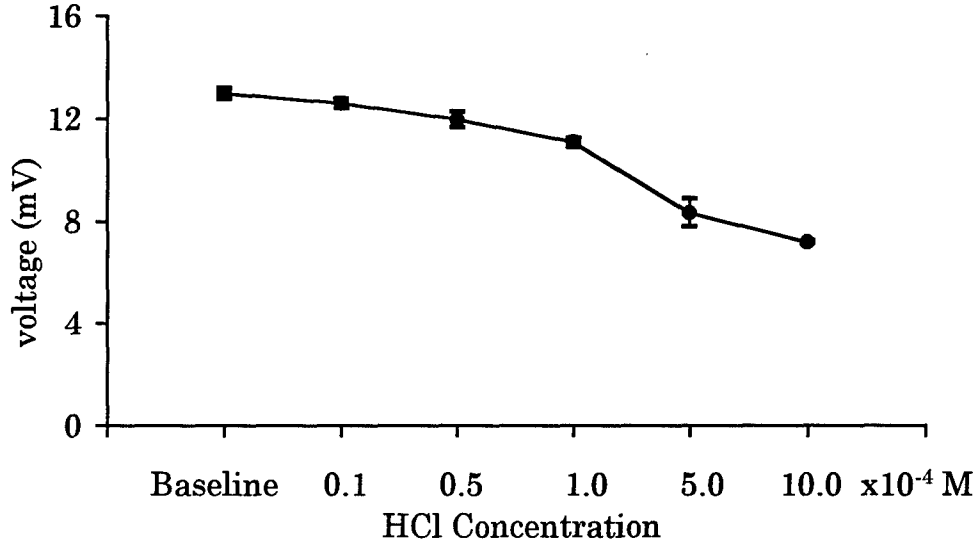


Figure 4-36. Maximum voltage ($V_{max}$) with HCl added (second series).

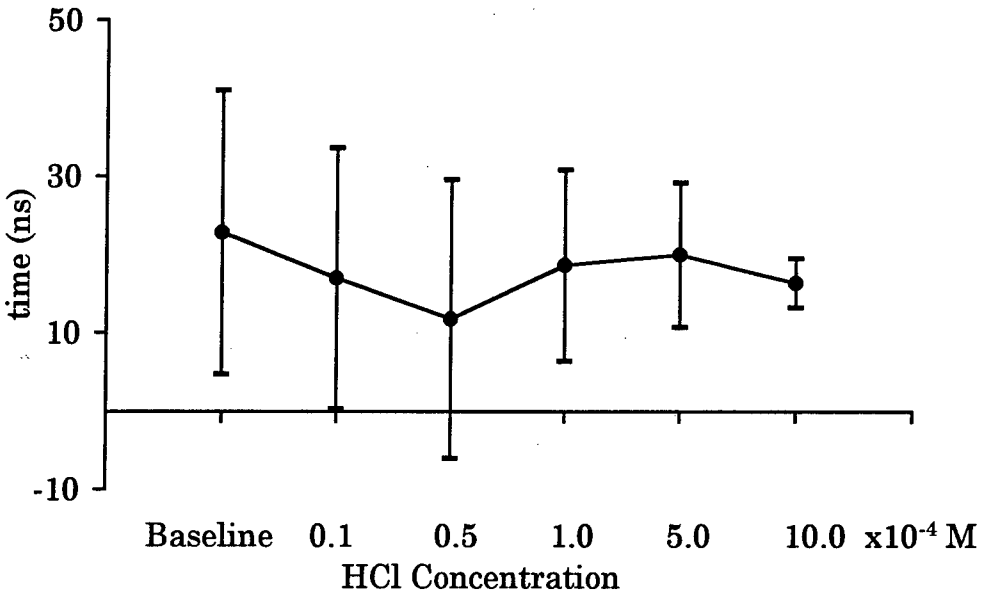


Figure 4-37. Fall-time with HCl added (second series).

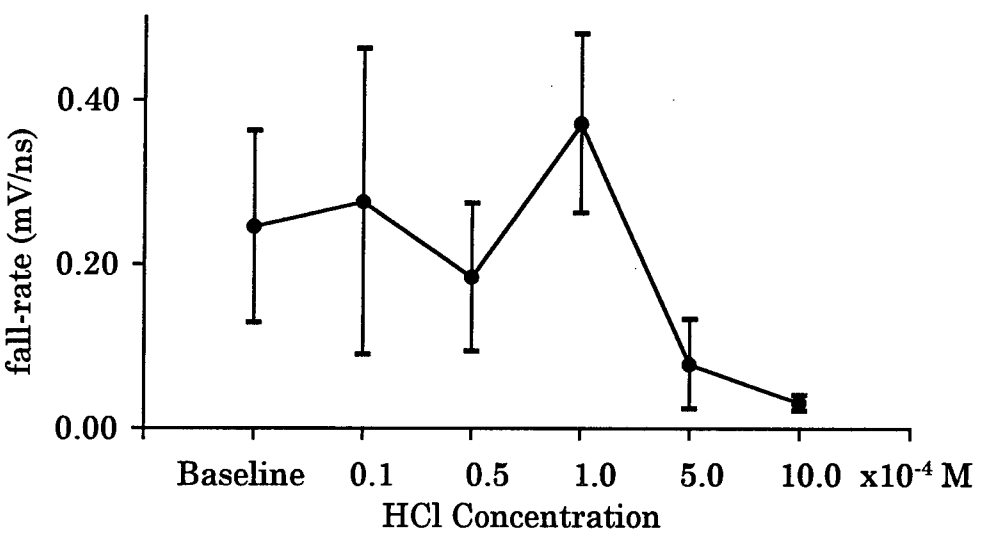


Figure 4-38. Fall-rate with HCl added (second series).

### 4.2.4 Polymer Coatings.

Figure 4-39 shows the waveforms for the shots fired using the different sets of polymer coatings. Figures 4-40 through 4-43 show the mean value and the standard deviation for the baseline and the value from the one shot of each of the different sets of polymer coatings. Since there was only one shot fired with each of the four combinations of the two polymer coatings, the standard deviation could not be calculated.

Three things are significant about the series of shots with the polymer coatings. The first is the data was collected using the new Tektronix SCD5000 digitizers, the second is the use of stainless steel electrodes, and the third is the second voltage "hump" seen on the baseline shots. On some of the previous shots, there would be a small rise in the voltage after the voltage dropped from its maximum but it was usually insignificant when compared to the main voltage pulse. This second voltage "hump" is seen in Figure 4-39 (solid line) and appears to be a reflection of the initial voltage pulse. Any type of coating on the electrodes would cause the reflection to disappear. Several attempts were made to recreate this phenomenon with the PSPICE model but proved to be unsuccessful. Also, when the copper tungsten electrodes were put back in the test chamber, the reflection disappeared again. The reflection seems to be caused by the use of the stainless steel electrodes but it is not clear why the type of electrode alone would cause such an effect.

### 4.2.5 Black Wax.

Figure 4-44 shows the average waveforms for the ten baseline shots and the ten shots fired with black wax on both electrodes. Figures 4-45 through 4-48 show the mean values and the standard deviations for the baseline signals and the signals with the black wax on the electrodes for each of the four parameters: $\tau_{eff}$, $V_{max}$, fall-time, and fall-rate.

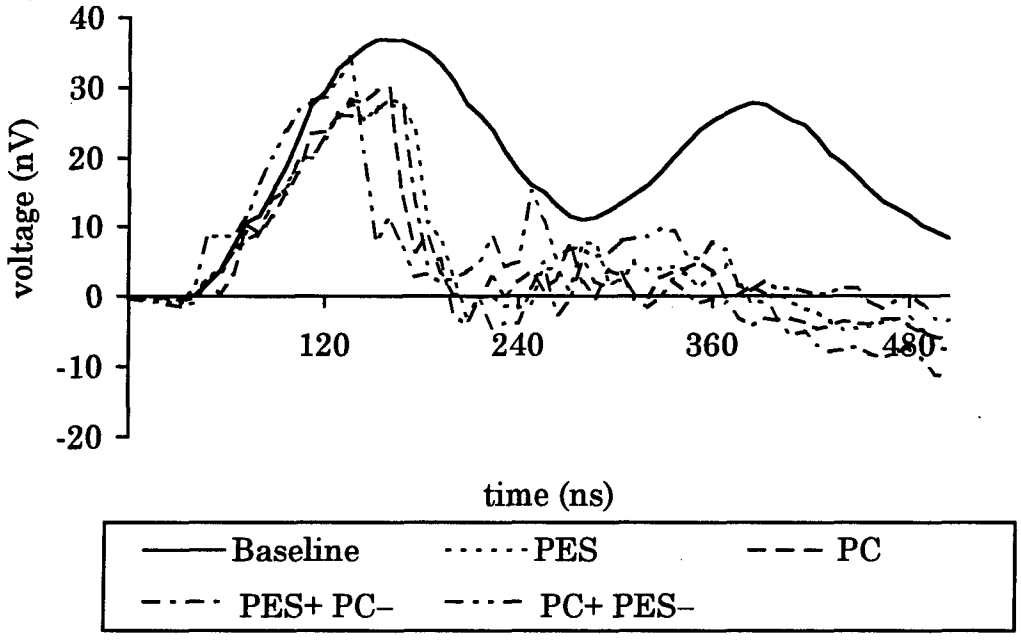


Figure 4-39. Average waveforms with polymer coatings on the electrodes.

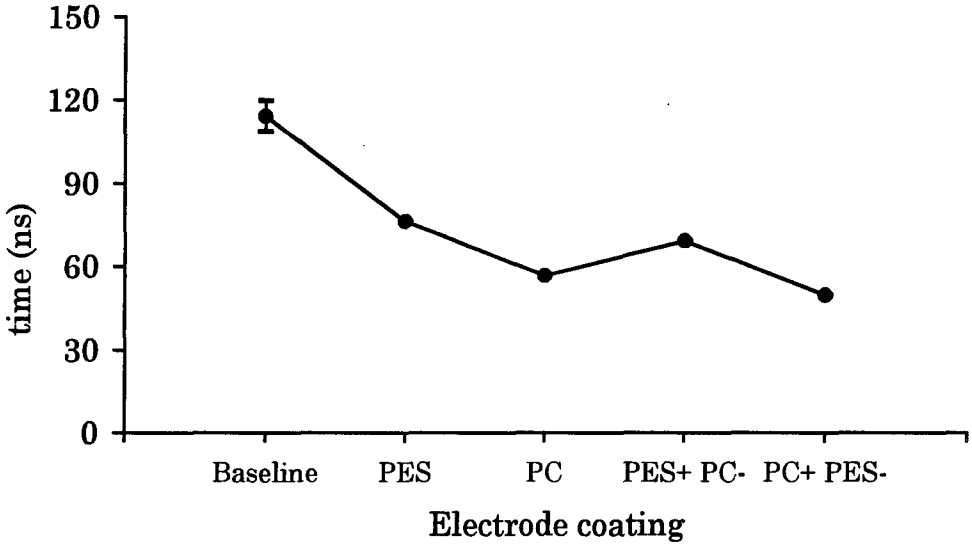


Figure 4-40. Effective time ($\tau_{eff}$) with polymer coatings on the electrodes.

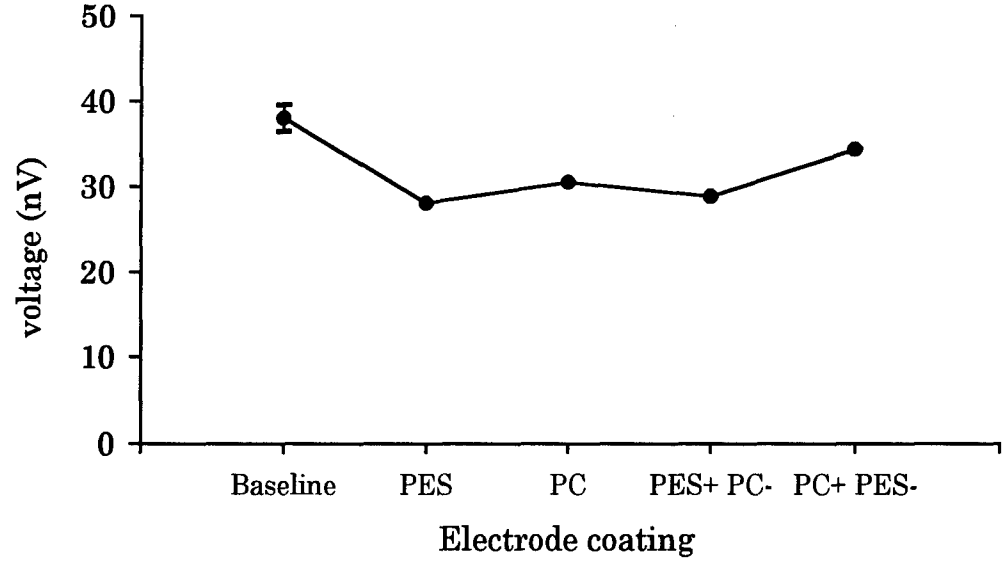


Figure 4-41. Maximum voltage ($V_{max}$) with polymer coatings on the electrodes.

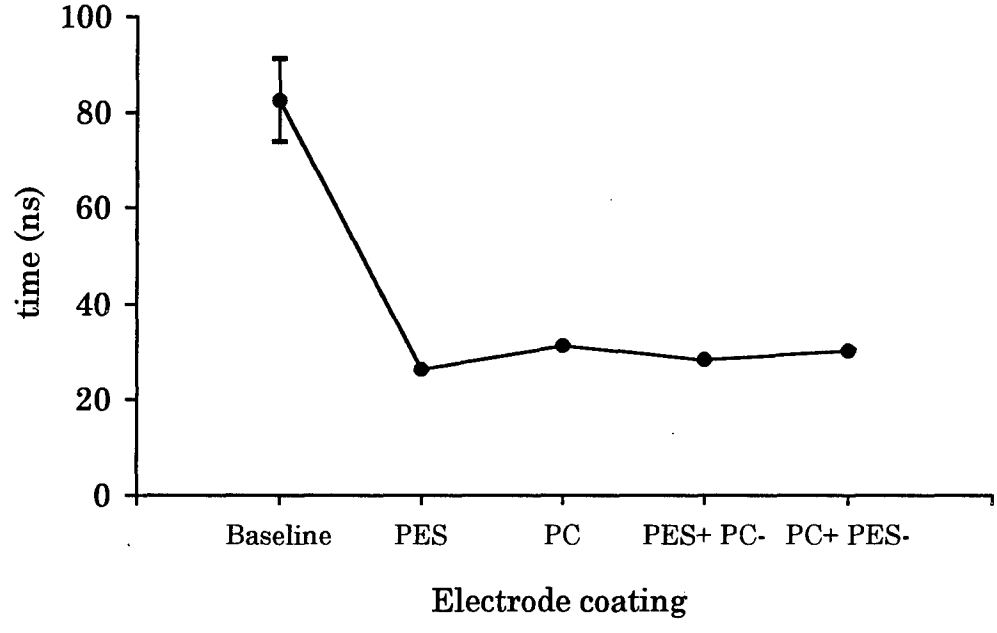


Figure 4-42. Fall-time with polymer coatings on the electrodes.

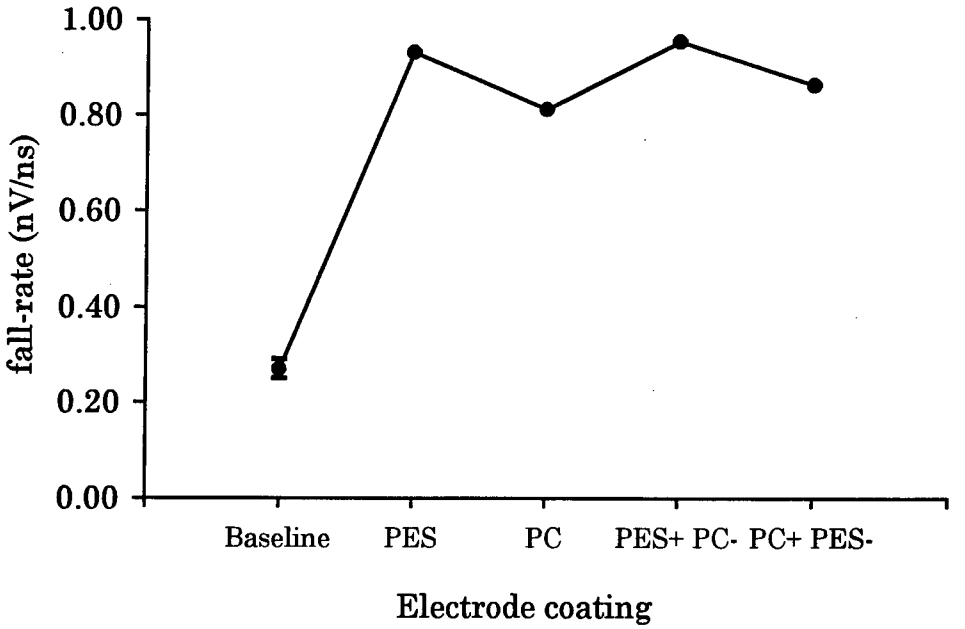


Figure 4-43. Fall-rate with polymer coatings on the electrodes.

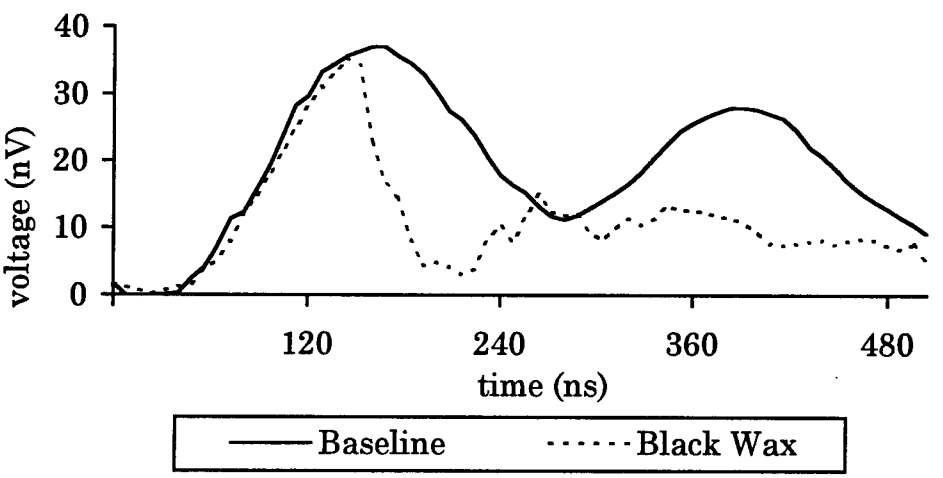


Figure 4-44. Average waveforms with black wax coatings on the electrodes.

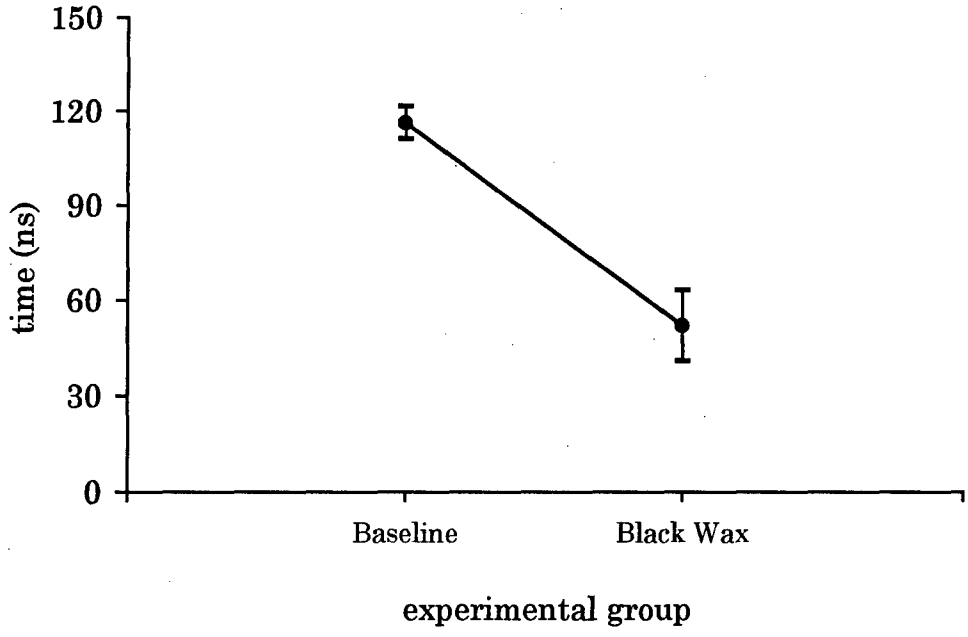


Figure 4-45. Effective time ($\tau_{eff}$) with black wax coatings on the electrodes.

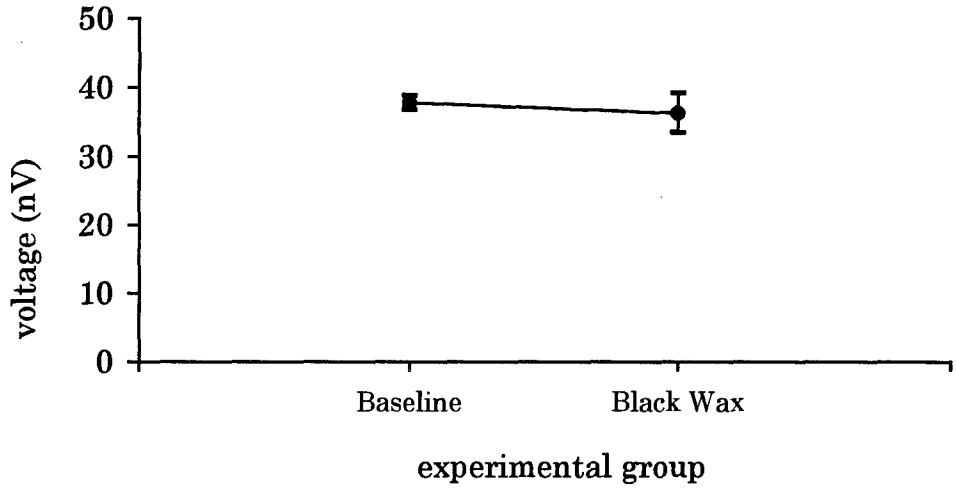


Figure 4-46. Maximum voltage ($V_{max}$) with black wax coatings on the electrodes.

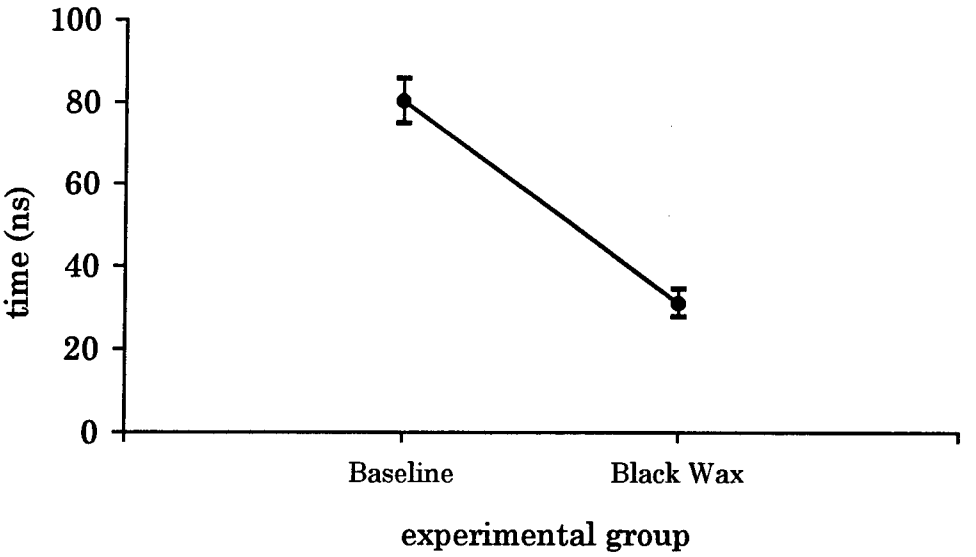


Figure 4-47. Fall-time with black wax coatings on the electrodes.

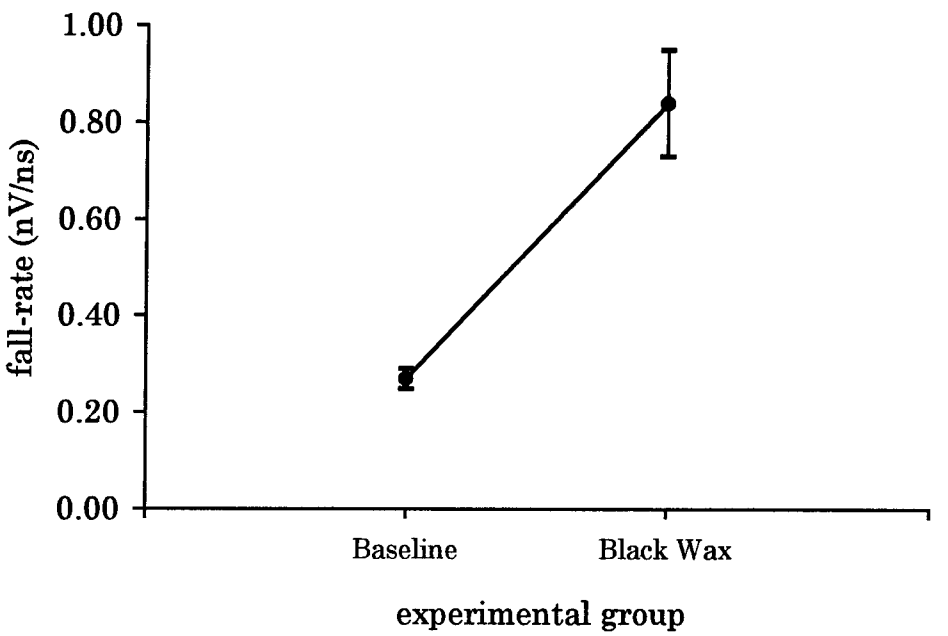


Figure 4-48. Fall-rate with black wax coatings on the electrodes.

4.2.6 Anodized Aluminum.

Figure 4-49 shows the average waveforms for the eight baseline shots and the two shots with anodized aluminum electrodes. Figure 4-50 shows the mean values and standard deviations for the $\tau_{eff}$ of the baseline versus anodized shots. The values for $V_{max}$ are shown in Figure 4-51, the fall-time values are shown in Figure 4-52, and the fall-rate values are in Figure 4-53.

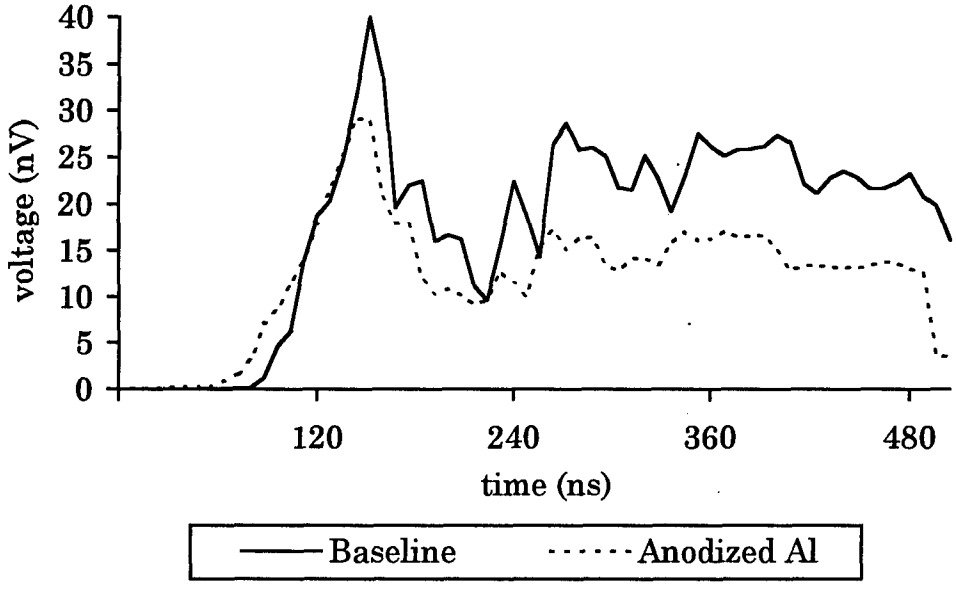


Figure 4-49. Average waveforms with anodized aluminum electrodes.

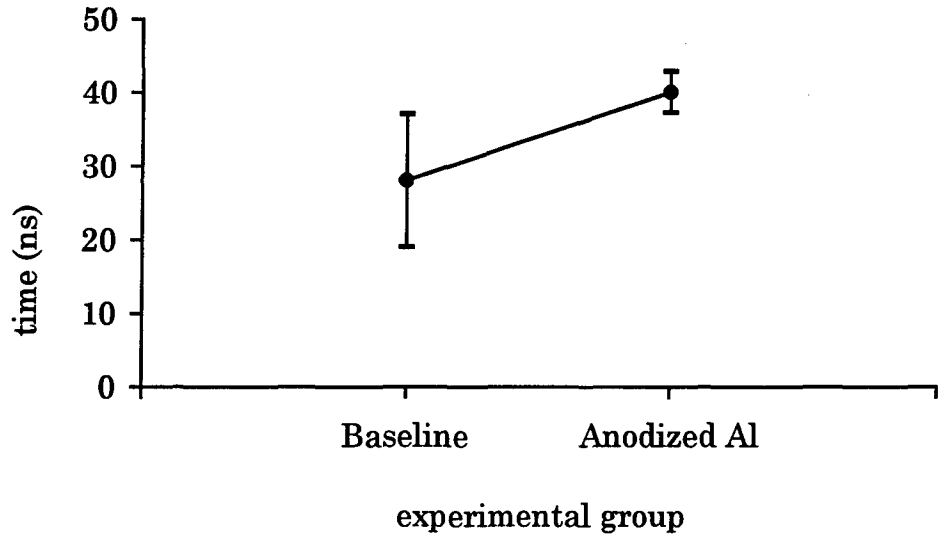


Figure 4-50. Effective time ($\tau_{eff}$) with anodized aluminum electrodes.

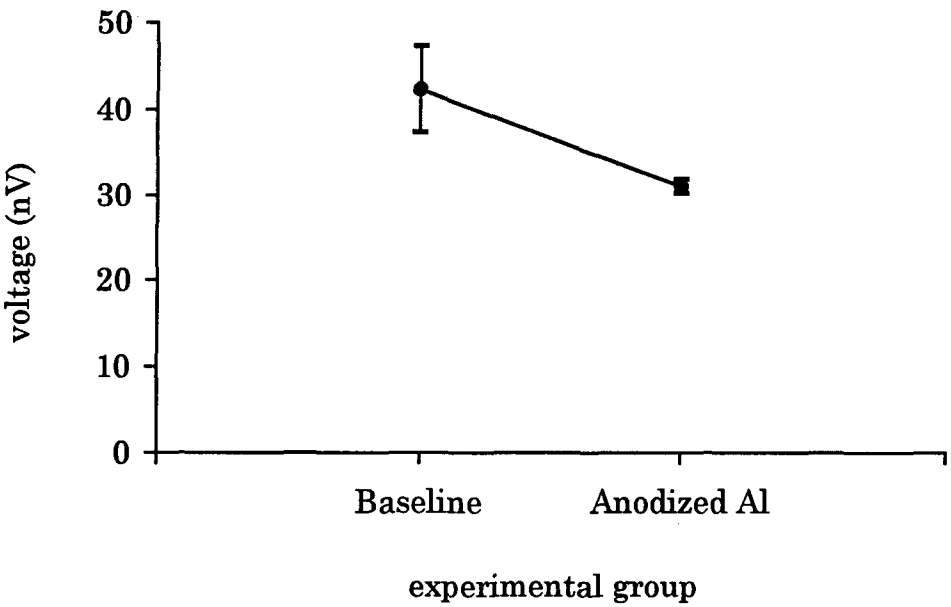


Figure 4-51. Maximum voltage ($V_{max}$) with anodized aluminum electrodes.

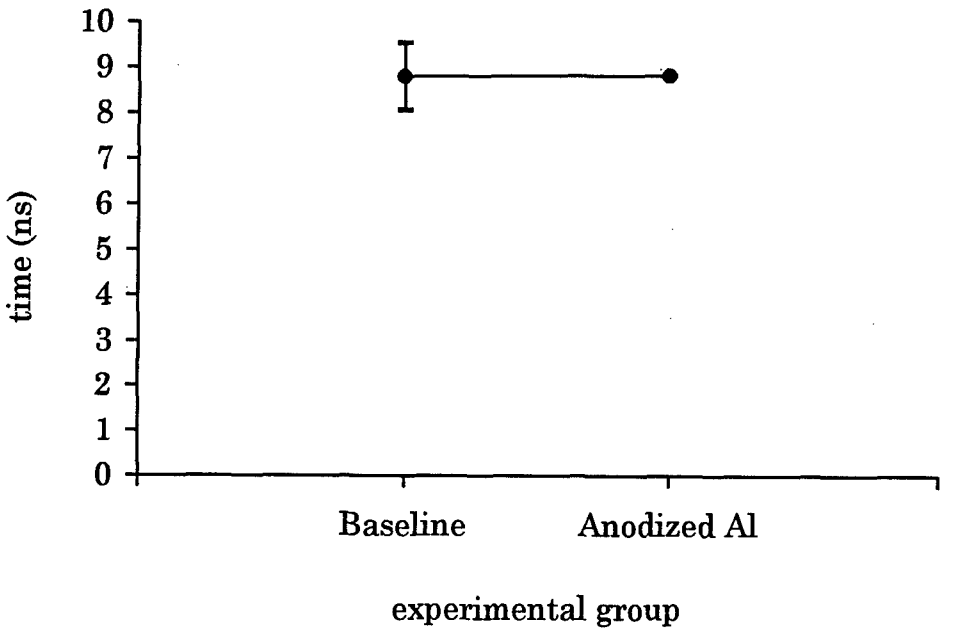


Figure 4-52. Fall-time with anodized aluminum electrodes.

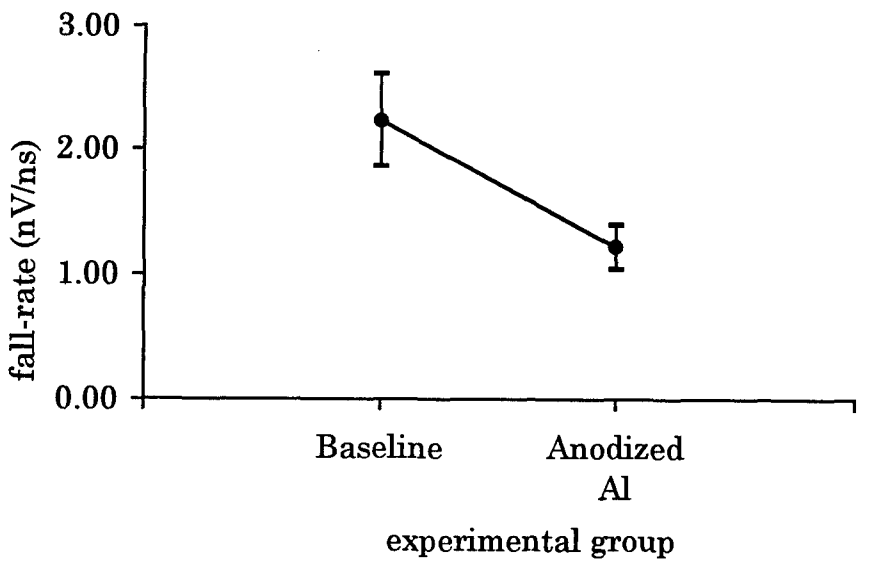


Figure 4-53. Fall-rate with anodized aluminum electrodes.

# SECTION 5
# CONCLUSIONS

Based on the data presented in Section 4, it is possible to generate some ideas as to what is happening in the water during the application of a high electric field. If the reader can accept the Russian breakdown model presented in Section 2, the results of this experiment must be able to support a breakdown process initiated by microbubbles and propagated through the water by proton transport. Looking at the previous research listed in the first part of Section 2, the methods that had significant effects on the breakdown field strength would affect either the occurrence of microbubbles or proton transport. In particular, water pressure showed some of the best results of all the methods presented. Even though it would not be practical in large systems, it is possible to double the breakdown field strength by applying very high pressures to the system. If it is microbubbles that initiate the discharge in the water gap, then applying high pressures would force out the bubbles from the electrode surface, decreasing the number of possible initiation sites, and also make the formation of bubbles from thermal heating more difficult.

Another technique used to increase the breakdown strength is to cool the water down to near freezing or, with additives, below freezing. In this case, more thermal energy is needed for the transition from near freezing liquid to the microbubble state.

The next area that has been researched is the type of electrode material used. Of particular note is the work presented in Section 2 that looked at different materials for the anode and cathode [6]. For example, using brass and aluminum electrodes, it is possible to almost double the breakdown field strength by switching from an aluminum anode and a brass cathode to an aluminum cathode and a brass anode. This is due principally to negative

charge injection. Again, looking at the Russian model, it would appear that the use of these two electrode materials together either enhance or inhibit the proton motion depending on the orientation of the electrodes.

The most promising technique for increasing the breakdown field strength is the use of diffusion electrodes for which the Russians have claimed a quadrupling of the field strength between the electrodes [1]. By applying a diffuse conducting layer on the electrode surface, the high intensity fields forming around the microbubbles are eliminated. This allows the field to build up to a higher level until the discharge is formed by a different process such as thermal conduction in the center of the gap.

The Russians have provided us with what seems to be a good workable model of the breakdown process. The results presented in Section 4 can now be put in context with this model. The effect of the magnetic field on the voltage output is particularly interesting because water has an electric dipole moment but does not have a magnetic dipole moment. So the magnetic fields would have no effect on the orientation or motion of the water molecules in their natural state but would have an effect on the movement of ions through the gap between the electrodes. The radius of the path of the charged particle moving through a magnetic field is given by

$$r = \frac{mv}{qB}, \tag{5.1}$$

where $m$ is the particle mass, $v$ is the velocity, $q$ is the charge, and $B$ is the magnetic field strength. Ovchinnikov et al. [18] measured the electron velocity in water to be approximately 1.5 x $10^3$ m/sec and Yanshin et al. [19] gives the proton velocity in water as 40 m/sec. With these velocities and using a magnetic field strength of 15 mT, the radii would be 0.6 μm and 27.8 μm for an electron and a proton, respectively, which are much smaller than the electrode gap. Of course, this assumes a transverse magnetic field which would not be the case here. However, with the copper-tungsten elec-

trodes, the discharge tended to begin on the edge of the edge of the electrode rather than in the center. If the initial discharge was from the edge of the electrode, then the charges would pass through almost transverse magnetic fields to get to the other electrode. The magnetic field may also affect the ability of the water molecule to interact with the proton to form the hydronium ion, thereby disrupting the current path being formed in the water. Magnetic fields have been demonstrated to be effective for shielding high voltage systems in vacuum and there may be a similar mechanism in water. The magnetic fields employed in this experiment were very small and may account for the small changes in the output but give an inducement to continue this line of research to see if increasing the magnetic field strength will increase the breakdown field strength.

The first experiment using the $SF_6$ gas gave some promising results with a significant increase in the $\tau_{eff}$. Sulfur hexafluoride was chosen because of its electro-negative quality which is why it is used in spark gap switches. The gas captures low energy electrons as they move across the gap thereby increasing the voltage holdoff of the spark gap switch. For this reason, the gas was used in the water to see if it would have a similar effect. The results seen in the first series of shots may have been due to a bad capacitor that was about to burst and is why that series was terminated. Two additional series of shots were run without the same increase in $\tau_{eff}$ seen in the first series. This may have been due to one of two things. The first was the inability to determine how much $SF_6$ was actually mixed into the water. It is possible that only trace amounts of the gas actually circulated in the water such that there was an insufficient quantity to cause any effect on the discharge in the gap. The other possibility is that if it is proton motion in the water that sets up the discharge, as suggested in the Russian model, then the electronegativity of the $SF_6$ would have no effect on the discharge. An interesting

follow-on would be to use an electro-positive gas, such as argon or helium, to see if it would have an effect.

The Russians showed in several experiments [15] that adding HCl and similar chemicals to the water decreased the conductivity of the water during the prebreakdown period. They did not look at the field strength or voltage holdoff of the water gap. The HCl experiments were conducted to see if the decreased conductivity (increased resistivity) would relate to an increase in the field strength or voltage holdoff. The addition of HCl to the water would increase the number of $H^+$ ions and was expected to interfere with the development of charge transfer by creating an excess of hydronium molecules. The other possible effect was that the $Cl^-$ ions capturing the protons as they left the electrode surface would decrease the number of protons available to start the discharge. The only effect that adding the HCl seemed to have was to spread the energy over a longer time period as the concentration of HCl increased. Perhaps the phenomena seen by the Russians occurs if there is not sufficient voltage to cause a discharge in the gap.

The use of coatings has shown some potential for small surface areas but has either not been successful or not tried with larger surface areas. Polymer coatings may prove to be useful but no real conclusions can be drawn from the research discussed here because of the limited number of trials conducted. Additional research in this area may yield some significant results. The black wax coating did not prove to be successful. This could have been due to the method used in coating the electrode or may be due to the inability of the wax to be effective over large areas. Black wax has been shown to be effective for systems with extremely small electrode surface areas but this effect may not scale to larger sizes [7].

The results of the anodized aluminum electrode experiment indicate that anodizing the electrodes decreased the voltage holdoff level. This is inconsistent with the results that Gehman [9] demonstrated which showed that the

breakdown voltage of anodized aluminum was about 15% higher than plain aluminum. Gehman used a mixture of ethylene glycol and water, cooled to –30°C, which may account for the difference in the results.

The results of the experiments using the two surfactants, dodecylamine and laric acid, did not show increased breakdown voltage or increased time to breakdown. In fact, the laric acid lowered the breakdown voltage by a factor of two. We still believe that the key to the results reported by the Russians is some sort of coating grown on the electrodes by some chemical agent which is added to the water. However, in the limited time available we were able to try only the most obvious chemical candidates. Presumably, there is a chemical agent we did not think of.

Future research should look at what is happening at the surface of the electrode on a microscopic level. The region where the metal surface and the water interface is where the electric field breakdown is initiated. By suppressing the initiation of the arc, the electric field can rise to much higher levels and will either increase the maximum voltage across the gap or increase the time that the gap can withstand the voltage before arcing. Whether it is microbubbles or high intensity field points on the surface of the electrode that cause the initiation of the arc, anything that lowers the electric fields on the surface of the electrode would be beneficial. A coating must be able to electrically "smooth" the microscopic surface of the electrode. This is essentially how the diffusion electrodes work. By having a thin layer of conductive water close to the surface of the electrode, the electric field enhancement due to surface irregularities is lowered. This allows the field to build up until it reaches the intrinsic maximum in the gap. The diffusion electrodes would not be practical in a very large system but, as mentioned in the introduction, the Russians claimed that they have found a practical way to do what the diffusion electrodes are doing [19]. Much of the previous research has shown that there is usually a tradeoff between $E_{BD}$, $\tau_{eff}$, and $\varepsilon_r$. This should be re-

membered when considering the Russian claims. Additional research may show that the technique developed by the Russians may yield a higher breakdown strength in the water but may, for instance, reduce the capacitance of the system by reducing $\varepsilon_r$.

Many techniques to increase the field strength of water have been tried with various levels of success. Some of these techniques have been very successful in a laboratory setting but would not be useful in practical system. These techniques help provide insight into the breakdown mechanism and are the key to finding a practical technique for increasing the field strength of water. A practical technique would have to be independent of the geometry of the conductor and the type of material the conductor is made of. It would have to work on systems that had either a closed or open water circulation, and must not be harmful to the filtration and de-ionization system. The technique needs to be self-healing or undisturbed if a breakdown occurs in the water. Ideally, it would not require changing the water after every shot.

## SECTION 6

## REFERENCES


(1). Vorov'ev, V. V., V. A. Kapitonov, E. P. Kruglyakov, and Yu. A. Tsidulko, "Breakdown of water in a system with 'diffusion' electrodes," Soviet Physics Technical Physics, Vol. 25, No. 5, pp. 598-602, May 1980. (UNCLASSIFIED)

(2) Abramyan, E. A., V. A. Kornilov, et al., "Megavolt Energy-Concentrating Device," Soviet Physics - Doklady, Vol. 16, No. 11, pp. 983, May, 1972. (UNCLASSIFIED)

(3) Sincerny, P. S., "Electrical Breakdown Properties of Water for Repetitively Pulsed Burst Conditions," Proceedings of the 3rd IEEE International Pulsed Power Conference, pp. 222-225, June, 1981. (UNCLASSIFIED)

(4) Fenneman, D. B., "Pulsed High-Voltage Dielectric Properties of Ethylene Glycol/Water Mixtures," Journal of Applied Physics, Vol. 53, No. 12, pp. 8961-8968, December, 1982. (UNCLASSIFIED)

(5) Noyel, G. A., L. J. Jorat, O. Derriche, and J. R. Huck, "Dielectric Properties of Normal Supercooled Water Obtained in Alcohol/Water Mixtures," IEEE Transactions on Electrical Insulation, Vol. 27, No. 6, pp. 1136-1143, December, 1992. (UNCLASSIFIED)

(6) Zahn, M., Y. Ohki, K. Rhoads, M. LaGasse, and H. Matsuzawa, "Electro-Optic Charge Injection and Transport Measurements in Highly Purified Water and Water/Ethylene Glycol Mixtures," IEEE Transactions on Electrical Insulation, Vol. EI-20, No. 2, pp. 199-211, April, 1985. (UNCLASSIFIED)

(7) Szklarczyk, M., R. C. Kainthla, and J. O' M. Bockris, "On the Dielectric Breakdown of Water: An Electrochemical Approach," Journal of Electrochemical Society, Vol. 136, No. 9, pp. 2512-2520, September, 1989. (UNCLASSIFIED)

(8) Fenneman, D. B., and R. J. Gripshover, "Experiments on Electrical Breakdown in Water in the Microsecond Regime," IEEE Transactions on Plasma Science, Vol. PS-8, No. 3, pp. 209-213, September, 1980. (UNCLASSIFIED)

(9) Gehman Jr., V. H., D. B. Fenneman, and R. J. Gripshover, "Electrode Surface Effects on Unipolar Charge Injection in Cooled Liquid Dielectric Mixtures," Digest of Technical Papers - 4th IEEE Pulsed Power Conference, pp. 316-322, June, 1983. (UNCLASSIFIED)

(10) McLeod, A. R., and V. H. Gehman, Jr., "Water Breakdown Measurements of Stainless Steel and Aluminum Alloys for Long-Charging Times," Digest of Technical Papers. Sixth IEEE Pulsed Power Conference, pp. 57-59, 1987. (UNCLASSIFIED)

(11) Kuzhekin, I. P., "Investigation of the Breakdown by Rectangular Voltage Pulses of a Liquid in an Inhomogeneous Field," Soviet Physics - Technical Physics, Vol. 11, No. 12, pp. 1585-1589, June, 1967. (UNCLASSIFIED)

(12) Buttram, M., and M. O'Malley, "Breakdown of Water Under Long Term Stress," Digest of Technical Papers - 4th IEEE Pulsed Power Conference, pp. 327-330, 1983. (UNCLASSIFIED)

(13) Vorov'ev, V. V., V. A. Kapitonov, and E. P. Kruglyakov, "Increase of Dielectric Strength of Water in a System with 'Diffusion' Electrodes," JETP Letters, Vol. 19, No. 2, pp. 58-59, January, 1974. (UNCLASSIFIED)

(14) Hasted, J. B., Aqueous Dielectrics, Chapter 2: The Experimental Data for Liquid Water, Chapman and Hall, London, pp. 37-40, 1993. (UNCLASSIFIED)

(15) Ovchinnikov, I. T., and E. V. Yanshin, "Relaxation of Proton Conduction in Water in Strong Pulsed Electric Fields," Soviet Physics - Technical Physics, Vol. 29, No. 12, pp. 1431-1432, December, 1984. (UNCLASSIFIED)

(16) Yanshin, E. V., I. T. Ovchinnikov, and Yu. N. Vershinin, "Optical Study of Nanosecond Prebreakdown Phenomena in Water," Soviet Physics - Technical Physics, Vol. 18, No. 10, pp. 1303-1306, April, 1974. (UNCLASSIFIED)

(17) Yanshin, E. V., K. V. Yanshin, S. M. Korobeynikov, "Space Charge and Pre-Breakdown Bubbles Formation Near Point Electrodes Under Pulse Voltage," Conference Record, Eighth International Conference on Conduction and Breakdown in Dielectric Liquids, pp. 194-198, July, 1984. (UNCLASSIFIED)

(18) Ovchinnikov, I. T., K. V. Yanshin, and E. V. Yanshin, "Use of the Kerr Effect to Study Pulsed Electric Fields Near a Sharp Point in Water," Soviet Physics - Technical Physics, Vol. 23, No. 12, pp. 1487-1489, December, 1978. (UNCLASSIFIED)

(19) Yanshin, E. V., S. M. Korobeynikov, I. T. Ovchinnikov, S. G. Sarin, K. V. Yanshin, V. M. Kopylov, and A. V. Klepikov, "Physical Processes Limiting the Pulse Energy Release in Liquid Dielectrics," Proc. Tenth IEEE Pulsed Power Conference, June, 1995, p. 574. (UNCLASSIFIED)

(20) Terman, F. E., Radio Engineers' Handbook, McGraw-Hill Book Company, Inc., New York, p. 53, 1943. (UNCLASSIFIED)

(21) Coulter, T. J., A Compact Megavolt Marx Bank Generator Design, Master's thesis, Texas Tech University, Lubbock, Texas, August, 1994. (UNCLASSIFIED)

(22) Francis, J. F., "High Voltage Pulse Techniques," Technical Report No. 5 on AFOSR Grant 74-2639 "Dense Plasma Heating and Radiation Generation," Plasma Laboratory, Department of Electrical Engineering, Texas Tech University, Lubbock, Texas, 79409, p. 102, December, 1976. (UNCLASSIFIED)

(23) Kristiansen, M., Basic Electromagnetic Field Theory, U. S. Air Force Pulsed Power Lecture Series, Texas Tech University, No. 3, p. 18, 1978. (UNCLASSIFIED)

(24) Kenyon, V., personal communication, Naval Surface Warfare Center, Silver Springs, Maryland, June 22, 1993. (UNCLASSIFIED)

(25) Miller, R., personal communication, Maxwell Laboratories, San Diego, California, June 22, 1993. (UNCLASSIFIED)

(26) Wilkinson, M., and E. Chu, "Calibration of Capacitive Voltage Probes in Water-Dielectric, High Power Pulse Generators," Maxwell Laboratories, Inc., pp. 59-68, 1982. (UNCLASSIFIED)

(27) Bruning, J. L., and B. L. Kintz, Computational Handbook of Statistics 2nd ed., Scott, Foresman and Company, Glenview, Illinois, 1977. (UNCLASSIFIED)

(28) Childers, K., personal communication, Physics International, San Leandro, California, January 27, 1995. (UNCLASSIFIED)

(29) Martin, T., personal communication, Sandia National Laboratory, Albuquerque, New Mexico, January 27, 1995. (UNCLASSIFIED)

# APPENDIX A
# WATER BREAKDOWN FORMULAS

## A.1 DESCRIBING WATER BREAKDOWN LEVELS

During the early 1960's, J. C. Martin did considerable experimental work on the voltage breakdown levels in water. His work was done on water at standard temperature and pressure (STP). Considerable work has been done with water under high pressure but Martin's work was not in this area. From the data collected, Martin wrote several equations to describe the data. The two most common equations are

$$F\tau_{eff}^{1/3}A^{1/10} = 0.3\,, \tag{A.1}$$

for positive polarity and

$$F\tau_{eff}^{1/3}A^{1/10} = 0.6\,, \tag{A.2}$$

for negative polarity, where $F$ is the electric field breakdown level in MV/cm, $A$ is the area in cm$^2$, and $\tau_{eff}$ is the effective time in μs. These equations will give the electric field necessary to have a breakdown in the water for a given effective time, over a given area. For example, let $\tau_{eff}$ = 1 μs, and $A$ =1 cm$^2$, then $F$ of the first equation is 0.3 MV/cm. If the electric field is greater than or equal to 0.3 MV/cm, then a breakdown in the water can almost be guaranteed [28]. This would be referred to operating "at the JCM level." To operate at 60% JCM, the system is designed so that the maximum field strength, for this example, is less than or equal to 0.18 MV/cm.

What will be seen if the breakdown field of many discharges are measured is a Gaussian distribution. A typical normalized Gaussian distribution for this example would look like (Figure A-1) with $F$ from Martin's equation at the maximum of the curve. The significance of operating at 60% JCM would be the very low probability of a breakdown occurring in the water.

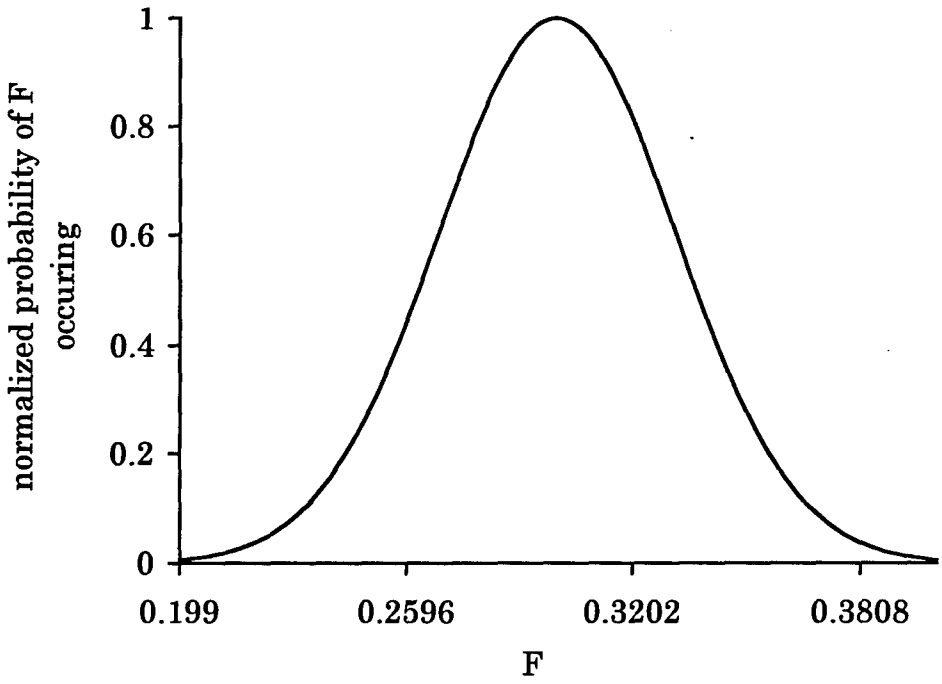


Figure A-1. Typical Gaussian curve.

A.2 SO, WHY DO NOT ALL MACHINES OPERATE AT 60% JCM?

Water is used as the insulator in pulsed power machines because it has a high relative dielectric constant ($\varepsilon_r$). This is important because the size of the machine depends on the amount of energy that can be stored in the insulator. Think of the water as the insulator in a parallel plate capacitor. The capacitance is given by

$$C = \frac{\varepsilon_o \varepsilon_r A}{d}, \tag{A.3}$$

where $\varepsilon_0$ is the dielectric constant of vacuum, $\varepsilon_r$ is the relative dielectric constant, $A$ is the surface area of the plate, and $d$ is the distance separating the two plates. With $\varepsilon_r$ of about 80, water becomes a very popular insulator for pulsed power machines. The energy stored in a capacitor is given by

$$E_c = \frac{1}{2} CV^2 \quad (A.4)$$

The electric field strength *(E)* is equal to the voltage *(V)* divided by the distance *(d)*. Substituting this into the energy equation gives you

$$E_c = \frac{1}{2} CE^2 d^2 . \quad (A.5)$$

So the energy stored in the capacitor increases to the square power of the electric field. This means that if the system is operating at 60% JCM then only 36% of the energy is stored that would be stored at 100% JCM. This has a significant impact on the design of the machine. Of course, it would not be a good idea to operate at JCM level because half of the shots would not be any good because of voltage breakdown in the water capacitor. In designing a machine, the cost of the size of the machine versus the number of bad shots tolerated would have to be weighed. This would not only be the data lost on a bad shot but the damage done to the machine.

## A.3 HOW CAN SANDIA OPERATE AT 120% JCM?

It should be remembered that the JCM equations at the beginning of this paper were based on empirical data and not theory [29]. This means that each of the parameters has a limited range for which the equations are valid. Extrapolating the equations outside of these ranges could cause trouble. The size of the pulsed power machines that are being built today are on a much larger scale than what was available at the time Martin did his experiments. The size and area dimensions of the Sandia machines are outside of the range of data for the JCM equations. Additional experiments were conducted by the Naval Research Laboratory in the late 1960's to expand Martin's equations. Considerable data were generated by W. H. Lupton and resulted in the Elbert-Lupton equations which are similar to the Martin equations.

The major difference is the exponent for the area term. The two Elbert-Lupton equations are

$$F\tau_{eff}^{1/3} A^{0.058} = 0.23, \tag{A.6}$$

for positive polarity, and

$$F\tau_{eff}^{1/3} A^{0.069} = 0.557, \tag{A.7}$$

for negative polarity. The Sandia machines operate under the Elbert-Lupton levels. For the area dimensions involved with the Sandia machines, if the Martin equations are used, it appears that the system is operating at the 120% level. PI uses the Elbert-Lupton equations to design their machines [28]. The DOUBLE EAGLE machine was designed at 60% Elbert-Lupton and has never had a breakdown in its water line.

The curves in Figure A-2 show the difference between the JCM levels and the Elbert-Lupton levels for various surface areas. The third trace is the 120% JCM level. As can be seen, for areas above 43,000 $cm^2$, the Elbert-Lupton curve crosses the 120% JCM curve.

The designers at Sandia [29] believe that the area term dependency disappears at very large areas, e.g., $A > 10^7$ $cm^2$.

## A.4 WHAT IS TEXAS TECH DOING?

The research conducted at Texas Tech investigates the effects of magnetic fields, electrode coatings and water additives on $E_{BD}$ and $\tau_{eff}$. No one has examined the effects of magnetic fields on water before. Various additives, such as alcohol and glycol, have been used to allow the water temperature to be lowered beyond its normal freezing point in order to increase $E_{BD}$ and $\tau_{eff}$. Additives that affect these two parameters directly have been looked at. Several different types of coatings on the electrode surfaces have been tried. The Texas Tech Pulsed Power Laboratory has used polymer and wax coatings on the surface of the electrodes. The Water Breakdown System in use at Texas

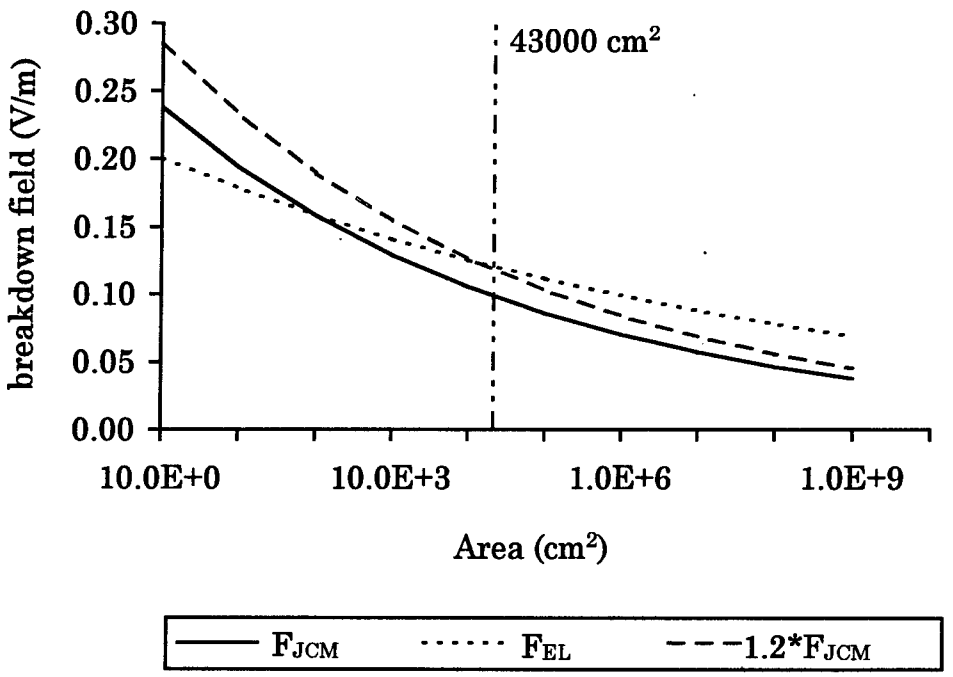


Figure A-2. Comparison of the breakdown field equations (F) versus surface area (A).

Tech is capable of delivering a 400 kV, 150 ns pulse to a 1.5 cm gap.

## A.4 ADDITIONAL WATER BREAKDOWN LEVEL INFORMATION

Starting with the equation for energy in a capacitor,

$$E_c = \frac{1}{2} C V^2, \tag{A.8}$$

where $E_c$ is in joules, C is in farads, and V is in volts. The equation for the electric field (F) for the simplest case of parallel plate geometry is

$$F = \frac{V}{d}, \tag{A.9}$$

where V is in volts and d is in meters. For other geometries, various field enhancement factors must be included. Combining the two equations yields

$$E_c = \frac{1}{2} C F^2 d^2 . \tag{A.10}$$

For a parallel plate capacitor, the equation for the capacitance is given by

$$C = \frac{\varepsilon_o \varepsilon_r A}{d}, \tag{A.11}$$

where $\varepsilon_o = 8.85 \times 10^{-12}$ farad/meter, $\varepsilon_r$ is the relative dielectric constant, $A$ is the area of the two plates in meter$^2$, and $d$ is the distance between the two plates in meters. Combining Eqs. (A.10) and (A.11) gives

$$E_c = \frac{1}{2} \frac{\varepsilon_o \varepsilon_r A}{d} F^2 d^2 , \tag{A.12}$$

which reduces to

$$E_c = \frac{1}{2} \varepsilon_o \varepsilon_r A F^2 d . \tag{A.13}$$

By picking

$$A F^2 d = \frac{2}{\varepsilon_o} \text{ (volts}^2 \text{ meter)}, \tag{A.14}$$

then

$$E_c \sim \varepsilon_r . \tag{A.15}$$

By graphing this along with three of the most common insulators - oil, ethylene glycol (antifreeze), water, the importance that water plays in pulsed power machines can be seen (Figure A-3).

Next, the effect of the insulating medium on the amount of energy stored in the capacitor as the electric field increases can be looked at. Going back to Eq. (A.16)

$$E_c = \frac{1}{2} \varepsilon_o \varepsilon_r A F^2 d , \tag{A.16}$$

and setting

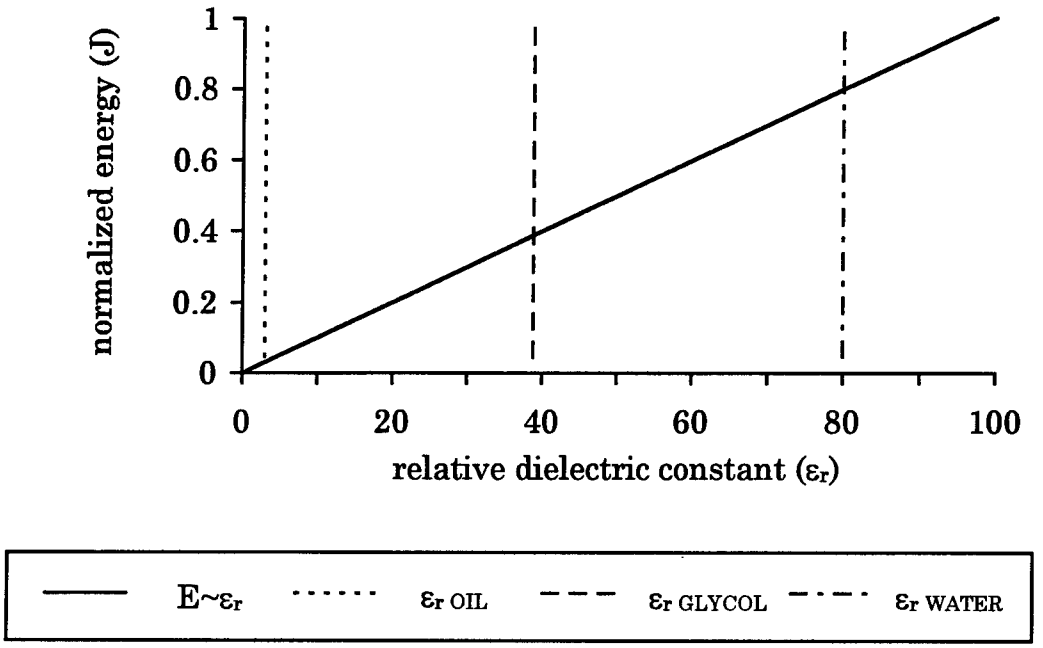


Figure A-3. Normalized Energy ($E_C$) versus relative dielectric constant ($\varepsilon_r$) for $AF^2d = 2/\varepsilon_o$.

$$Ad = \frac{2}{\varepsilon_o}\ (\mathrm{m}^3), \tag{A.17}$$

then

$$E_c \sim \varepsilon_r F^2 . \tag{A.18}$$

Remember that $\varepsilon_r$ for oil, ethylene glycol, and water are 2.2, 39, and 80, respectively. Figure A-4 shows the effects of $\varepsilon_r$ on the energy stored as the electric field ($F$) increases.

Next, how the energy changes with respect to the area can be shown. The four cases for water using the J. C. Martin and Elbert-Lupton equations need to be looked at. J. C. Martin showed that

$$F\tau_{eff}^{1/3} A^{1/10} = 0.3, \tag{A.19}$$

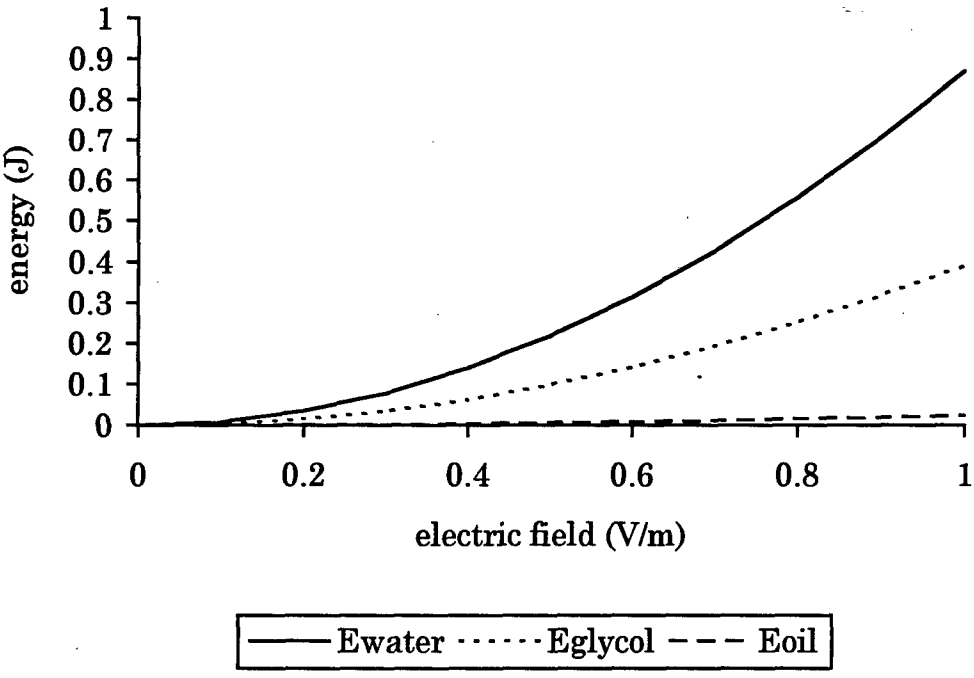


Figure A-4. Normalized energy ($E_C$) versus normalized electric field (F) for $Ad = 2/\varepsilon_o$.

for positive polarity and

$$F\tau_{eff}^{1/3}A^{1/10} = 0.6, \tag{A.20}$$

for negative polarity, where $F$ is the electric field breakdown level in MV/cm, $A$ is the area in cm$^2$, and $\tau_{eff}$ is the effective time in μs. Solving these two equations for $F$ gives us

$$F = \frac{0.3}{\tau_{eff}^{1/3}A^{1/10}}, \tag{A.21}$$

and

$$F = \frac{0.6}{\tau_{eff}^{1/3}A^{1/10}}. \tag{A.22}$$

The significance of the polarity dependence is that in non-parallel plate geometry, e.g., coaxial, the high field electrode (the smallest one), i.e., the inner coaxial electrode, should be negative. Reversing the polarity on coaxial systems is, therefore, not a good idea. It will lower the hold-off voltage by a factor of two and thus the energy by a factor of four.

Elbert-Lupton showed that

$$F\tau_{eff}^{1/3}A^{0.058} = 0.23, \tag{A.23}$$

for positive polarity, and

$$F\tau t_{eff}^{1/3}A^{0.069} = 0.557, \tag{A.24}$$

for negative polarity. Again, solving for $F$ gives

$$F = \frac{0.23}{\tau_{eff}^{1/3}A^{0.058}}, \tag{A.25}$$

for positive polarity, and

$$F = \frac{0.557}{\tau_{eff}^{1/3}A^{0.069}}, \tag{A.26}$$

for negative polarity. A set of four energy equations which have been designated as $E_{JCM+}$, $E_{JCM-}$, $E_{EL+}$, and $E_{EL-}$ for JCM positive, JCM negative, Elbert-Lupton positive, and Elbert-Lupton negative, respectively, can be derived.

For $E_{JCM+}$, start with Eq. (A.27) again

$$E_c = \frac{1}{2}\varepsilon_o\varepsilon_r AF^2 d. \tag{A.27}$$

Substituting Eq. (A.21) into Eq. (A.27) gives

$$E_{JCM+} = \frac{1}{2}\varepsilon_o\varepsilon_r A\left(\frac{0.3}{\tau_{eff}^{1/3}A^{1/10}}\right)^2 d. \tag{A.28}$$

The $A$ in Eq. (A.16) is in meter$^2$ while the $A$ in Eq. (A.21) is in cm$^2$. The easiest way to make these terms compatible is to convert the first $A$ to cm$^2$. This gives

$$E_{JCM+} = \frac{10^4}{2} \varepsilon_o \varepsilon_r A \left( \frac{0.3}{\tau_{eff}^{1/3} A^{1/10}} \right)^2 d . \qquad \text{(A.29)}$$

Rearranging and combining the terms now gives

$$E_{JCM+} = \frac{10^4}{2\tau_{eff}^{2/3}} \varepsilon_0 \varepsilon_R dA \frac{(0.3)^2}{A^{2/10}}, \qquad \text{(A.30)}$$

which gives, for a fixed $d$ and $\tau_{eff}$, the following proportionality relationship

$$E_{JCM+} \sim (0.3)^2 A^{(1-2/10)} . \qquad \text{(A.31)}$$

This gives the area relationship for $E_{JCM+}$. Doing the same for the other three equations -- Eqs. (A.22), (A.25), (A.26) -- gives

$$E_{JCM-} \sim (0.6)^2 A^{(1-2/10)}, \qquad \text{(A.32)}$$

$$E_{EL+} \sim (0.23)^2 A^{(1-2\cdot 0.058)}, \qquad \text{(A.33)}$$

and,

$$E_{EL-} \sim (0.557)^2 A^{(1-2\cdot 0.069)} . \qquad \text{(A.34)}$$

Graphing these four equations gives Figure A-5 which shows the relationships between the area and the energy for the four equations. As can be seen, there is a significant effect at very large areas on the amount of energy that can be stored depending on which set of equations used.

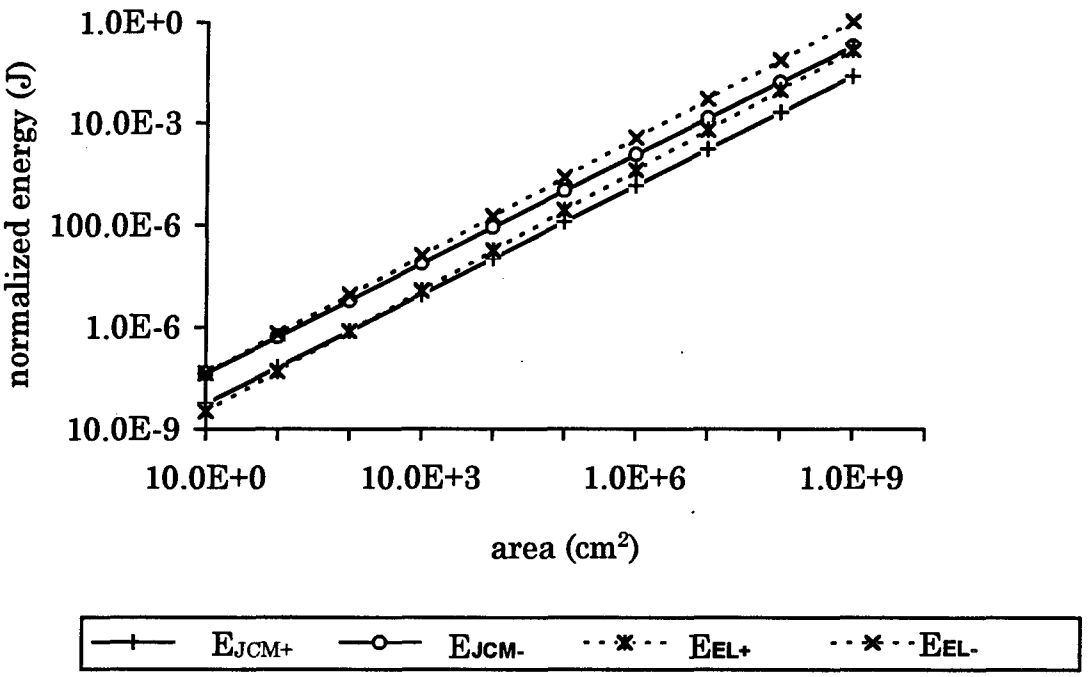


Figure A-5. Normalized energy versus area for the JCM and EL equations.

# APPENDIX B

## BIBLIOGRAPHY


Abramyan, E. A., V. A. Kornilov, et al., "Megavolt Energy-Concentrating Device," Soviet Physics - Doklady, Vol. 16, No. 11, pp. 983, May, 1972.

Adamian, Y. A., V. V. Titkov, and G. A. Shneerson, "Water Line with the Electrostatic Concentrator," Digest of Technical Papers, Ninth IEEE International Pulsed Power Conference, pp. 103-106, June, 1993.

Alkhimov, A. P., V. V. Vorob'ev, V. F. Klimkin, A. G. Ponomarenko, and R. I. Soloukhin, "The Development of Electrical Discharge in Water," Soviet Physics - Doklady, Vol. 15, No. 10, pp. 959-961, April, 1971.

Angell, C. A., Water a Comprehensive Treatise, Volume 7, Water and Aqueous Solutions at Subzero Temperatures, Chapter 1, "Supercooled Water," Edited by Felix Franks, Plenum Press, New York, NY, pp. 1-81.

Antonov, E. A., L. N. Gnatyuk, B. M. Stepanov, Yu. I. Filenko, and V. Ya. Tsarfin, "Holographic Investigation of Electrical Explosions of Conductors," High Temperature, Vol. 10, No. 6, pp. 1087-1091, 1971.

Arensburg, A., and S. Wald, "X-Ray Diagnostics of a Plasma-Jet-Liquid Interaction in Electrothermal Guns," Journal of Applied Physics, Vol. 73, No. 5, pp. 2145-2154, March, 1993.

Atten, P., and A. Saker, "Streamer Propagation Over a Liquid/Solid Interface," IEEE Transactions on Electrical Insulation, Vol. 28, No. 2, pp. 230-242, April, 1993.

Babula, E., A. Sierota, S. Zoledziowski, and J. H. Calderwood, "The Effect of Moisture on Partial Discharges in Dielectric Liquids," Conference Record, Eight International Conference on Conduction and Breakdown in Dielectric Liquids, pp. 209-213, July, 1984.

Baksht, R. B., I. M. Datsko, A. F. Korostelev, V. V. Loskutov, A. V. Luchinskii, and A. A. Chertov, "Nanosecond electrical explosion of thin wires," Soviet Journal of Applied Physics, Vol. 9, No. 6, pp. 706-710, 1983.

Balygin, I.E., "Electrical Breakdown of Liquid Dielectrics (A Review)," Translation of Elektrichestvo (Electricity), No. 1, pp. 89, 1954. Foreign Technology Report FTD-HT-23-772-72, 20 October 1972.

Bartnikas, R., "Dielectric Loss in Insulating Liquids," IEEE Transactions on Electrical Insulation, Vol. EI-2, No. 1, April, 1967.

Bell, W. R., "Influence of Specimen Size on the Dielectric Strength of Transformer Oil," IEEE Transactions on Electrical Insulation, Vol. EI-12, No. 4, August, 1977.

Berger, N., and P. Jay, "A New Impregnant for HV Power Capacitors," IEEE Transactions on Electrical Insulation, Vol. EI-21, No. 1, pp. 59-63, February, 1986.

Berger, T. L., "Effects of Surrounding Medium on Electrically Exploded Aluminum Foil Fuses," IEEE Transactions on Plasma Science, Vol. PS-8, No. 3, pp. 213-216, September, 1980.

Bernardes, J., and M. F. Rose, "Electrical Breakdown Characteristics of Sodium Chloride - Water Mixtures," Digest of Technical Papers - 4th IEEE Pulsed Power Conference, pp. 308-311, June, 1983.

Beroual, A., "Behavior of Charged and Uncharged Bubbles in Dielectric Liquids Subjected to Electric Stress," Journal of Applied Physics, Vol. 71, No. 3, pp. 1142-1145, February, 1992.

Beroual, A., "Electronic and Gaseous Processes in the Prebreakdown Phenomena of Dielectric Liquids," Journal of Applied Physics, Vol. 73, No. 9, pp. 4528-4533, May, 1993.

Beroual, A., and R. Tobazeon, "Prebreakdown Phenomena in Liquid Dielectrics," IEEE Transactions on Electrical Insulation, Vol. EI-21, No. 4, pp. 613-627, August, 1986.

Beruchev, N. G., E. P. Bol'shakov, et al., "Nanosecond High-Current Electron Accelerator," Instruments and Experimental Techniques, Vol. 26, Pt 1, No. 6, pp. 1259-1265, November-December, 1983.

Binns, D. F., and A. Jaberansari, "Effect of Temperature on the Electrical Breakdown of Conductor Samples in R-Temp and Envirotemp," Conference Record, Eighth International Conference on Conduction and Breakdown in Dielectric Liquids, pp. 250-254, July, 1984.

Birlaskedaran, S., and M. Darveniza, "Microdischarges from Particles in Transformer Oil," IEEE Transactions on Electrical Insulation, Vol. EI-11, No. 4, pp. 162-163, December, 1976.

Borsi, H., and U. Schroder, "Initiation and Formation of Partial Discharges in Mineral-Based Insulating Oil," IEEE Transactions on Dielectrics and Electrical Insulation, Vol. 1, No. 3, pp. 419-425, June, 1994.

Bozzo, R., G. Coletti, P. Molfino, and G. Molinari, "Electrode Systems for Dielectric Strength Controlling the Electro-Dielectrophoretic Effects," Conference Record, Eighth International Conference on Conduction and Breakdown in Dielectric Liquids, pp. 265-269, July, 1984.

Brzostek, E., and J. Kedzia, "Static Electrification in Aged Transformer Oil," IEEE Transactions on Electrical Insulation, Vol. EI-21, No. 4, pp. 609-612, August, 1986.

Burton, J. K., D. Conte, et al., "Multiple Channel Switching in Water Dielectric Pulse Generators," Proceedings of the 5th Symposium on Engineering Problems of Fusion Research, pp. 679-683, 1973.

Buttram, M., and M. O'Malley, "Breakdown of Water Under Long Term Stress," Digest of Technical Papers - 4th IEEE Pulsed Power Conference, pp. 327-330, 1983.

Camarcat, N., J. Delvaux, B. Etlicher, D. Mosher, G. Raboisson, and A. Perronnet, "Electrical pulsed power generators of the 1 TW class," Laser and Particle Beams, Vol. 3, part 4, pp. 415-455, 1985.

Cesari, S., and S. Yakov, "Considerations About the Impulse Breakdown and Power Frequency Partial Discharge Inception Voltages of Insulating Liquids," Conference Record, Eighth International Conference on Conduction and Breakdown in Dielectric Liquids, pp. 230-234, July, 1984.

Chadband, W. G., "On Variations in the Propagation of Positive Discharges Between Transformer Oil and Silicone Fluids," Journal Physics D: Applied Physics, Vol. 13, pp. 1299-1307, 1980.

Chadband, W. G., "The Ubiquitous Positive Streamer," IEEE Transactions on Electrical Insulation, Vol. 23, No. 4, pp. 697-706, August, 1988.

Chadband, W. G., and T. M. Sufian, "Experimental Support for a Model of Positive Streamer Propagation in Liquid Insulation," IEEE Transactions on Electrical Insulation, Vol. EI-20, No. 2, pp. 239-246, April, 1985.

Chiu, C., C. W. Smith, and J. H. Calderwood, "Investigation of a Critical Region Between Corona and Discharge Channels in Highly Stressed Dielectric Liquids," Conference Record, Eighth International Conference on Conduction and Breakdown in Dielectric Liquids, pp. 164-170, July, 1984.

Colson, S. D., and T. H. Dunning, Jr., "The Structure of Nature's Solvent: Water," Science, Vol. 265, pp. 43-44, July, 1994.

Curry, R., P.D'A. Champney, C. Eichenberger, J. Fockler, D. Morton, R. Sears, I. Smith, R. Conrad, "The Development and Testing of Subnanosecond-Rise, Kilohertz Oil Switches for the Generation of High-Frequency Impulses," IEEE Transactions on Plasma Science, Vol. 20, No. 3, pp. 383-392, June, 1992.

Danikas, M., "Technical Report: Particles in Transformer Oil," IEEE Electrical Insulation Magazine, Vol. 7, No. 2, pp. 39-40, March/April, 1991.

Demidov, B. A., M. V. Ivkin, V. A. Petrov, and S. D. Fanchenko, "A High-Voltage Water Spark Gap with Laser Firing," Instruments and Experimental Techniques, Vol. 17, No. 1, pp. 131-133, 1974.

Denholm, A. S., J. J. Moriarty, W. R. Bell, J. R. Uglum, G. K. Simcox, J. Hipple, and S. V. Nablo, "Review of Dielectrics and Switching," Technical Report No. AFWL-TR-72-88, AFWL/DYX, Kirtland AFB, New Mexico 87117, 1988, (Limited Distribution).

Devins, J. C., S. J. Rzad, and R. J. Schwabe, "Breakdown and Prebreakdown Phenomena in Liquids," Journal of Applied Physics, Vol. 52, No. 7, pp. 4531-4545, July, 1981.

Dimeler, G. R., I. W. Mills, and J. J. Melchiore, "The Scope of Hydrogenation as a Refining Tool for the Manufacture of Transformer Oils," IEEE Transactions on Electrical Insulation, Vol. EI-4, No. 1, pp. 7-12, 1969.

Dingjiu, L., and C. Shoushen, "The Breakdown Voltage of Deionized Water and Transformer Oil in the Microsecond and Nanosecond Regions," Proceedings, Second International Conference on Properties and Applications of Dielectric Materials, Vol. 1, pp. 63-66, 1988.

Dotoku, K., H. Yamada, and S. Sakamoto, "Field Emission into Nonpolar Organic Liquids," Journal of Chemical Physics, Vol. 69, No. 3, pp. 1121-1125, August, 1978.

Duval, M., and C. Lamarre., "The Characterization of Electrical Insulating Oils by High-Performance Liquid Chromatography," IEEE Transactions on Electrical Insulation, Vol. EI-12, No. 5, pp. 340-348, October, 1977.

Duval, M., and D. Cauchon, "Paraffinic Transformer Oils for Use at Low Temperatures," IEEE Transactions on Electrical Insulation, Vol. EI-18, No. 6, pp. 586-590, December, 1983.

Eish, T. D., Y. A. Abed, and G. M. El-Salam, "Breakdown Phenomena in Transformer Oil Subjected to Direct Voltages with Ripple," Conference Record, Eighth International Conference on Conduction and Breakdown in Dielectric Liquids, pp. 245-249, July, 1984.

El-Sulaiman, A. A., and A. S. Ahmed, "Effects of Field Strength and Filtration on Burst Phenomena in Aged Transformer Oil Under High Non-Uniform DC Field," IEEE Transactions on Electrical Insulation, Vol. EI-18, No. 2, pp. 163-166, April, 1983.

Energy Sciences, Inc., "The Influence of Hydrostatic Pressure Upon the Dielectric Properties of Deionized Water," Performed under Contract No. F29601-71-C-0034, Air Force Weapons Laboratory, Kirtland AFB, NM, May, 1972.

Etlicher, B., N. Camarcat, C. Bruno, G. Roboisson, and A. Perronnet, "Scaling of the J. C. Martin breakdown equations to generators of the 1-TW class," Digest of Technical Papers - 4th IEEE Pulsed Power Conference, pp. 331-334, 1983.

Federov, V. M., "High Power Nanosecond Discharge Channel in Water," 5th Megagauss Conference, pp. 319-326, 1990.

Felici, N. J., "Blazing a Fiery Trail with the Hounds," IEEE Transactions on Electrical Insulation, Vol. 23, No. 4, pp. 497-503, August, 1988.

Fenneman, D. B., "Pulsed High-Voltage Dielectric Properties of Ethylene Glycol/Water Mixtures," Journal of Applied Physics, Vol. 53, No. 12, pp. 8961-8968, December, 1982.

Fenneman, D. B., and R. J. Gripshover, "Experiments on Electrical Breakdown in Water in the Microsecond Regime," IEEE Transactions on Plasma Science, Vol. PS-8, No. 3, pp. 209-213, September, 1980.

Fenneman, D. B., and R. J. Gripshover, "High Power Dielectric Properties of Water Mixtures," Digest of Technical Papers - 4th IEEE Pulsed Power Conference, pp. 302-307, June, 1983.

Fleszynski, J., and B. Lutynski, "Macroparticle-Initiated Breakdown of Insulating Oil," Conference Record, Eighth International Conference on Conduction and Breakdown in Dielectric Liquids, pp. 275-279, July, 1984.

Forster E. O., "Critical Assessment of the Electrical Breakdown Process In Dielectric Fluids," IEEE Transactions on Electrical Insulation, Vol. EI-20, No. 5, pp. 891-896, October, 1985.

Forster, E. O., "Electric Conductance in Liquid Hydrocarbons," IEEE Transactions on Electrical Insulation, Vol. EI-2, No. 1, pp. 10-18, April, 1967.

Forster, E. O., "Partial Discharges and Streamers in Liquid Dielectrics, the Significance of the Inception Voltage," IEEE Transactions on Electrical Insulation, Vol. 28, No. 6, pp. 941-946, December, 1993.

Forster, E. O., "Progress in the Field of Electric Properties of Dielectric Liquids," IEEE Transactions on Electrical Insulation, Vol. 25, No. 1, pp. 45-53, February, 1990.

Forster, E. O., "Research in the Dynamics of Electrical Breakdown in Liquid Dielectrics," IEEE Transactions on Electrical Insulation, Vol. EI-15, No. 3, pp. 182-185, June, 1980.

Forster, E. O., and P. Wong, "High Speed Laser Schlieren Studies of Electrical Breakdown in Liquid Hydrocarbons," IEEE Transactions on Electrical Insulation, Vol. EI-12, No. 4, pp. 435-442, December, 1977.

Frei, C. J., "Weibull Statistical Analysis of Dielectric Breakdown in N-Hexane," Conference Record, Eighth International Conference on Conduction and Breakdown in Dielectric Liquids, pp. 217-224, July, 1984.

Friedman, M., and M. Ury, "Chemically Enhanced Opening Switch for Generating High-Voltage Pulses," Review of Scientific Instruments, Vol. 48, No. 3, pp. 279-281, March, 1977.

Fuhr, J., and W. F. Schmidt, "Time-Resolved Current-Voltage Measurement of the Spark Breakdown in Liquid N-Hexane," Conference Record, Eighth International Conference on Conduction and Breakdown in Dielectric Liquids, pp. 235-240, July, 1984.

Fuhr, J., W. F. Schmidt, and S. Sato, "Spark Breakdown of Liquid Hydrocarbons. I. Fast Current and Voltage Measurements of the Spark Breakdown in Liquid n-hexane," Journal of Applied Physics, Vol. 59, No. 11, pp. 3694-3701, June, 1986.

Fuhr, J., and W. F. Schmidt, "Spark Breakdown of Liquid Hydrocarbons. II. Temporal Development of the Electric Spark Resistance in n-pentane, n-hexane, 2,2 dimethylbutane, and n-decane," Journal of Applied Physics, Vol. 59, No. 11, pp. 3702-3708, June, 1986.

Garton, G. C., E. C. Rogers, and E. H. Reynolds, "Discussion on Dielectric Loss and Voltage Breakdown in Liquid Nitrogen and Hydrogen," IEEE Transactions on Electrical Insulation, pp. 47-48, March, 1971.

Gavrilov, G. N., V. V. Petukhov, A. G. Ryabinin, G. A. Ryabinin, and T. V. Brublevskaya "Total Hydrodynamic Efficiency of an Underwater Electric Discharge," Soviet Physics - Technical Physics, Vol. 22, No. 7, pp. 868-870, July, 1977.

Gavrilov, I. M., V. R. Kukhta, V. V. Lopatin, and P. G. Petrov, "Dynamics of Prebreakdown Phenomena in a Uniform Field in Water," IEEE Transactions on Dielectrics and Electrical Insulation, Vol. 1, No. 3, pp. 496-502, June, 1994.

Gehman Jr., V. H., D. B. Fenneman, and R. J. Gripshover, "Electrode Surface Effects on Unipolar Charge Injection in Cooled Liquid Dielectric Mixtures," Digest of Technical Papers - 4th IEEE Pulsed Power Conference, pp. 316-322, June, 1983.

Girdinio, P., G. Liberti, P. Molfino, G. Molinari, and A. Viviani, "A New Class of Uniform Field Electrodes for Dielectric Strength Tests in Dielectric Liquids," Conference Record, Eighth International Conference on Conduction and Breakdown in Dielectric Liquids, pp. 225-229, July, 1984.

Gomer, R., "Field Emission and Field Ionization in Condensed Phases," Accounts of Chemical Research, Vol. 5, No. 2, pp. 41-48, February, 1972.

Graneau, P., and P. N. Graneau, "Electrodynamic Explosions in Liquids," Applied Physics Letters, Vol. 46, No. 5, pp. 468-470, March, 1985.

Guenther, A. H., G. L. Zigler, J. R. Bettis, and R. P. Copeland, "Laser triggered switching of a pulsed, charged, oil filled spark gap," Review of Scientific Instruments, Vol. 46, No. 7, pp. 914-920, 1975.

Hakim, R. M., "The Effect of Oxidation on the Dielectric Properties of an Insulating Oil," IEEE Transactions on Electrical Insulation, Vol. EI-7, No. 4, pp. 185-195, December, 1972.

Hakim, R. M., "The Properties of an Insulating Oil and Its Fractions at Low Temperatures," IEEE Transactions on Electrical Insulation, Vol. EI-10, No. 4, pp. 124-134, December, 1975.

Hakim, R. M., R. G. Oliver, and H. St-Onge, "The dielectric properties of silicone fluids," Erratum: IEEE Transactions on Electrical Insulation, Vol. EI-13, No. 1, p. 65, 1978.

Halpern, B., and R. Gomer, "Field Emission in Liquids," The Journal of Chemical Physics, Vol. 51, No. 3, pp. 1031-1047, August, 1969.

Halpern, B., and R. Gomer, "Field Ionization in Liquids," The Journal of Chemical Physics, Vol. 51, No. 3, pp. 1048-1056, August, 1969.

Hasted, J. B., Aqueous Dielectrics, Chapman and Hall, London, 1993.

Hasted, J. B., Water a Comprehensive Treatise, Volume 1, The Physics and Physical Chemistry of Water, Chapter 7, "Liquid Water: Dielectric Properties," Edited by Felix Franks, Plenum Press, New York, NY, pp. 255-309, 1972.

Hasted, J. B., Water a Comprehensive Treatise, Volume 2, Water in Crystalline Hydrates Aqueous Solutions of Simple Nonelectrolytes, Chapter 7, "Dielectric Properties," Edited by Felix Franks, Plenum Press, New York, NY, pp. 405-458, 1973.

Hausler, E., and L. Stein, "Fokussierbare Unterwasserimpulsschallquellen," Acustica, Vol. 49, No. 4, pp. 273-279, 1981, (German).

Hayashi, M., O. Yamamoto, H. Isa, C. Uenosono, Y. Mino, and T. Tani, "Studies on Corona in Transformer Oil by Measurement of Space Charge," Conference Record, Eighth International Conference on Conduction and Breakdown in Dielectric Liquids, pp. 204-208, July, 1984.

Hebner, R. E., E. F. Kelley, E. O. Forster, and G. J. Fitzpatrick, " Observation of Prebreakdown and Breakdown Phenomena in Liquid Hydrocarbons Under Nonuniform Field Conditions," Conference Record, Eighth International Conference on Conduction and Breakdown in Dielectric Liquids, pp. 185-189, July, 1984.

Henson, B. L., "Corona Discharge from Fine Points in Liquid Helium," Physics Letters, Vol. 33A, No. 2, pp. 91-92, October, 1970.

Hosticka, C., "Dependence of Uniform/Nonuniform Field Transformer Oil Breakdown on Oil Composition," IEEE Transactions on Electrical Insulation, Vol. EI-14, No. 1, pp. 43-50, February, 1979.

Huck, J. R., G. A. Noyel, and L. J. Jorat, "Dielectric Properties of Supercooled Glycerol-Water Solutions," IEEE Transactions on Electrical Insulation, Vol. 23, No. 4, pp. 627-638, August, 1988.

Inuishi, Y., "Effect of Space Charge and Structure on Breakdown of Liquid and Solid," IEEE Transactions on Electrical Insulation, Vol. EI-17, No. 6, pp. 488-492, December, 1982.

Itahashi, S., M. Sone, and H. Mitsui, "Effect of dissolved water in several kinds of liquid dielectrics on conduction," Proceedings of the 1991 CEIDP, pp. 482-487.

Jaksts, A. and A. D. Cross, "High Speed Streak Photography of the Breakdown of Transformer Oil and the Dependence of its Nature on Local Stored Energy," IEEE Transactions on Electrical Insulation, Vol. EI-18, No. 6, pp. 599-604, December, 1983.

Jefferies, M., and K. Mathes, "Dielectric Loss and Voltage Breakdown in Liquid Nitrogen and Hydrogen," IEEE Transactions on Electrical Insulation, Vol. EI-5, No. 3, pp. 83-91, September, 1970.

Johnson, D. L., and J. P. VanDevender, "Low Prepulse, High Power Density Water Dielectric Switching," Digest of Technical Papers - 2nd IEEE International Pulsed Power Conference, pp. 191-194, June, 1979.

Johnson, D. L., and J. P. VanDevender, and T. H. Martin, "High Power Density Water Dielectric Switching," IEEE Transactions on Plasma Science, Vol. PS-8, No. 3, pp. 204-209, September, 1980.

Jones, H. M., and E. E. Kunhardt, "Development of Pulsed Dielectric Breakdown in Liquids," Journal of Physics D: Applied Physics, Vol. 28, No. 1, p. 178, 1995.

Jones, H. M., and E. E. Kunhardt, "Electron Impact Ionization and Dielectric Breakdown in Liquid Xe and Ar," Conference Record of the 1994 IEEE International Symposium on Electrical Insulation, pp. 442-445, June 1994.

Jones, H. M., and E. E. Kunhardt, "Monte Carlo Investigation of Electron-Impact Ionization in Liquid Xenon," Physical Review B, Vol. 48, No. 13, pp. 9382-9387, October 1993.

Jones, H. M., and E. E. Kunhardt, "Pulsed Dielectric Breakdown of Pressurized Water and Salt Solutions," Journal of Applied Physics, Vol. 77, No. 2, p. 795, 1995.

Jones, H. M., and E. E. Kunhardt, "Submicrosecond Breakdown and Prebreakdown Phenomena in Water: Influence of Pressure, Conductivity, and Gap Separation," Conference Record of the 1994 IEEE International Symposium on Electrical Insulation, pp. 442-445, June 1994.

Jones, H. M., and E. E. Kunhardt, "The Influence of Pressure and Conductivity on the Pulsed Breakdown of Water," IEEE Transactions on Dielectrics and Electrical Insulation, Vol. 1, No. 6, pp. 1016-1025, December, 1994.

Kadish, A., and W. B. Maier, II, "Electromagnetic Radiation from Abrupt Current Changes in Electrical Discharges." Journal of Applied Physics, Vol. 70, No. 11, pp. 6700-6711, December, 1991.

Kaneko, T., M. Hara, and M. Akazaki, "Effects of Voltage on Dielectric Breakdown Characteristics in Gaps Partially Immersed in Liquid Nitrogen," Conference Record, Eighth International Conference on Conduction and Breakdown in Dielectric Liquids, pp. 270-274, July, 1984.

Kang, B. P., "Stability of Electrical-Insulating Oils," IEEE Transactions on Electrical Insulation, Vol. EI-5, No. 2, pp. 41-46, June, 1970.

Kang, B. P., "Thermal Dependency of Viscosity, Power Factor, and Ion Content of Electrical Insulating Oils-III Predictions of Power Factor of Oil Blends Through the Concept of Ion Content," IEEE Transactions on Electrical Insulation, Vol. EI-2, No. 2, pp. 121-128, August, 1967.

Kang, B. P., "Thermal Dependency of Viscosity, Power Factor, and Ion Content of Electrical Insulating Oils-II Characteristics of Blended Insulating Oils," IEEE Transactions on Electrical Insulation, Vol. EI-2, No. 1, pp. 55-69, April, 1967.

Kao, K., and J. McMath, "Time-Dependent Pressure Effect in Liquid Dielectrics," IEEE Transactions on Electrical Insulation, Vol. EI-5, No. 3, pp. 64-68, September, 1969.

Kao, K., and M. Rashwan, "On the Thermal Activation Energy for High-Field Electric Conduction in Dielectric Liquids," IEEE Transactions on Electrical Insulation, Vol. EI-13, No. 2, pp. 86-93, April, 1978.

Kao, K. C., "Theory of high-field electric conduction and breakdown in dielectric liquids," IEEE Transactions on Electrical Insulation, Vol. EI-11, No. 4, pp. 121-128, 1976.

Kedzia, J., and E. Brozostek, "Static Electrification in Transformer Oil as a Measure of its Aging," IEEE Transactions on Electrical Insulation, Vol. EI-19, No. 2, pp. 101-106, April, 1984.

Kelly, E. F., and R. E. Hebner Jr., "Electro-Optic Field Measurement at a Needle Tip and Streamer Initiation in Nitrobenzene," 1986 Annual Report Conference on Electrical Insulation and Dielectric Phenomena, IEEE, pp. 272-277, 1986.

Kelly, E. F., and R. E. Hebner Jr., "The Electric Field Distribution Associated with Prebreakdown Phenomena in Nitrobenzene," Journal of Applied Physics, Vol. 52, No. 1, pp. 191-195, January, 1981.

Khalifa, M., and A. Nosseir, "Temporal Variation of Conduction Currents in Liquid Insulants Under High Direct Voltages," IEEE Transactions on Electrical Insulation, Vol. EI-11, No. 2, pp. 51-54, June, 1976.

Kitani, I., and K. Arii, "Impulse Tree and Discharge Light in PMMA Subjected to Nanosecond Pulses," IEEE Transactions on Electrical Insulation, Vol. EI-19, No. 4, pp. 281-287, August, 1984.

Klimkin, V., "Mechanisms of Electrical Breakdown of Water from Pointed Anode in the Nanosecond Range," Soviet Technical Physics Letters, Vol. 16, No. 2, pp. 146-147, February, 1990.

Koldamasov, A. I., "Plasma Formation in Cavitating Dielectric Liquid," Soviet Physics - Technical Physics, Vol. 36, No. 2, pp. 234-235, 1991.

Korobeynikov, S. M., and E. V. Yanshin, "Bubble Model: Time Dependent Pressure Effect in Liquids," Conference Record of the 10th International Conference on Conduction and Breakdown in Dielectric Liquids, pp. 360-364, 1990.

Korobeynikov, S. M., and E. V. Yanshin, "Dynamics of the Electrostriction Pressure in a Fluid Near a Spherical Electrode," Soviet Physics - Technical Physics, Vol. 28, No. 10, pp. 1288-1290, October, 1983.

Kovsharov, N. F., A. V. Luchinskii, et al., "SNOP-3 Pulse Generator," Instruments and Experimental Techniques, Vol. 30, No. 6, Part 1, pp. 1367-1373, May, 1988.

Krasucki, Z., High Voltage Technology, Chapter 7, "Breakdown of Commercial Liquid and Liquid-Solid Dielectrics," Edited by L. L. Alston, Oxford University Press, London, pp. 129-143, 1968,

Krivitskii, E. V., "On the Destruction of Phase Uniformity in Liquid Dielectrics Subjected to a Pulsed Voltage," Soviet Physics - Technical Physics, Vol. 36, No. 1, pp. 4-7, January, 1991.

Krivitskii, E. V., V. D. Kustovskii, and A. P. Slivinskii, "Effect of the Initial Conditions on the Dynamics of an Underwater Spark. I. Effect of the Parameters of the Generator and the Medium," Soviet Physics - Technical Physics, Vol. 25, No. 8, pp. 993-998, August, 1980.

Kuffel, E., and W. S. Zaengl, High Voltage Engineering, Section 5.14.2, Breakdown in Liquids, Pergamon Press, New York, pp. 411-421, 1984.

Kuleshov, V. M., S. L. Nedoseev, V. P. Smirnov, and A. M. Spektor, "Switching characteristics of a discharge in water," Soviet Physics - Technical Physics, Vol. 19, No. 1, pp. 150-151, 1974.

Kuskova, N. I., "Mechanisms of Electrical Breakdown in Water," Soviet Technical Physics Letters, Vol. 15, No. 12, December, 1989.

Kuzhekin, I. P., "Investigation of the Breakdown by Rectangular Voltage Pulses of a Liquid in an Inhomogeneous Field," Soviet Physics - Technical Physics, Vol. 11, No. 12, pp. 1585-1589, June, 1967.

Lagunov, V. M., and V. M. Fedorov, "Use of Water Insulation in the Pulsed Current Sources and Electron Accelerators of the Novosibirsk Institute of Nuclear Physics," Soviet Journal of Applied Physics, Vol. 4, No. 3, pp. 396-403, May-June, 1978.

Lee, W. M., and R. D. Ford, "Pressure Measurements Correlated with Electrical Explosion of Metals in Water," Journal of Applied Physics, Vol. 64, No. 8, pp. 3851-3854, October, 1988.

Lesaint, O., and R. Tobazeon, "Study of the Generation by Acute Electrodes of a Gaseous Phase in Dielectric Liquids Subjected to High A. C. or Step Voltages," Conference Record, Eighth International Conference on Conduction and Breakdown in Dielectric Liquids, pp. 176-179, July, 1984.

Lewis, T. J., High Voltage Technology, Chapter 6, The Electrical Conduction and Strength of Pure Liquids, Edited by L. L. Alston, Oxford University Press, London, pp. 111-127, 1968.

Lhiaubet, C., and R. M. Meyer, "Method of Indirect Determination of the Anodic and Cathodic Voltage Drops in Short High-Current Electric Discharges in a Dielectric Liquid," Journal of Applied Physics, Vol. 52, No. 6, pp. 3929-3934, June, 1981.

Lischer, D. W., and A. Ramrus, "Laser Initiated Conduction of an Overvolted Water Spark Gap," Digest of Technical Papers - 3rd IEEE International Pulsed Power Conference, IEEE, New York, NY, pp. 478-481, 1981.

Mahajan, S. M., and T. S. Sudarshan, "Measurement of the Space Charge Field in Transformer Oil Using its Kerr Effect," IEEE Transactions on Dielectrics and Electrical Insulation, Vol. 1, No. 1, pp. 63-70, February, 1994.

Maksiejewski, J. L., "The Breakdown Process of a Liquid Trigatron," IEEE Transactions on Electrical Insulation, Vol. 23, No. 2, pp. 227-230, April, 1988.

Maksiejewski, J. L., "The Effect of Additives on the Time Characteristics of a Liquid Trigatron," IEEE Transactions on Electrical Insulation, Vol. EI-22, No. 3, pp. 237-239, June, 1987.

Maksiejewski, J. L., "Time-Lags of Triggered Spark Gaps in Liquid Hydrocarbons," Conference Record, Eighth International Conference on Conduction and Breakdown in Dielectric Liquids, pp. 260-264, July, 1984.

Maruska, H. P., E. O. Forster, and J. H. Enard, "Electrical Transport Processes in Heavy Hydrocarbon Fluids," IEEE Transactions on Electrical Insulation, Vol. EI-20, No. 6, pp. 947-955, December, 1985.

Mathes, K. N., "Influence of Electrical Discharges in Oil and Combinations of Oil and Paper." IEEE Transactions on Electrical Insulation, Vol. EI-11, No. 4, pp. 164-180, December, 1976.

McClintock, P. V. E., "Field Emission in Liquid Helium," Physics Letters, Vol. 29A, No. 8, pp. 453-454, June, 1969.

McGrath, P. B., and H. I. Marsden, "DC-Induced prebreakdown Events in N-Hexane," IEEE Transactions on Electrical Insulation, Vol. EI-21, No. 4, pp. 669-672, August, 1986.

McKenny, P. J., and P. B. McGrath, "Anomalous Positive Point Prebreakdown Behavior in Dielectric Liquids," IEEE Transactions on Electrical Insulation, Vol. EI-19, No. 2, pp. 93-100, April, 1984.

McLeod, A. R., and V. H. Gehman, Jr., "Water Breakdown Measurements of Stainless Steel and Aluminum Alloys for Long-Charging Times," Digest of Technical Papers. Sixth IEEE Pulsed Power Conference, pp. 57-59, 1987.

Megahed, I. Y., and A. A. Zaky, "Influence of Temperature and Pressure on Conduction Currents in Transformer Oil," IEEE Transactions on Electrical Insulation, Vol. EI-4, No. 4, pp. 99-103, December, 1969.

Mel'nikov, N. P., G. A. Ostroumov, and M. Yu. Stoyak, "The Development of an Electric Discharge in Aqueous Electrolytes," Soviet Physics - Doklady, Vol. 8, No. 2, pp. 176, August, 1963.

Melchiore, J. J., and I. W. Mills, "Factors Affecting Stability of Electrical Insulating Oils," IEEE Transactions on Electrical Insulation, Vol. EI-2, No. 2, pp. 150-155, 1967.

Messerschmitt, J., "Investigations of the Pressure Dependence of Electrical Breakdown of Purified Water and Saline Solutions," Digest of Technical Papers, Ninth IEEE International Pulsed Power Conference, pp. 56-58, June, 1993.

Miller, A. R., "Sub-Ohm Coaxial Pulse Generators, Blackjack 3, 4, and 5," 3rd IEEE International Pulsed Power Conference, pp. 200-205, 1981.

Moore, W. B., R. W. Stinnett, and D. H. McDaniel, "Supermite Vacuum Interface Design," Digest of Technical Papers. 5th IEEE Pulsed Power Conference, pp. 315-318, 1985.

Morcos, I., and F. Rizk, "A Surface Chemistry Approach to the Study of Solid Electrodes in Insulating Liquids," IEEE Transactions on Electrical Insulation, Vol. EI-12, No. 4, pp. 309-312, August, 1977.

Nakao, Y., H. Itoh, Y. Sakai, and H. Tagashira, "Studies of the Creepage Discharge on the Surface of Liquids," IEEE Transactions on Electrical Insulation, Vol. 23, No. 4, pp. 677-687, August, 1988.

Nelson, J. K., "Dielectric Fluids in Motion," IEEE Electrical Insulation Magazine, Vol. 10, No. 3, pp. 16-28, May/June, 1994.

Nosseir, A., "Effect of Dissolved Gases, Stress, and Gap Spacing on High-Field Conductivity in Liquid Insulants," IEEE Transactions on Electrical Insulation, Vol. EI-10, No. 2, pp. 58-62, June, 1975.

Noyel, G. A., L. J. Jorat, O. Derriche, and J. R. Huck, "Dielectric Properties of Normal Supercooled Water Obtained in Alcohol/Water Mixtures," IEEE Transactions on Electrical Insulation, Vol. 27, No. 6, pp. 1136-1143, December, 1992.

Ohashi, A., and M. Ueda, "Thermal Breakdown of Silicone Liquids Under Pulsed High-Frequency Field," IEEE Transactions on Electrical Insulation, Vol. EI-8, No. 4, pp. 128-133, December, 1973.

Oliveri, S., and R. Kattan, "Numerical Study of Single-Vapor-Bubble Dynamics in Insulating Liquids Initiated by Electrical Current Pulses," Journal of Applied Physics, Vol. 71, No. 1, pp. 108-112, January, 1982.

Ovchinnikov, I. T., and E. V. Yanshin, "A High-Voltage Pulse Electrooptical Bridge," Instruments and Experimental Techniques, Vol. 26, No. 1, pp. 100-103, 1983.

Ovchinnikov, I. T., and E. V. Yanshin, "Dipolar-Ion-Mediated Relaxation of Conduction in Water Associated with High-Voltage Impurities," Soviet Physics - Technical Physics, Vol. 29, No. 12, pp. 1430-1431, December, 1984.

Ovchinnikov, I. T., and E. V. Yanshin, "Relaxation of Proton Conduction in Water in Strong Pulsed Electric Fields," Soviet Physics - Technical Physics, Vol. 29, No. 12, pp. 1431-1432, December, 1984.

Ovchinnikov, I. T., K. V. Yanshin, and E. V. Yanshin, "Investigating Prebreakdown Fields in Water by Means of the Kerr Effect," Soviet Physics - Technical Physics, Vol. 19, No. 2, pp. 294-295, August, 1974.

Ovchinnikov, I. T., K. V. Yanshin, and E. V. Yanshin, "Use of the Kerr Effect to Study Pulsed Electric Fields Near a Sharp Point in Water," Soviet Physics - Technical Physics, Vol. 23, No. 12, pp. 1487-1489, December, 1978.

Pellinen, D. G., and I. Smith, "A reliable multimegavolt voltage divider," Review of Scientific Instruments, Vol. 43, No. 2, pp. 299-301, 1972.

Perkins, J. R., "Selection of Materials for Use as Electrical Insulation-A Philosophical and Systematic Approach," IEEE Transactions on Electrical Insulation, Vol. EI-6, No. 3, pp. 106-110, September, 1971.

Perret, J., "Study of the Dielectric Breakdown of Insulating Mineral Oils Under Impulse Voltages," IEEE Transactions on Electrical Insulation, Vol. EI-16, No. 4, pp. 339-345, August, 1981.

Petrovic, K., and D. Vitorvic, "Examination of Insulating Oils for Transformers by Instrumental Methods," IEEE Transactions on Electrical Insulation, Vol. EI-18, No. 6, pp. 591-598, December, 1983.

Pompili, M., C. Mazzetti, and E. O. Forster, "Partial Discharge Distributions in Liquid Dielectrics," IEEE Transactions on Electrical Insulation, Vol. 27, No. 1, pp. 99-105, February, 1992.

Prikhod'ko, N. "Electrical Breakdown of Dielectrics With a Dipole Structure," Translation of Tomsk Universitet Sibirskiy Fiziko-Tekhnicheskiv Institut Trudy, (High Voltage Laboratory), Vol. 6, No. 2, pp. 114-119, 1945. Foreign Technology Report NO. FTD-HC-23-1176-72, 20 July 1972.

Qui, Y., A. Sun, and E. Kuffel, "Improved Dielectric Strength of SF6 Gas with a Trichlorotrifluoroethane Vapor Additive," IEEE Transactions on Electrical Insulation, Vol. EI-22, No. 6, pp. 763-768, December, 1987.

Rabe, J. G., and W. F. Schmidt, "Discussion: Decomposition Products of Silicone Liquids due to Electric Discharges," IEEE Transactions on Electrical Insulation, Vol. EI-18, No. 6, pp. 662-663, December, 1983.

Ramu, T. S., and Y. N. Rao, "On the Evaluation of Conductivity of Mixtures of Liquid Dielectrics," IEEE Transactions on Electrical Insulation, Vol. EI-7, No. 2, pp. 55-60, June, 1972.

Rao, Y. N., and T. S. Ramu, "Determination of the Permittivity and Loss Factor of Mixtures of Liquid Dielectrics," IEEE Transactions on Electrical Insulation, Vol. EI-7, No. 4, December, 1972.

Ridah, S., "Shock Waves in Water," Journal of Applied Physics, Vol. 64, No. 1, pp. 152-158, July, 1988.

Rudenko, N. S., and V. I. Tsvetkov, "An Investigation of the Electric Strength of Some Liquid Dielectrics Subject to Nanosecond Voltage Pulses," Soviet Physics - Technical Physics, Vol. 10, No. 10, pp. 1417-1419, April, 1966.

Rudenko, N. S., and V. I. Tsvetkov, "Study of the Pulse Electrical Strength of Some Liquids," Soviet Physics - Technical Physics, Vol. 9, No. 6, pp. 837-839, December, 1964.

Rzad, S. J., and J. C. Devins, "The Influence of a DC Bias on Streamers Produced by Step Voltages in Transformer Oil and Over Solid-Liquid Interfaces," IEEE Transactions on Electrical Insulation, Vol. EI-18, No. 1, pp. 1-10, February, 1983.

Sacchi, C. A., "Laser-Induced Electric Breakdown in Water," Journal of the Optical Society Am B, Vol. 8, No. 2, pp. 337-344, February, 1991.

Saikan, S. and F. Shimizu, "Water Spark Gap for a Nitrogen Laser," Review of Scientific Instruments, Vol.46, No. 12, pp. 1700-1701, December, 1975.

Sakamoto, S., and H. Yamada, "Optical Study of Conduction and Breakdown in Dielectric Liquids," IEEE Transactions on Electrical Insulation, Vol. EI-15, No. 3, pp. 171-181, June, 1980.

Sarin, S. G., E. V. Yanshin, and S. M. Korobeynikov, "EHD Instabilities Registration in Liquids," Proceedings of the 3rd International Conference on Properties and Applications of Dielectric Materials, pp. 898-900, July, 1991.

Sawada, T., and T. Kitamori, "Detection of Ultrafine Particles in Ultrapure Water by Laser-Induced Breakdown Acoustic Effect," IEE 1988 Ultrasonics Symposium, pp. 711-716, 1988.

Sazama, F. J., and V. L. Kenyon, "A Streamer Model for High-Voltage Water Switches," IEEE Transactions on Plasma Science, Vol. PS-8, No. 3, pp. 198-203, September, 1980.

Schmidt, W. F., "Elementary Processes in the Development of the Electrical Breakdown of Liquids (A Review)," IEEE Transactions on Electrical Insulation, Vol. EI-17, No. 6, pp. 478-483, December, 1982.

Schmidt, W. F., and W. Schnabel, "Electron Injection into Dielectric Liquids by Field Emission," Zeitschrift fur Naturforschung A (Astrophysik, Physik, und Physikalische Chemie), Vol. 26A, No. 1, pp. 169-170, 1971.

Schnabel, W., and W. Schmidt, "Polymerization by High Electric Fields: Field Emission and Field Ionization," Journal of Polymer Science, Symposium No. 42, 273-280, 1973.

Schwinkendorf, W. E., "Development of Water as a High Energy Density Dielectric," Air Force Weapons Laboratory, Kirtland Air Force Base, New Mexico, December, 1976, Report No. AFWL-TR-76-113 (Limited Distribution).

Schwinkendorf, W. E., "Review of Electrical Breakdown Processes in Water," Air Force Weapons Laboratory, Kirtland Air Force Base, New Mexico, December, 1976, Report No. AFWL-TR-76-110 (Limited Distribution).

Schwinkendorf, W. E., "Study of Conduction and Electrical Breakdown of Dielectric Liquids," Air Force Weapons Laboratory, Kirtland Air Force Base, New Mexico, December, 1976, Report No. AFWL-TR-76-112 (Limited Distribution).

Sharbaugh, A. H., and P. K. Watson, "The Electric Strength of Hexane Vapor and Liquid in the Critical Region," Journal of Applied Physics, Vol. 48, No. 3, pp. 943-950, March, 1977.

Sharbaugh, A. H., J. C. Devins and S. J. Rzad, "Progress in the Field of Electric Breakdown in Dielectric Liquids," IEEE Transactions on Electrical Insulation, Vol. EI-13 No. 4, pp. 249-276, August, 1978.

Sharbaugh, A. H., J. C. Devins, and S. J. Rzad, "Review of past work on liquid breakdown," IEEE Transactions on Electrical Insulation, Vol. EI-15, No. 3, pp. 167-170, June, 1980.

Shaw, D. G., and S. W. Cichanowski, "A Changing Capacitor Technology-Failure Mechanisms and Design Innovations," IEEE Transactions on Electrical Insulation, Vol. EI-16, No. 5, pp. 399-413, October, 1981.

Shipman Jr., J. D., "Design and Performance of the New Multichannel Oil Output Switch on the Gamble IIA Water Dielectric Pulse Power Generator at NRL," Digest of Technical Papers - 3rd IEEE International Pulsed Power Conference, IEEE, New York, NY, pp. 475-477, 1981.

Shirai, M., and T. Ishii, "Evolution of Hydrogen from Insulating Oil in Transformers," IEEE Transactions on Electrical Insulation, Vol. EI-12, No. 4, pp. 266-272, August, 1977.

Shirai, M., S. Shimoji, and T. Ishii, "Thermodynamic study on the thermal decomposition of insulating oil," IEEE Transactions on Electrical Insulation, Vol. EI-12, No. 4, pp. 272-280, 1977.

Sincerny, P. S., "Electrical Breakdown Properties of Water for Repetitively Pulsed Burst Conditions," Proceedings of the 3rd IEEE International Pulsed Power Conference, pp. 222-225, June, 1981.

Skvarenina, T. L., "An Introduction to Electrical Breakdown in Dielectrics," USAF Air Command and Staff College, Maxwell AFB, AL, Report No. 85-2470, April, 1985.

Spence, P. W., Y. G. Chen, G. Frazier, and H. Calvin, "Inductance and Resistance Characteristics of Single-Site Untriggered Water Switches in Water Transfer Capacitor Circuits," Digest of Technical Papers - 2nd IEEE International Pulsed Power Conference, pp. 359-362, June, 1979.

Srebrov, B. A., L. P. Dishkova, and F. I. Kuzmanova, "Electrical Breakdown of a Small Gap Filled with Distilled Water," Soviet Technical Physics Letters, Vol. 16, No. 1, pp. 70-71, January, 1990.

Stekol'nikov, I. S., and V. Ya. Ushakov, "Discharge Phenomena in Liquids," Soviet Physics - Technical Physics, Vol. 10, No. 9, pp. 1307-1313, March, 1966.

Stricklett, K., and R. Brunt, "Partial Discharge and Dielectric Liquid Research," Research for Electric Energy Systems - An Annual Report, pp. 32-45, December, 1991.

Sueda, H., and K. C. Kao, "Prebreakdown Phenomena in High-Viscosity Dielectric Liquids," IEEE Transactions on Electrical Insulation, Vol. EI-17, No. 3, pp. 221-227, June, 1982.

Sufian, T. M., and W. G. Chadband, "Positive Streamer Propagation in Liquid Insulation," Conference Record, Eighth International Conference on Conduction and Breakdown in Dielectric Liquids, pp. 153-158, July, 1984.

Suzuki, T., and S. Murakami, "Decomposition Products of Silicone Liquid due to Electric Discharge," IEEE Transactions on Electrical Insulation, Vol. EI-18, No. 2, pp. 152-157, April, 1983.

Suzuki, T., H. Hiramoto, and M. Umeda, "Dependence of Breakdown Voltage of Silicone Liquid on Temperature," IEEE Transactions on Electrical Insulation, Vol. EI-18, No. 4, pp. 462-590, August, 1983.

Szklarczyk, M., R. C. Kainthla, and J. O'M. Bockris, "On the Dielectric Breakdown of Water: An Electrochemical Approach," Journal of Electrochemical Society, Vol. 136, No. 9, pp. 2512-2520, September, 1989.

Tobazeon, R., "Prebreakdown Phenomena in Dielectric Liquids," IEEE Transactions on Dielectrics and Electrical Insulation, Vol. 1, No. 6, pp. 1132-1147, December, 1994.

Tobazeon, R., and D. Philippe, "Prebreakdown Currents and Optical Events in Insulating Liquids Subjected to a Voltage Step in Point-Plane Geometry," Conference Record, Eighth International Conference on Conduction and Breakdown in Dielectric Liquids, pp. 190-193, July, 1984.

Tobazeon, R., J. C. Filippini, and C. Marteau, "On the Measurement of the Conductivity of Highly Insulating Liquids," IEEE Transactions on Dielectrics and Electrical Insulation, Vol. 1, No. 6, pp. 1000-1004, December, 1994.

Toriyama, Y., and U. Shinohara, "Electric Breakdown Field Intensity of Water and Aqueous Solutions," Physics Review, Vol. 51, No. 8, pp. 680, April, 1937.

Tsukioka, H., K. Sugawara, E. Mori, S. Hukumori, and S. Sakai, "New Apparatus for Detecting H2, CO, and CH4 Dissolved in Transformer Oil," IEEE Transactions on Electrical Insulation, Vol. EI-18, No. 4, pp. 409-419, August, 1983.

Ushakov, V. Ya., "Development of a Discharge in a Liquid Dielectric with Ramp Function Voltage Pulses," Soviet Physics - Technical Physics, Vol. 10, No. 10, pp. 1420-1423, April, 1966.

VanDevender, J. P., "The Resistive Phase of a High Voltage Water Spark," Journal of Applied Physics, Vol. 49, No. 5, pp. 2616-2620, May, 1978.

VanDevender, J. P., and T. H. Martin, "Untriggered water switching," IEEE Transactions on Nuclear Science, Vol. NS-22, No. 3, pp. 979-982, 1975.

Van Heesch, E. J. M., R. H. P. Lemmens, B. Franken, K. J. Ptasinski, and F. L. S. Geurts, "Pulsed Corona for Breaking up Air Bubbles in Water," IEEE Transactions on Dielectrics and Electrical Insulation, Vol. 1, No. 3, pp. 426-431, June, 1994.

Von Hippel, A., "The Dielectric Relaxation Spectra of Water, Ice, and Aqueous Solutions, and their Interpretation. 1. Critical Survey of the Status-quo for Water," IEEE Transactions on Electrical Insulation, Vol. 23, No. 5, pp. 801-816, October, 1988.

Von Hippel, A., "The Dielectric Relaxation Spectra of Water, Ice, and Aqueous Solutions, and their Interpretation. 2. Tentative Interpretation of the Relaxation Spectrum of Water in the Time and Frequency Domain," IEEE Transactions on Electrical Insulation, Vol. 23, No. 5, pp. 817-823, October, 1988.

Von Hippel, A., "The Dielectric Relaxation Spectra of Water, Ice, and Aqueous Solutions, and their Interpretation. 3. Proton Organization and Proton Transfer in Ice," IEEE Transactions on Electrical Insulation, Vol. 23, No. 5, pp. 825-840, October, 1988.

Vorob'ev, V. V., V. A. Kapitonov, and E. P. Kruglyakov, "Increase of Dielectric Strength of Water in a System with 'Diffusion' Electrodes," JETP Letters, Vol. 19, No. 2, pp. 58-59, January, 1974.

Vyvolokin, A. E., "Generation of SHF-Fields by Nontraditional Sources," Digest of Technical Papers, Ninth IEEE International Pulsed Power Conference, pp. 616-617, June, 1993.

Watson, P. K., and A. H. Sharbaugh, "The Electric Strength of Nitrogen at Elevated Pressures and Small Gap Spacings," Journal of Applied Physics, Vol. 40, No. 1, pp. 328-334, January, 1969.

Watson, P. K., W. G. Chadband, and W. Y. Mak, "Bubble Growth in Viscous and Non-Viscous Liquids Following a Localized Electrical Discharge," Conference Record, Eighth International Conference on Conduction and Breakdown in Dielectric Liquids, pp. 180-184, July, 1984.

Weber, B. V., R. J. Commisso, G. Cooperstein, J. M. Grossmann, D. D. Hinshelwood, D. Mosher, J. M. Neri, P. F. Ottinger, and S. J. Stephanakis, "Plasma Erosion Opening Switch Research at NRL," IEEE Transactions on Plasma Science, Vol. PS-15, No. 6, pp. 635-648, December, 1987.

Wilkinson, G. M., "Time-Dependent Capacitance Effects in Water Dielectric Switching," Digest of Technical Papers - 4th IEEE Pulsed Power Conference, pp. 323-326, June, 1983.

Wilkinson, G. M., and A. R. Miller, "Untriggered, Multisite Switching in Water at Microsecond Charging Times," presented at the 1986 High Voltage Workshop, (limited distribution).

Wong, P. P., and E. O. Forster, "The Dynamics of Electrical Breakdown in Liquid Hydrocarbons," IEEE Transactions on Electrical Insulation, Vol. EI-17, No. 3, pp. 203-220, June, 1982.

Xie, H. K., and K. C. Kao, "A Study of the Low-Density Regions Developed in Liquefied Polyethylene Under High Electric Fields," Conference Record, Eighth International Conference on Conduction and Breakdown in Dielectric Liquids, pp. 199-203, July, 1984.

Yamada, H., and T. Sato, "Electro-Optical Measurement of Pre-Breakdown Current in Dielectric Liquids," Conference Record, Eighth International Conference on Conduction and Breakdown in Dielectric Liquids, pp. 171-175, July, 1984.

Yamashita, H., E. O. Forster, and M. Pompili, "Streamer Formation in Perfluoropolyether Under Impulse Conditions," IEEE Transactions on Electrical Insulation, Vol. 28, No. 3, pp. 324-329, June, 1993.

Yamashita, H., T. Okada, and H. Amano, "Pre-Breakdown Current and Light Emission in Transformer Oil," Conference Record, Eighth International Conference on Conduction and Breakdown in Dielectric Liquids, pp. 159-163, July, 1984.

Yamazawa, K., M. Uemura, H. Yamashita, and E. O. Foster, "Pulse Measurements Using LED in Dielectric Liquids Under Impulse Voltages," IEEE Transactions on Dielectrics and Electrical Insulation, Vol. 1, No. 3, pp. 391-396, June, 1994.

Yanshin, E. V., and I. T. Ovchinnikov, "High Field Conduction Measurements in Water by Pulse Electrooptical Bridge," Conference Record of the 8th International Conference on Conduction and Breakdown in Dielectric Liquids, pp. 83-87, July, 1984.

Yanshin, E. V., K. V. Yanshin, S. M. Korobeynikov, "Space Charge and Pre-Breakdown Bubbles Formation Near Point Electrodes Under Pulse Voltage," Conference Record, Eighth International Conference on Conduction and Breakdown in Dielectric Liquids, pp. 194-198, July, 1984.

Yanshin, E. V., I. T. Ovchinnikov, and Yu. N. Vershinin, "Optical Study of Nanosecond Prebreakdown Phenomena in Water," Soviet Physics - Technical Physics, Vol. 18, No. 10, pp. 1303-1306, April, 1974.

Yasufuku, S., "Calorimetric Measurements of Water Dissolved in Dielectric Fluids," IEEE Transactions on Electrical Insulation, Vol. EI-17, No. 5, pp. 464-468, October, 1982.

Yasufuku, S., "General Properties of Mixtures of Naphthenic Insulating Oil with Alkyl-benzenes," IEEE Transactions on Electrical Insulation, Vol. EI-14, No. 6, pp. 343-346, December, 1979.

Yasufuku, S., and Y. Ishioka, "General Properties of Mixtures of Paraffinic Insulating Oil with Alkybenzenes," IEEE Transactions on Electrical Insulation, Vol. EI-15, No. 5, pp. 429-433, October, 1980.

Yasufuku, S., J. Ise, and S. Kobayashi, "Radiation-Induced Degradation Phenomena in Electrical Insulating Oils," IEEE Transactions on Electrical Insulation, Vol. EI-13, No. 1, pp. 45-50, February, 1978.

Yasufuku, S., T. Umemura, and T. Tanii, "Electric Conduction Phenomena and Carrier Mobility Behavior in Dielectric Fluids," IEEE Transactions on Electrical Insulation, Vol. EI-14, No. 1, pp. 28-35, February, 1979.

Yehia, S., and A. A. Zaky, "Some Factors Affecting the Direct Breakdown Voltage of Silicone Oil Under Nonuniform Fields," IEEE Transactions on Electrical Insulation, Vol. EI-18, No. 1, pp. 86-88, February, 1983.

Yoshino, K., "Dependence of Dielectric Breakdown of Liquids on Molecular Structure," IEEE Transactions on Electrical Insulation, Vol. EI-15, No. 3, pp. 186-200, June, 1980.

Yoshino, K., "Electrical Conduction and Dielectric Breakdown in Liquid Dielectrics," IEEE Transactions on Electrical Insulation, Vol. EI-21, No. 6, pp. 847-853, December, 1986.

Yoshino, K., S. H. Kim, K. Kaneto, and Y. Inuishi, "Dielectric Breakdown of Liquid Helium and Influence of Electrode Coating," Conference Record, Eighth International Conference on Conduction and Breakdown in Dielectric Liquids, pp. 241-244, July, 1984.

Young, D. R., "Electric Breakdown in CO2 from Low Pressures to the Liquid State," Journal of Applied Physics, Vol. 21, pp. 222-231, March, 1950.

Zahn, M., "Transform Relationship Between Kerr-Effect Optical Phase Shift and Non-uniform Electric Field Distributions," IEEE Transactions on Dielectrics and Electrical Insulation, Vol. 1, No. 2, pp. 235-246, April, 1994.

Zahn, M., S. Voldman, T. Takada, and D. B. Fenneman, "Charge Injection and Transport in High Voltage Water/Glycol Capacitors," Journal of Applied Physics, Vol. 54, No. 1, pp. 315-325, January, 1983.

Zahn, M., Y. Ohki, K. Rhoads, M. LaGasse, and H. Matsuzawa, "Electro-Optic Charge Injection and Transport Measurements in Highly Purified Water and Water/Ethylene Glycol Mixtures," IEEE Transactions on Electrical Insulation, Vol. EI-20, No. 2, pp. 199-211, April, 1985.

Zaky, A. A., and I. Megahed, "Effect of Organic Additives, Gas Phase, Stress, and Temperature on the Gassing Characteristics of Insulating Liquids," IEEE Transactions on Electrical Insulation, Vol. EI-7, No. 3, pp. 145-152, September, 1972.

Zaky, A. A., I. Y. Megahed, and S. A. Yehia, "The Direct Breakdown Voltage of Silicone Oil Under Uniform Fields," Conference Record, Eighth International Conference on Conduction and Breakdown in Dielectric Liquids, pp. 255-259, July, 1984.

Zaky, A. A., I. Y. Megahed, M. S. Khalil, "Effect of Dissolved Gases, Organic Additives and Field Configuration on Co-Field Motion in Insulating Oils," IEEE Transactions on Electrical Insulation, Vol. EI-14, No. 1, pp. 21-27, February, 1979.

Zaky, A. A., M. E. Zein Eldine, and R. Hawley, "Influence of electrode coatings on the breakdown strength of transformer oil," Nature, Vol. 202, pp. 687-688, 1964.

Zavtrak, S. T., and E. V. Korobko, "Behavior of Gas Bubbles in Liquid Dielectrics in the Presence of an External Electric Field," Soviet Physics - Technical Physics, Vol. 36, No. 3, March, 1991.

Zutavern, F., and M. Buttram, "Area and Time Dependence of the Breakdown of Water Under Long Term Stress," Annual Report. IEEE 1983 Conference on Electrical Insulation and Dielectric Phenomena, pp. 251-256, 1983.

**DISTRIBUTION LIST**
**DSWA-TR-97-30**

**DEPARTMENT OF DEFENSE**

BALLISTIC MISSILE DEFENSE OFFICE
ATTN: T/SL

DEFENSE INFORMATION SYSTEMS AGENCY
ATTN: COMMANDER

DEFENSE INTELLIGENCE AGENCY
ATTN: DT-4A
ATTN: DT-4C
ATTN: TWJ

DEFENSE SPECIAL WEAPONS AGENCY
ATTN: ES, JOAN MA PIERRE
2 CYS ATTN: ESA
ATTN: ESA, G DAVIS
ATTN: ESA, W SUMMA
ATTN: ESE, R C WEBB
ATTN: ESE, W J SCOTT
ATTN: EST, K WARE
ATTN: EST, L PRESSLEY
ATTN: EST, R GULLICKSON
ATTN: R SCHNEIDER
ATTN: OPS
ATTN: PMPO
ATTN: PMPO, P HEBERT
2 CYS ATTN: TRC
ATTN: WEL
ATTN: WEP, T KENNEDY

DEFENSE TECHNICAL INFORMATION CENTER
2 CYS ATTN: DTIC/OCP

FC DEFENSE SPECIAL WEAPONS AGENCY
ATTN: FCT-S, G BALADI
ATTN: FCTI
ATTN: FCTO
ATTN: FCTR, R W SHOUP

NATIONAL DEFENSE UNIVERSITY
ATTN: NWCO

NATIONAL SECURITY AGENCY
ATTN: TECHNICAL LIBRARY

NET ASSESSMENT OFC OF SEC OF DEFENSE
ATTN: DOCUMENT CONTROL

**DEPARTMENT OF THE ARMY**

ARMY RESEARCH LABORATORIES
ATTN: TECH LIB
ATTN: AMSEL-WT-NH/KEHS
ATTN: AMSRL-WT-KEHS

ARMY SPACE & STRATEGIC DEFENSE CMD
ATTN: CSSD-ES-E1, R CROWSON

DEFENSE ADVANCED RSCH PROJECTS AGENCY
ATTN: DED

DEP CH OF STAFF FOR OPS & PLANS
ATTN: DAMO-ODW

U S ARMY WAR COLLEGE
ATTN: LIBRARY

U S ARMY VULNERABILITY ASSESSMENT LAB
ATTN: SLCVA-TAC

U S ARMY THAAD PROJECT OFFICE
ATTN: CSSD-WD

**DEPARTMENT OF THE NAVY**

NAVAL SEA SYSTEMS COMMAND
ATTN: PMS 423

NAVAL RESEARCH LABORATORY
ATTN: CODE 6720, J DAVIS
ATTN: CODE 6770, G COOPERSTEIN

NAVAL SURFACE WARFARE CENTER
ATTN: B DEPARTMENT

OFFICE OF NAVAL INTELLIGENCE
ATTN: DEOO
ATTN: LIBRARY

NAVAL AIR SYSTEMS COMMAND
ATTN: AIR-5161
ATTN: AIR-5164
ATTN: AIR-933

SPACE & NAVAL WARFARE SYSTEMS CMD
ATTN: PMW-145
ATTN: TECHNICAL LIBRARY

**DEPARTMENT OF THE AIR FORCE**

AFIWC/MSO
ATTN: TECHNICAL LIBRARY

AIR FORCE CTR FOR STUDIES & ANALYSIS
ATTN: AFSAA/SAI, RM 1D363 PENTAGON

AIR UNIVERSITY LIBRARY
ATTN: AUL-LSE

PHILLIPS LABORATORY
ATTN: PL/WSP, J KIUTTU
ATTN: PL/WSP, J DEGNAN

SAN ANTONIO AIR LOGISTICS CTR
ATTN: ALC/SW MR F CRISTADORO

SSP-27334 TRIDENT
ATTN: J BURTLE
ATTN: K TOBIN

USAF ROME LAB TECHNICAL LIBRARY, FL2810
ATTN: RBCM
ATTN: RBCT

USAF/AEDC/DOT
ATTN: DOT, MAJ J ROWLEY

**DEPARTMENT OF ENERGY**

LAWRENCE LIVERMORE NATIONAL LAB
ATTN: L-477, L SUTER
ATTN: L-84, G SIMONSON

LOS ALAMOS NATIONAL LABORATORY
ATTN: D-410, C EKDAHL
ATTN: MS D408
ATTN: MS F617
ATTN: MS H827
ATTN: MS-J970, R REINOVSKY

SANDIA NATIONAL LABORATORIES
ATTN: M HEDEMANN
ATTN: M K MATZEN
ATTN: D COOK
ATTN: TECH LIB
ATTN: W BALLARD
ATTN: W BEEZHOLD

U S DEPT OF ENERGY IE-24
ATTN: D CRANDALL

U S DEPT OF ENERGY
ATTN: C B HILLAND, DP-243
ATTN: C KEANE, DP-16
ATTN: R GUNDERSON, OMA/DP-252

**OTHER GOVERNMENT**

CENTRAL INTELLIGENCE AGENCY
ATTN: OSWR/SSD/SWB
ATTN: OSWR/STD/TTB
ATTN: OSWR, J PINA

FEDERAL EMERGENCY MANAGEMENT AGENCY
ATTN: SL-CD-MP

**DEPARTMENT OF DEFENSE CONTRACTORS**

ALME AND ASSOCIATES
ATTN: JOHN F DAVIS
ATTN: S SEILER, G101

APTEK, INC.
ATTN: T MEAGHER

BERKELEY RSCH ASSOCIATES, INC.
ATTN: N PEREIRA

CHARLES STARK DRAPER, INC.
ATTN: LIBRARY

DEFENSE GROUP, INC
ATTN: ROBERT POLL

E-SYSTEMS, INC.
ATTN: TECH INFO CTR

HY-TECH RESEARCH CORP.
2 CY ATTN: E J YADLOWSKY

INSTITUTE FOR DEFENSE ANALYSES
ATTN: TECH INFO SERVICES

JAYCOR
ATTN: M TREADAWAY

JAYCOR
ATTN: CYRUS P KNOWLES

KAMAN SCIENCES CORPORATION
ATTN: CLAUDE FORE

KAMAN SCIENCES CORPORATION
ATTN: DASIAC
ATTN: DASIAC/DARE

KTECH CORP.
ATTN: FRANK DAVIES

LOGICON R AND D ASSOCIATES
ATTN: E QUINN
ATTN: I VITKOVITSKY

LOGICON R AND D ASSOCIATES
ATTN: ROGER LEWIS

MAXWELL TECHNOLOGIES
ATTN: JOHN THOMSON
ATTN: PHIL COLEMAN
ATTN: WILLIAM H RIX

MISSION RESEACH CORP.
ATTN: K STRUVE

MISSION RESEARCH CORP.
ATTN: J R HENLEY

PRIMEX PHYSICS INTERNATIONAL
ATTN: B FAILOR
ATTN: C STALLINGS
ATTN: J RIORDAN
ATTN: P SINCERNY
ATTN: S L WONG

PULSE SCIENCE, INC.
ATTN: I D SMITH
ATTN: P W SPENCE
ATTN: TECHNICAL LIBRARY

SCIENCE APPLICATIONS INTL CORP
ATTN: W CHADSEY

SRI INTERNATIONAL
ATTN: ELECTROMAG SCI LAB TECH LIB

SVERDRUP INC AEDC
ATTN: L S CHRISTENSEN
ATTN: V KENYON

TEXAS TECH UNIVERSITY
2 CY ATTN: L HATFIELD
2 CY ATTN: M KRISTIANSEN

THE AEROSPACE CORP
ATTN: LIBRARY ACQUISITION M1/199
ATTN: T PARK M2/241